

IS-T 1698

Dynamic NMR Studies of Restricted Arene Rotation in the Chromiu
Tricarbonyl Thiophene and Selenophene Complexes

by

Sanger, Michael J.

MS Thesis submitted to Iowa State University

Ames Laboratory, U.S. DOE

Iowa State University

Ames, Iowa 50011

Date Transmitted: May 27, 1994

PREPARED FOR THE U.S. DEPARTMENT OF ENERGY
UNDER CONTRACT NO. W-7405-Eng-82.

MASTER

RECEIVED

OCT 25 1994

OSTI

DISTRIBUTION OF THIS DOCUMENT IS UNLIMITED

878

DISCLAIMER

This report was prepared as an account of work sponsored by an agency of the United States Government. Neither the United States Government nor any agency thereof, nor any of their employees, makes any warranty, express or implied, or assumes any legal liability or responsibility for the accuracy, completeness or usefulness of any information, apparatus, product, or process disclosed, or represents that its use would not infringe privately owned rights. Reference herein to any specific commercial product, process, or service by trade name, trademark, manufacturer, or otherwise, does not necessarily constitute or imply its endorsement, recommendation, or favoring by the United States Government or any agency thereof. The views and opinions of authors expressed herein do not necessarily state or reflect those of the United States Government or any agency thereof.

DISCLAIMER

**Portions of this document may be illegible
in electronic image products. Images are
produced from the best available original
document.**

TABLE OF CONTENTS

	Page
ACKNOWLEDGMENTS	iii
GENERAL INTRODUCTION	
Summary of Research	1
Thesis Organization	1
RESTRICTED ROTATIONAL BARRIERS IN $\text{Cr}(\text{CO})_3(\eta^6\text{-ARENE})$ COMPLEXES	
Introduction	2
Steric Rotational Barriers	6
Electronic Rotational Barriers	15
DYNAMIC NMR STUDIES OF THE RESTRICTED ROTATION OF THIOPHENES (Th) AND SELENOPHENES (Seln) IN THE $\text{Cr}(\text{CO})_3(\eta^5\text{-Th})$ AND $\text{Cr}(\text{CO})_3(\eta^5\text{-Seln})$ COMPLEXES	
Abstract	22
Introduction	23
Experimental Section	26
Results and Discussion	40
Supplementary Materials	60
References Cited	80
GENERAL CONCLUSIONS	90
REFERENCES CITED	91

ACKNOWLEDGMENTS

At this time, I would like to take the opportunity to thank a number of people who have helped me in my studies at Iowa State University.

Dr. Robert J. Angelici has always been helpful and has taught me a great deal about teaching and research at the graduate level.

Lisa Berreau has been a good friend to me during my stay at ISU and has always been available for discussion or an encouraging word.

My sincere thanks go out to the past and present members of the A-Team: Dr. John Benson, Dr. Mary Rottink, Dr. Mitchell Robertson, Dr. Hyoung Jun, Carter White, Dongmei Wang, Chip Nataro, James Rudd, Wayde Konze, and Allyn Ontko. Throughout my time in this group, the A-Team members have taught me everything I needed to know about research and life as a graduate student. I would like to offer special thanks to Dr. John Benson, who showed the patience of a saint in answering all of my questions when I first joined the group.

Most importantly, I would like to thank my parents, John and Dorothy Sanger, and my two sisters, Judy and Marilyn Sanger, for their support during a very long and trying time.

This work was performed at Ames Laboratory under Contract No. W-7405-Eng-82 with the U.S. Department of Energy. The United States Government has assigned the DOE Report Number IS-T-1698 to this thesis.

GENERAL INTRODUCTION

Summary of Research

This thesis contains the results of organometallic studies of thiophene and selenophene coordination in transition metal complexes. Chromium tricarbonyl complexes of thiophene, selenophene, and their alkyl-substituted derivatives were prepared and variable-temperature ^{13}C NMR spectra of these complexes were recorded in dimethyl ether. Bandshape analyses of these spectra yielded activation parameters for restricted rotation of the thiophene and selenophene ligands in these complexes. Extended Hückel molecular orbital calculations (EHMO) of the free thiophene and selenophene ligands and selected chromium tricarbonyl thiophene complexes were performed to better explain the activation barriers of these complexes. The structure of $\text{Cr}(\text{CO})_3(\eta^5\text{-2,5-dimethylthiophene})$ was established by a single crystal X-ray diffraction study.

Thesis Organization

This thesis consists of two chapters: the first is a literature review of restricted rotation in chromium tricarbonyl arene complexes; the second contains the results of my research as they were submitted for journal publication. Literature citations and figures are numbered independently in the literature review and the paper. Following the paper is a general summary of this work and the references cited in the literature review.

**RESTRICTED ROTATIONAL BARRIERS IN
 $\text{Cr}(\text{CO})_3(\eta^6\text{-AREN}E)$ COMPLEXES**

Introduction

Restricted Rotation in $\text{Cr}(\text{CO})_3(\eta^6\text{-C}_6\text{H}_6)$. A molecular structure of chromium tricarbonyl benzene, $\text{Cr}(\text{CO})_3(\eta^6\text{-C}_6\text{H}_6)$ (**1**), determined by Rees and Coppens¹ in 1973 suggests a slight localization of the double bonds in the benzene ring upon coordination to the $\text{Cr}(\text{CO})_3$ fragment. This study revealed that $\text{Cr}(\text{CO})_3(\eta^6\text{-C}_6\text{H}_6)$ exists in the solid state as the *staggered* conformer (structure **1a** in Figure 1) in which the C-C bonds are eclipsed by the carbonyl ligands; the *eclipsed* conformer (structure **1b** in Figure 1) has three of the carbon atoms in the ring eclipsed to the CO ligands. This study also demonstrated that the three C-C bonds eclipsed by the CO ligands are on average 0.018(2) Å longer than the *staggered* C-C bonds, consistent with octahedral hybridization of the chromium atom. The octahedral coordination of the Cr atom in this structure raises the question as to whether the metal-arene bonding is better described as localized metal-olefin bonds or in terms of a delocalized π -electron system of

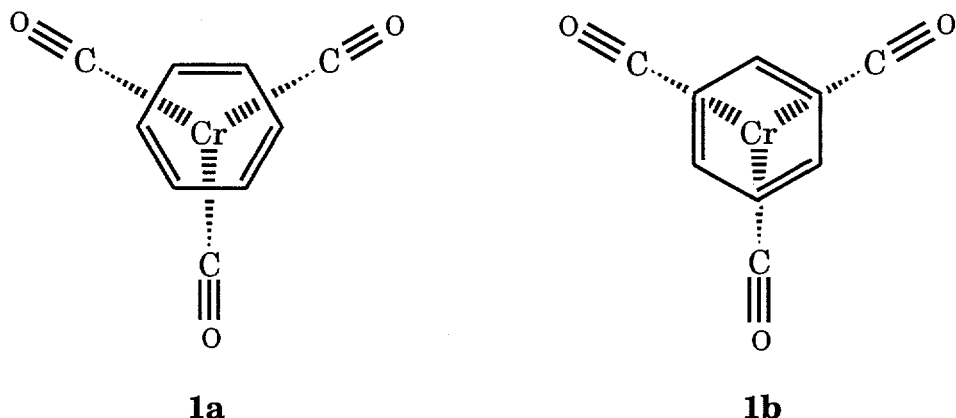


Figure 1. *Staggered* (**1a**) and *eclipsed* (**1b**) conformers of $\text{Cr}(\text{CO})_3(\eta^6\text{-C}_6\text{H}_6)$.

roughly cylindrical symmetry. The former case implies a large energy barrier to arene rotation; the latter allows relatively free rotation of the ring.

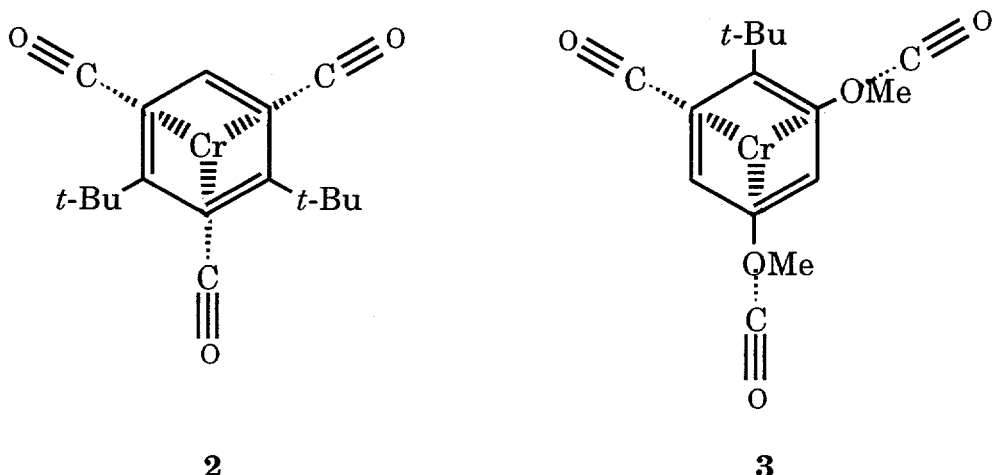
A variable-temperature ^1H NMR study² of the spin-lattice relaxation time (T_1) in crystalline $\text{Cr}(\text{CO})_3(\eta^6\text{-C}_6\text{H}_6)$ showed a minimum T_1 value at -90°C; this corresponds to an activation barrier of 4.2(1) kcal/mol for the intramolecular rotation of benzene. Comparison of this value with the rotational barrier measured in solid benzene (4.4 kcal/mol),³ however, suggests that the measured activation energy of **1** is due more to the crystal-packing forces present in the solid than to any interactions between benzene and the $\text{Cr}(\text{CO})_3$ fragment. This conclusion is supported by a ^{13}C NMR spin-lattice relaxation study⁴ of $\text{Cr}(\text{CO})_3(\eta^6\text{-C}_6\text{H}_6)$ in CDCl_3 in which an upper limit for the rotational barrier for the benzene ring was estimated to be 0.55 kcal/mol. Similarly, an electron diffraction study⁵ of gaseous $\text{Cr}(\text{CO})_3(\eta^6\text{-C}_6\text{H}_6)$ at 140°C suggested that this complex is essentially an unhindered internal rotor in the vapor phase that exists as a mixture of several conformations which differ only in the relative orientations of the arene ring and the CO ligands.

In 1977, Hoffmann and co-workers⁶ performed extended Hückel molecular orbital calculations (EHMO) on several $\text{ML}_3(\text{polyene})$ transition metal complexes, including $\text{Cr}(\text{CO})_3(\eta^6\text{-C}_6\text{H}_6)$. These calculations were directed at understanding the conformational preferences and barriers to internal rotation of the polyenes with respect to the ML_3 fragment. EHMO calculations for **1** predicted that the *staggered* conformer (structure **1a** in Figure 1) is 0.3 kcal/mol more stable than the *eclipsed* conformer (structure **1b** in Figure 1), which is in accord with the crystal structure reported previously.¹ The overlap populations calculated for the C-C bonds eclipsed by the CO ligands are smaller than those of the

staggered C-C bonds and this is consistent with the distortion of the C-C bonds noted in the X-ray study. The authors suggested that the more the ML_3 (polyene) complex resembles an octahedron, the greater the rotational barrier of the polyene with respect to the ML_3 fragment. Indeed, calculations of the rotational barrier in $Cr(CO)_3(\eta^6\text{-cyclohexatriene})$, in which the three double bonds in the benzene ring have been completely localized, resulted in a value of 19.4 kcal/mol.

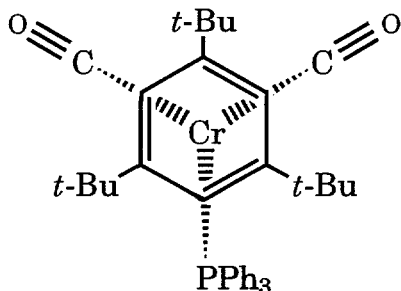
Initial ^{13}C NMR Studies of Substituted $\text{Cr}(\text{CO})_3(\eta^6\text{-Arene})$ Complexes.

In an attempt to measure arene rotational barriers on the NMR timescale, Jackson and co-workers⁷ studied the ¹³C NMR spectra of Cr(CO)₃(η⁶-1,3-(*t*-Bu)₂-C₆H₄) (**2**) and Cr(CO)₃(η⁶-1-(*t*-Bu)-2,4-(OMe)₂C₆H₃) (**3**) in CDCl₃. Although



the electronic effects of the *t*-Bu groups favor the rotamer in which they are eclipsed by the CO ligands, the steric effects of these bulky groups predominate, resulting in the ground state shown in **2**. The ^{13}C NMR spectra of **2**, however, showed no broadening of the CO resonance at -60°C , which would be indicative of restricted arene rotation on the NMR timescale. Methoxy groups are good π -

electron donors that increase the electron density on the *ortho* and *para* carbons of the benzene ring. Because chromium prefers octahedral coordination with relatively electron-rich carbons, this complex strongly favors the ground state shown in **3**; the steric effects of the *t*-Bu group also favor this ground state. However, the ^{13}C NMR spectrum of **3** showed no broadening of the CO resonance at -60°C. The ^{13}C NMR spectrum of the triphenylphosphine-substituted complex $\text{Cr}(\text{CO})_2(\text{PPh}_3)(\eta^6\text{-1,3,5-(}t\text{-Bu)}_3\text{C}_6\text{H}_3)$ (**4**) was also studied in CDCl_3 .⁸ The



4

authors had hoped that the sizes of the bulky PPh_3 ligand and the *t*-Bu groups would allow them to observe restricted arene rotation in this complex, but the ^{13}C NMR spectrum of this complex in CDCl_3 at -60°C showed no splitting of the *t*-Bu or the aromatic carbon resonances.

These studies demonstrated that in the absence of exceptional steric or electronic effects, barriers to arene rotation in the $\text{Cr}(\text{CO})_3(\eta^6\text{-arene})$ complexes are too small to be detected by NMR spectroscopy. In this section, a review of the dynamic NMR studies of selected $\text{Cr}(\text{CO})_3(\eta^6\text{-arene})$ complexes is presented for complexes that have steric or electronic factors that are substantial enough to lead to restricted rotation on the NMR timescale.

Steric Rotational Barriers

Restricted Rotation of Arene Substituents. When the solid state ^{13}C NMR spectrum of chromium tricarbonyl hexaethylbenzene, $\text{Cr}(\text{CO})_3(\eta^6\text{-C}_6\text{Et}_6)$ (**5**), was reported,⁹ it was noted that the methyl, methylene, and aromatic carbons each appeared as pairs of equally intense peaks. This observation is consistent with the molecular structure of **5**¹⁰ in which the arene appears in the *1,3,5-distal-2,4,6-proximal* conformation (structure **5a** in Figure 2); this conformation is also present in free C_6Et_6 .¹¹ In the ^{13}C NMR of **5** at room temperature in CD_2Cl_2 , the methyl, methylene, and aromatic carbons all appear as singlets; however, at lower temperatures these resonances are split, as seen in the solid state.

Because each ethyl group on the ring can be either *proximal* or *distal* to the metal and the arene ring can be either *eclipsed* or *staggered* with respect to the $\text{Cr}(\text{CO})_3$ fragment (Figure 1), there are 36 stereoisomers possible for $\text{Cr}(\text{CO})_3(\eta^6\text{-C}_6\text{Et}_6)$.¹² However, if it is postulated for steric reasons that an Et group eclipsed by a carbonyl cannot be *proximal* and that the two Et groups of a C-C bond eclipsed by a CO ligand must be *distal*, the number of conformers possible is now restricted to five (Figure 2). The *eclipsed* conformer of **5d** has

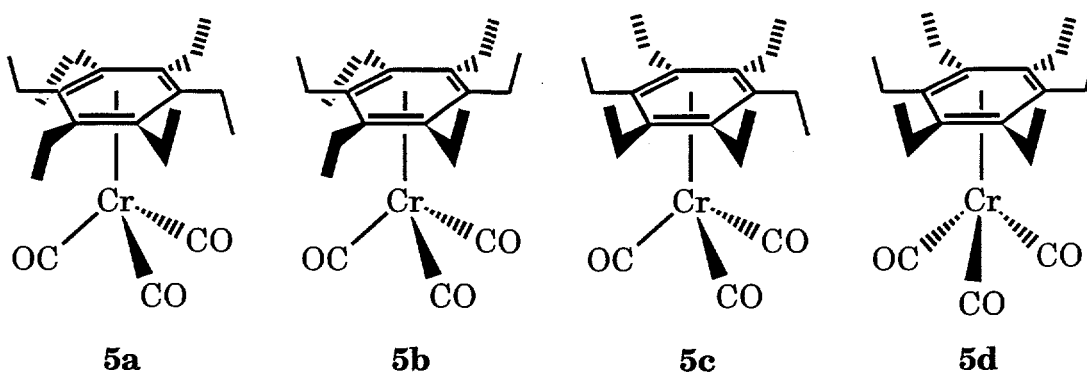


Figure 2. Allowed stereoisomers for $\text{Cr}(\text{CO})_3(\eta^6\text{-C}_6\text{Et}_6)$ (**5**).

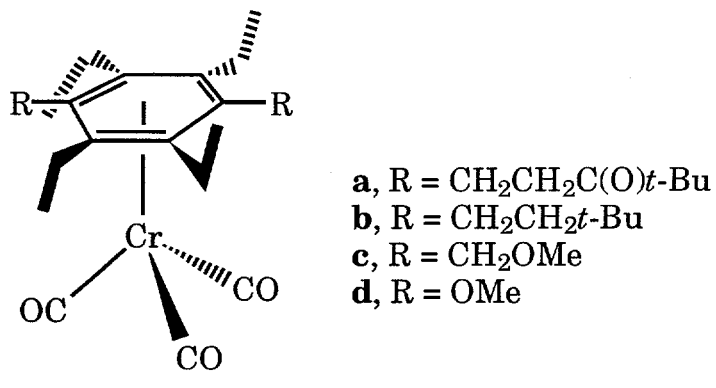
been ignored since hexa-substituted arene rings with local C_{6v} symmetry invariably bind to the $\text{Cr}(\text{CO})_3$ fragment as the *staggered* conformer.^{1,10,13} Examples of each of these stereoisomers have been reported in the molecular structures of **5** and its phosphine, thiocarbonyl, and nitrosyl derivatives: **5a** [$\text{Cr}(\text{CO})_2\text{L}(\eta^6\text{-C}_6\text{Et}_6)$, where $\text{L} = \text{CO}$,¹⁰ CS ,¹⁴ and NO^+ ,¹⁵ and $\text{Cr}(\text{CO})(\text{CS})(\text{NO})(\eta^6\text{-C}_6\text{Et}_6)^+$], **5b** [$\text{Cr}(\text{CO})_2(\text{PMe}_3)(\eta^6\text{-C}_6\text{Et}_6)^+$]¹⁶, **5c** [$\text{Cr}(\text{CO})_2(\text{PR}_3)(\eta^6\text{-C}_6\text{Et}_6)$, where $\text{R} = \text{Me}$, Et ,¹² and Ph ¹⁰], and **5d** [$\text{Cr}(\text{CO})_2(\text{PR}_3)(\eta^6\text{-C}_6\text{Et}_6)$, where $\text{R} = \text{Et}$ and Ph]. The authors argued¹⁵ that sterically nondemanding ligands such as CO , CS , and NO^+ allow the ring to exist in the lowest energy conformer **5a** in which there are no Et-Et non-bonding interactions. However, as increasingly steric phosphine ligands are used, the PR_3 -Et repulsive interactions increase in magnitude and force more of the Et groups to occupy *proximal* positions with a concomitant increase in the Et-Et repulsions. Hence, crystals of the PMe_3 complex contain 80% **5b** and 20% **5c**, crystals of the PEt_3 complex contain 50% **5c** and 50% **5d**, and crystals of the PPh_3 complex contain 33% **5c** and 67% **5d**.

The ^{13}C NMR of $\text{Cr}(\text{CO})_3(\eta^6\text{-C}_6\text{Et}_6)$ at room temperature in CD_2Cl_2 displayed four singlets corresponding to the methyl, methylene, aromatic carbon, and CO ligand resonances.^{10b} At 10°C, the first three carbon signals broaden and at -30°C these signals appear as pairs of equally intense peaks. The ΔG_{300^\ddagger} value of 11.5(6) kcal/mol was determined by bandshape analysis of the variable-temperature ^{13}C NMR spectra. This value is comparable to that estimated for free C_6Et_6 (11.8 kcal/mol) using empirical force field calculations (EFF). Bandshape analyses performed on the ^{13}C NMR spectra of $\text{Cr}(\text{CO})_2(\text{CS})(\eta^6\text{-C}_6\text{Et}_6)$, $\text{Cr}(\text{CO})_2(\text{NO})(\eta^6\text{-C}_6\text{Et}_6)^+$, and $\text{Cr}(\text{CO})(\text{CS})(\text{NO})(\eta^6\text{-C}_6\text{Et}_6)^+$ yielded ΔG_{300^\ddagger} values of 11.5(5),¹⁴ 11.5(4),¹⁵ and 11.4(4)¹⁵ kcal/mol, respectively. Comparison of ΔG^\ddagger

values calculated for the free arene and the CO, CS, and NO⁺ derivatives of **5** reveals that ML₃ fragments with sterically nondemanding ligands do not affect the rotational barriers of the Et groups in C₆Et₆.

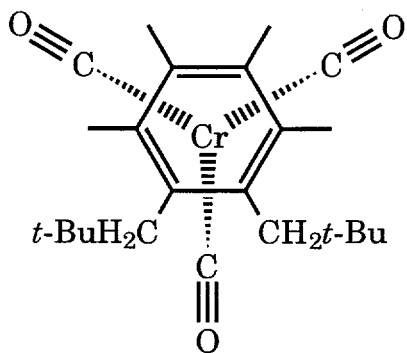
The molecular structure of the hexa-*n*-propylbenzene complex Cr(CO)₃(η^6 -C₆(*n*-Pr)₆)¹⁷ shows the same *1,3,5-distal-2,4,6-proximal* conformation present in **5**. The variable-temperature ¹³C NMR spectra of this complex in toluene-d₈ also showed a decoalescence of the arene and *n*-propyl signals. Bandshape analysis of these spectra yielded a value of $\Delta G_{300}^\ddagger = 11.9(7)$ kcal/mol. This value is the same as that seen in the C₆Et₆ complexes and suggests that Et and *n*-Pr groups offer similar steric constraints to the Cr(CO)₃ fragment.

Kilway and Siegel¹⁸ reported the rotational barriers of the arene substituents for 1,4-disubstituted derivatives of hexaethylbenzene and their chromium tricarbonyl complexes, Cr(CO)₃(η^6 -1,4-R₂C₆Et₄), where R = CH₂CH₂C(O)*t*-Bu (**6a**), CH₂CH₂*t*-Bu (**6b**), CH₂OMe (**6c**), and OMe (**6d**). In these studies, the



authors discovered that these barriers are only slightly affected by metal complexation, as evidenced by the ΔG^\ddagger values for the free arenes and their Cr(CO)₃ complexes, respectively: **6a** (11.3(3) and 11.8(3) kcal/mol),^{18a} **6b** (11.2(3) and

11.8(3) kcal/mol,^{18b} **6c** (9.4(3) and 8.9(3) kcal/mol,^{18b} and **6d** (7.7(3) and 6.6(3), kcal/mol).^{18b} These results are in contrast with a study¹⁹ in which the rotational barrier of the *neo*-pentyl groups in 1,2-di-*neo*-pentyltetramethylbenzene dropped from 16.2 kcal/mol in the free arene to 12 kcal/mol in the Cr(CO)₃ complex (**7**).



7

Although the ¹³C NMR spectra of Cr(CO)₃(PPh₃)(η⁶-C₆Et₆) demonstrated that only the all-*distal* conformer (similar to structure **5d** in Figure 2) is present in solution,¹⁰ the ¹³C NMR spectra of other Cr(CO)₂(PR₃)(η⁶-C₆Et₆) complexes (R = Me, Et, and OPh) are considerably more complex^{16,20} and are indicative of the presence of more than one of the possible rotamers. Variable-temperature ³¹P NMR spectra of these complexes showed a decoalescence of the single peak present at room temperature into two peaks for PEt₃ (**5c-5d**),²⁰ three peaks for P(OPh)₃ (**5b-5d**),²⁰ and four peaks for PMe₃ (**5a-5d**).^{16,20} Bandshape analyses of these ³¹P NMR spectra resulted in ΔG[‡] values of 8.9(5), 8.8(5), and 9.3(2) kcal/mol for the PR₃ complexes, where R = Me, Et, and OPh, respectively. These values are lower than that seen for **5** (11.8 kcal/mol)¹⁰ and the authors suggested²⁰ that the lower barriers in the phosphine complexes reflect a destabilization

of the ground state resulting from increased non-bonding repulsive interactions among the ethyl groups and between the ethyl groups and the PR_3 ligand.

Restricted Rotation of Phosphine Ligands. Although a variable-temperature ^{13}C NMR study¹⁰ of $\text{Cr}(\text{CO})_2(\text{PPh}_3)(\eta^6\text{-C}_6\text{Et}_6)$ demonstrated no decoalescence phenomena in the arene, ethyl, or CO ligand peaks, the phenyl resonances for the PPh_3 ligand showed a decoalescence into two signals of intensity 2:1 at low temperatures.²¹ These resonances are consistent with restricted rotation about the Cr-P bond in this complex with rapid rotation about the Cr-arene and P-C(*ipso*) bonds. Hunter and co-workers²¹ reported the variable-temperature ^{13}C NMR spectra of the homosubstituted hexaalkylbenzene complexes $\text{Cr}(\text{CO})_2(\text{PPh}_3)(\eta^6\text{-C}_6\text{R}_6)$, where R = H, Me, Et, and *n*-Pr. In this study, the authors reported that restricted rotation about the Cr-P bond was observed in all but the benzene (R = H) complex. Bandshape analyses of these spectra yielded ΔG_{200}^\ddagger values of 9.2(4), 9.1(4), and 9.0(4) kcal/mol for the C_6Me_6 , C_6Et_6 , and $\text{C}_6(n\text{-Pr})_6$ complexes, respectively. The restricted rotation about the Cr-P bond was attributed to steric difficulties experienced by the phenyl groups as they attempt to rotate past the coordinated arene. The fact that the benzene complex experienced no restricted rotation about the Cr-P bond while the other complexes experienced the same rotational barrier suggests that there is some minimum steric requirement for restricted Cr-P rotation that is met for all of these complexes except the benzene complex.

An additional study by Hunter and co-workers²² of the ^{13}C NMR spectra of the methyl-substituted benzene complexes $\text{Cr}(\text{CO})_2(\text{PPh}_3)(\eta^6\text{-C}_6\text{H}_x\text{Me}_{6-x})$, where x = 0-6, demonstrated that rotation about the Cr-P bond is not restricted

when two adjacent positions on the ring are unsubstituted. Therefore, the only tri-substituted complex that showed restricted rotation is the $\eta^3\text{-Me}_3\text{C}_6\text{H}_3$ complex; similarly, all tetra-substituted benzene complexes showed restricted rotation except $\text{Cr}(\text{CO})_3(\eta^6\text{-1,2,3,4-Me}_4\text{C}_6\text{H}_2)$. The penta- and hexa-substituted complexes also showed restricted Cr-P rotation. The ΔG_{200}^\ddagger values determined by bandshape analysis of the ^{13}C NMR spectra vary from 8.1(3) to 9.2(5) kcal/mol; however, there is no significant trend in ΔG_{200}^\ddagger with respect to methyl substitution. This study suggested that two adjacent unsubstituted sites on the benzene ring allow adequate room for unrestricted phosphine rotation on the NMR timescale.

Chromium dicarbonyl triphenylphosphine complexes of the all-*syn* and the *syn-anti-syn* cyclotrimers of bicyclo[2.2.1]hept-2-yne (structures **8a** and **8b** in Figure 3, $\text{L} = \text{PPh}_3$) also showed restricted rotation of the Cr-P bond at low temperatures.²³ In both cases, the $\text{Cr}(\text{CO})_2(\text{PPh}_3)$ fragment is bound to the sterically less-demanding face of these ligands; therefore, the all-*syn* complex has three

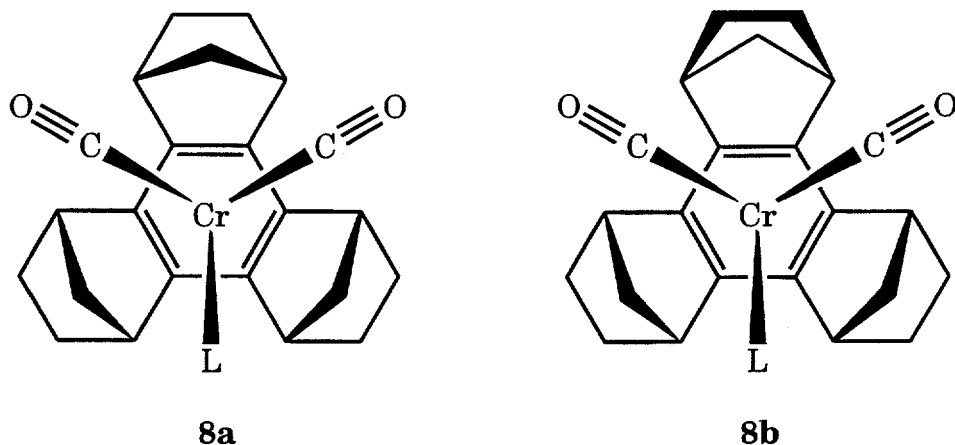


Figure 3. The $\text{Cr}(\text{CO})_2(\text{L})$ complexes of the all-*syn* (**8a**) and *syn-anti-syn* (**8b**) cyclotrimers of bicyclo[2.2.1]hept-2-yne

methylene groups *proximal* to the metal and the *syn-anti-syn* complex has two methylene groups and one ethylene group *proximal* to the chromium. The ΔG_{200}^\ddagger values for the Cr-P bond rotation in the *all-syn* and *syn-anti-syn* complexes were estimated to be 6.2 and 8.4 kcal/mol, respectively. The larger ΔG_{200}^\ddagger value for the $\text{Cr}(\text{CO})_2(\text{PPh}_3)$ complex of **8b** versus **8a** ($\text{L} = \text{PPh}_3$) reflects the increased steric demands of the *proximal* ethylene group compared to the *proximal* methylene group.

Restricted Rotation of Arene Ligands. Because the C_{3v} symmetry of $\text{Cr}(\text{CO})_3(\eta^6\text{-C}_6\text{Et}_6)$ in its *1,3,5-distal-2,4,6-proximal* stereoisomer (structure **5a** in Figure 2) prevents the observation of any restricted arene rotation, McGlinchey and co-workers prepared desymmetrized derivatives of **5** using the sterically non-demanding thiocarbonyl^{14,15} and nitrosyl¹⁵ ligands. These complexes also adopt the *1,3,5-distal-2,4,6-proximal* stereoisomer in solution and the ethyl and arene carbons in these complexes experience local C_{3v} symmetry with rapid arene ring rotation. However, upon restricted arene rotation these carbons no longer experience the same environment and their resonances are split.

In 1983, McGlinchey and co-workers¹⁴ reported that the methyl, methylene, and aromatic carbon resonances of $\text{Cr}(\text{CO})_2(\text{CS})(\eta^6\text{-C}_6\text{Et}_6)$ exhibit a 2:1:2:1 pattern at 163 K, which is consistent with slowed arene rotation of the *1,3,5-distal-2,4,6-proximal* stereoisomer. Hunter and Mislow²⁴ later suggested that the 2:1:2:1 pattern could be explained without invoking restricted arene rotation by the presence of the *1,2,3,5-distal-4,6-proximal* stereoisomer (structure **5b** in Figure 2). However, after a detailed analysis of the low temperature ^{13}C NMR spectrum of $\text{Cr}(\text{CO})_2(\text{CS})(\eta^6\text{-C}_6\text{Et}_6)$, McGlinchey *et al.*²⁵ reported that the only

complex present in solution is the *1,3,5-distal-2,4,6-proximal* stereoisomer and the 2:1:2:1 splitting requires restricted rotation of the arene ligand. The ^{13}C NMR spectra of $\text{Cr}(\text{CO})_2(\text{NO})(\eta^6\text{-C}_6\text{Et}_6)^+$ demonstrated a decoalescence of the ethyl and arene resonances into the 2:1:2:1 pattern similar to that seen for the CS complex.¹⁵ The ^{13}C NMR spectrum of $\text{Cr}(\text{CO})(\text{CS})(\text{NO})(\eta^6\text{-C}_6\text{Et}_6)^+$ complex at -105°C showed different environments for each carbon atom in the arene ligand. Analysis of the ^{13}C chemical shifts suggests that three ethyl groups are *proximal* and three are *distal*; this can only be attributed to the presence of the *1,3,5-distal-2,4,6-proximal* stereoisomer and restricted rotation of the arene ring. The activation barriers for arene rotation have been determined by bandshape analyses to be 9.2(2) kcal/mol for the $\text{Cr}(\text{CO})_2(\text{CS})$ complex²⁶ and 9.5(4) kcal/mol for both the $\text{Cr}(\text{CO})_2(\text{NO})^+$ and $\text{Cr}(\text{CO})(\text{CS})(\text{NO})^+$ complexes.¹⁵ The fact that the arene rotational barriers of these complexes do not change upon substitution of CO ligands by the more π -basic CS and NO⁺ ligands confirms that these barriers are based on the steric interactions between the three *proximal* ethyl groups and the three ligands on the chromium atom and not on any electronic factors. By analogy, these studies also suggest that the rotational barrier of the arene in $\text{Cr}(\text{CO})_3(\eta^6\text{-C}_6\text{Et}_6)$ should be about 9 to 9.5 kcal/mol.

In an attempt to estimate the arene rotational barrier in $\text{Cr}(\text{CO})_3(\eta^6\text{-C}_6\text{Et}_6)$, McGlinchey and co-workers²⁷ prepared $\text{Cr}(\text{CO})_3(\eta^6\text{-C}_6\text{Et}_5\text{C}(\text{O})\text{Me})$, a complex in which the arene ring has only mirror symmetry. Slowed arene rotation in this complex would be reflected by a splitting of the threefold symmetry of the $\text{Cr}(\text{CO})_3$ fragment. A detailed analysis of the ^{13}C NMR spectrum in CD_2Cl_2 at -100°C demonstrated that the only stereoisomer present is the *1-proximal-acetyl-3,5-proximal-2,4,6-distal*-pentaethyl conformer. The CO ligand resonance

in this spectrum is split into a 2:1 pattern at -100°C, which is consistent with slowed arene rotation with a ΔG^\ddagger value of 9.0(5) kcal/mol. Although it has been suggested²⁶ that the acetyl group perturbs the electronic structure of the arene ring and it is this perturbation that leads to restricted arene rotation, these authors reported²⁷ that the ^{13}C NMR shift of the organic carbonyl in both the free and complexed ring are indicative of steric interactions with the ethyl groups that prevent coplanarity of the carbonyl and the ring.

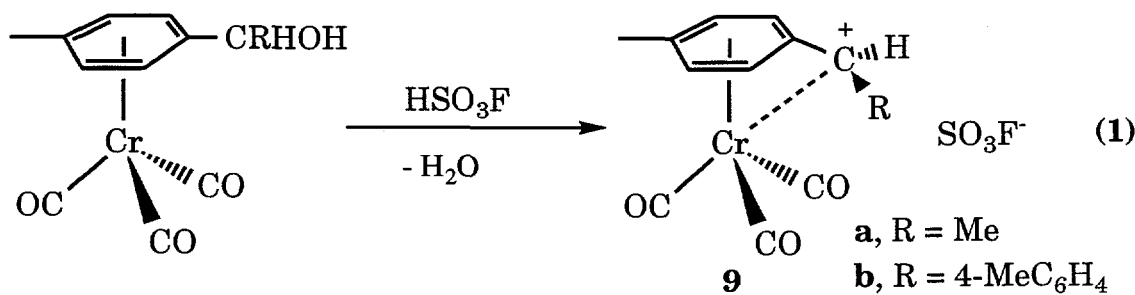
A similar study^{18a} was performed on 1,4-bis(4,4-dimethyl-3-oxopentyl)-tetraethylbenzene ($1,4-(\text{CH}_2\text{CH}_2\text{C}(\text{O})t\text{-Bu})_2\text{C}_6\text{Et}_4$) and its chromium tricarbonyl complex **6a**. The ^{13}C NMR spectra of **6a** showed decoalescence of the ring substituents into the *1,3,5-distal-2,4,6-proximal* stereoisomer. At lower temperatures, the spectra showed decoalescence of the CO ligands consistent with slowed arene rotation on the NMR timescale. The fact that the restricted arene rotation is largely steric in nature is supported by the larger arene rotational barrier for the $\text{Cr}(\text{CO})_3$ complex (9.5(5) kcal/mol)^{18a} than for the analogous $\text{Mo}(\text{CO})_3$ complex (6.7(5) kcal/mol).²⁸ The studies of $\text{Cr}(\text{CO})_3$ complexes with desymmetrized derivatives of C_6Et_6 , along with the studies of CS and NO^+ derivatives of $\text{Cr}(\text{CO})_3(\eta^6\text{-C}_6\text{Et}_6)$, suggest that the arene rotational barrier in $\text{Cr}(\text{CO})_3(\eta^6\text{-C}_6\text{Et}_6)$ is about 9 to 9.5 kcal/mol.

The ^{13}C NMR of the $\text{Cr}(\text{CO})_2\text{L}$ complexes, where $\text{L} = \text{CO}$, CS, and PPh_3 , of the all-*syn* and *syn-anti-syn* cyclotrimers of bicyclo[2.2.1]hept-2-yne (Figure 3) were studied in an attempt to observe restricted arene rotation. The $\text{Cr}(\text{CO})_3$ complex of the *syn-anti-syn* cyclotrimer showed a broadening of the carbonyl resonance in the ^{13}C NMR at -130°C, which corresponds to an activation barrier of about 6.5 kcal/mol.²⁹ The CS and PPh_3 complexes of the *syn-anti-syn* cyclo-

trimer are expected to have activation barriers similar to and larger than that estimated for the $\text{Cr}(\text{CO})_3$ complex, respectively. However, decoalescence phenomena were not observed for these complexes;²³ presumably this is due to the fact that the expected ground state still retains the C_s symmetry present in the complex with rapid arene rotation. Although the C_{3v} symmetry present in the $\text{Cr}(\text{CO})_3$ complex of the all-*syn* cyclotrimer precludes the observation of slowed arene rotation, the CS complex showed no evidence for slowed arene rotation.²³ In contrast, the PPh_3 complex of the all-*syn* cyclotrimer showed complex broadening of the ^{13}C NMR that is attributed to slowed rotation of both the Cr-P bond and the arene ring and corresponds to a ΔG^\ddagger value of 6.2(13) kcal/mol. The authors reported²³ that steric interactions with the metal ligands increase in the order **8a** < **8b** < **5** and is consistent with the increasing activation barrier of the $\text{Cr}(\text{CO})_3$ complexes (less than 6.2, 6.5, and 9.5 kcal/mol, respectively, L = CO).

Electronic Rotational Barriers

Restricted Rotation of Benzyl Cations. In 1977, Ceccon and co-workers³⁰ reported the variable-temperature ^{13}C NMR spectra of the chromium tricarbonyl benzyl cations $\text{Cr}(\text{CO})_3(\eta^6\text{-4-MeC}_6\text{H}_4\text{CRH})^+$, where R = Me (**9a**) and 4-MeC₆H₄ (**9b**), which were prepared by the protonation (with loss of H₂O) of the $\text{Cr}(\text{CO})_3$ - $(\eta^6\text{-4-MeC}_6\text{H}_4\text{CRHOH})$ complexes in HSO₃F (eq 1). Although the authors



reported that the CO ligand resonances were split into a 1:1:1 pattern at -50°C and attributed this splitting to restricted arene rotation, no activation barrier was calculated in this study. In 1992, McGlinchey and co-workers³¹ repeated these experiments. The ¹³C NMR spectra of **9a** was monitored over the temperature range of -60 to -25°C (at which point the complex showed clear signs of decomposition) and fully confirmed Ceccon's original assertions. Bandshape analysis of the ¹³C NMR spectra yields a ΔG_{248}^\ddagger value of 11.7(4) kcal/mol.

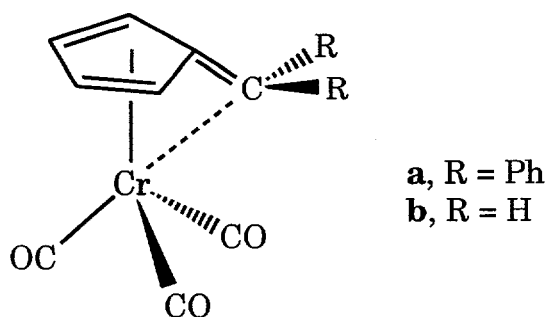
Initial EHMO calculations performed by Hoffmann and co-workers³² predicted that the methylene carbon in $\text{Cr}(\text{CO})_3(\eta^6\text{-C}_6\text{H}_5\text{CH}_2)^+$ will bend about 11° toward the chromium atom. This distortion increases the overlap of the vacant p_z orbital on the benzyl carbon with a filled metal orbital, which leads to a delocalization of the positive charge onto the metal and stabilizes the cationic complex. These calculations also predict that the *staggered* conformer of the benzyl complex is 6.8 kcal/mol more stable than the *eclipsed* conformer. Recent EHMO studies performed by McGlinchey and co-workers³¹ predicted that the methylene carbon in $\text{Cr}(\text{CO})_3(\eta^6\text{-C}_6\text{H}_5\text{CH}_2)^+$ will bend 22° toward the metal, resulting in a calculated activation barrier of 7.4 kcal/mol.

McGlinchey and co-workers³¹ suggested that the placement of an electron-donating substituent such as Me or OMe at the *para* position of the benzylic ring should reinforce the localization of relatively electron-rich sites at the *ipso* and *meta* positions of the ring. In contrast, a Me or OMe substituent in the *meta* position of the benzylic ring should counteract the charge localization of the benzyl cation. The former case should raise the activation barrier; the latter should lower it. This idea is supported by EHMO calculations that predicted activation barriers of 7.5 and 5.1 kcal/mol and measured ΔG^\ddagger values of 11 and 10 kcal/mol

for the *para* and *meta* complexes of $\text{Cr}(\text{CO})_3(\eta^6\text{-}(\text{OMe})\text{C}_6\text{H}_4\text{CH}_2)^+$, respectively. The discrepancies between the experimental ΔG^\ddagger values and those calculated by EHMO studies have been explained by the fact that the experimental values not only include the barrier to internal ring rotation, but also the energy needed to bend the methylene fragment away from the metal to allow free arene rotation.

EHMO calculations also suggested that in the tertiary benzyl complex $\text{Cr}(\text{CO})_3(\eta^6\text{-C}_6\text{H}_5\text{CMe}_2)^+$, bending of the methylene carbon toward the metal is energetically disfavored. The authors suggested that a tertiary cation is better suited to stabilize the cationic charge than a primary cation and thus needs less assistance from the metal to stabilize the complex. This argument is supported by the larger ΔG^\ddagger value reported for the primary benzyl complex $\text{Cr}(\text{CO})_3(\eta^6\text{-}4\text{-MeC}_6\text{H}_4\text{CH}_2)^+$ (12.5(4) kcal/mol) with respect to the secondary benzyl complex $\text{Cr}(\text{CO})_3(\eta^6\text{-}4\text{-MeC}_6\text{H}_4\text{CHMe})^+$ (11.7(4) kcal/mol).

Restricted Rotation of Fulvene Complexes. The molecular structures of $\text{Cr}(\text{CO})_3(\eta^6\text{-C}_5\text{H}_4\text{CPh}_2)^{33}$ (**10a**) and $\text{Cr}(\text{CO})_3(\eta^6\text{-C}_5\text{H}_4\text{CH}_2)^{34}$ (**10b**) demonstrated that the exocyclic methylene carbon is bent towards the $\text{Cr}(\text{CO})_3$ fragment by 35° and 30° , respectively, and that the CO ligands are *staggered* with respect to the



methylene carbon. EHMO calculations suggested³² that the *staggered* conformer present in these structures is 7.3 kcal/mol more stable than the *eclipsed* conformer; this value increases to 9.3 kcal/mol when the methylene carbon is bent 30° towards the metal. Preliminary studies done by Kreiter (cited in reference 32) suggested that the arene rotation in $\text{Cr}(\text{CO})_3(\eta^6\text{-C}_5\text{H}_4\text{CMe}_2)$ is slowed at 183 K; this corresponds to a ΔG^\ddagger value from 7 to 9 kcal/mol. Behrens and co-workers³⁴ reported a 2:1 splitting of the CO ligand resonance in the ^{13}C NMR spectrum in $\text{Cr}(\text{CO})_3(\eta^6\text{-C}_5\text{H}_4\text{CH}_2)$ consistent with an arene activation barrier of 11.3 kcal /mol. Recently, McGlinchey and co-workers³¹ reported the variable-temperature ^{13}C NMR spectra of $\text{Cr}(\text{CO})_3(\eta^6\text{-C}_5\text{H}_4\text{CPh}_2)$ and $\text{Cr}(\text{CO})_3(\eta^6\text{-C}_5\text{H}_4\text{CPhMe})$. In the former complex, the CO resonances were split into a 2:1 pattern while the latter complex showed CO resonances in a 1:1:1 ratio. The ΔG^\ddagger value calculated for both complexes is 11.0(5) kcal/mol. With the exception of Kreiter's study of $\text{Cr}(\text{CO})_3(\eta^6\text{-C}_5\text{H}_4\text{CMe}_2)$, the arene activation barriers of chromium tricarbonyl fulvene complexes are about 11 kcal/mol and are independent of the substituents on the exocyclic carbon atom.

Restricted Rotation of Terphenylene and Starphenylene Complexes. In order to minimize steric strain in the cyclobutadiene rings in the planar *angular*-terphenylene (benzo[3,4]cyclobuta[1,2a]biphenylene, **11a**) and starphenylene (**11b**) ligands (Figure 4), the C-C bonds of the central ring that are shared by the cyclobutadiene fragments are lengthened with respect to those between the butadiene rings. The resulting Kekulé character of the central ring in **11a** can be seen by the average C-C single bond length of 1.45 Å and the average C-C double bond length of 1.35 Å;³⁵ the 2,3,6,7,10,11-hexakis(trimethylsilyl) derivative of

11b demonstrates a more extreme Kekulé structure with an average C-C single bond length of 1.49 Å and an average C-C double bond length of 1.34 Å.³⁶ The bond alternation present in **11a** and **11b** is indicative of a net localization of the double bonds in the central benzene ring. EHMO calculations performed by Hoffmann and co-workers⁶ predicted that the rotational barrier for Cr(CO)₃(η^6 -cyclohexatriene), in which the three double bonds in the benzene ring are completely localized, is 19.4 kcal/mol. These calculations suggest that the *endo*-Cr(CO)₃ complexes of **11a** and **11b** should demonstrate significant rotational barriers.

The molecular structure of the *endo*-Cr(CO)₃(η^6 -angular-terphenylene)³⁷ demonstrated that the CO ligands are eclipsed by the cyclobutadiene rings, resulting in a conformation in which the chromium atom is octahedrally coordinated by the three CO ligands and the shorter C-C bonds of the central ring. The activation barrier measured for the restricted arene rotation in *endo*-Cr(CO)₃(η^6 -angular-terphenylene) is 9.4(5) kcal/mol.

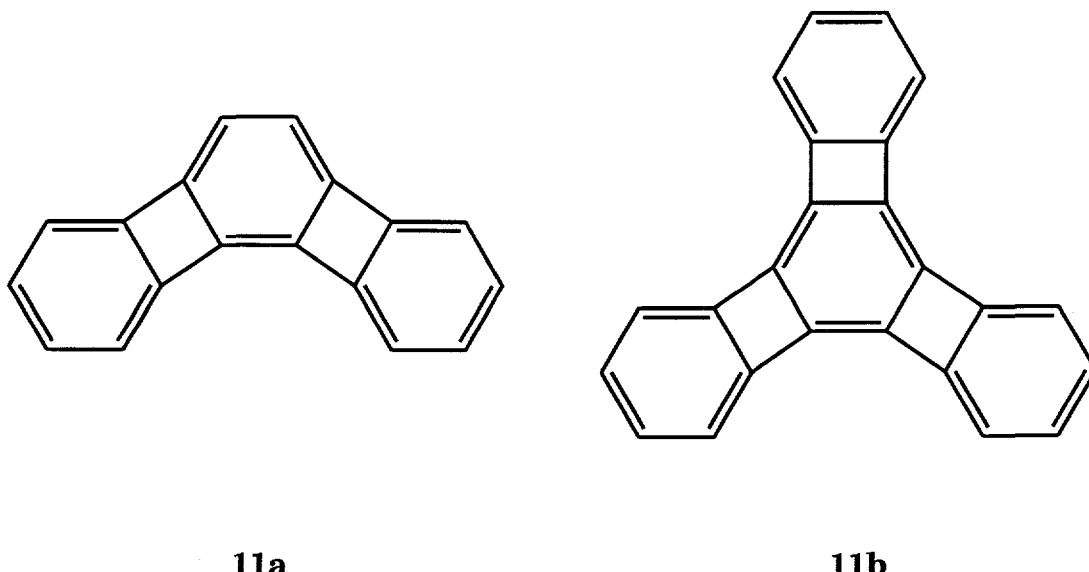
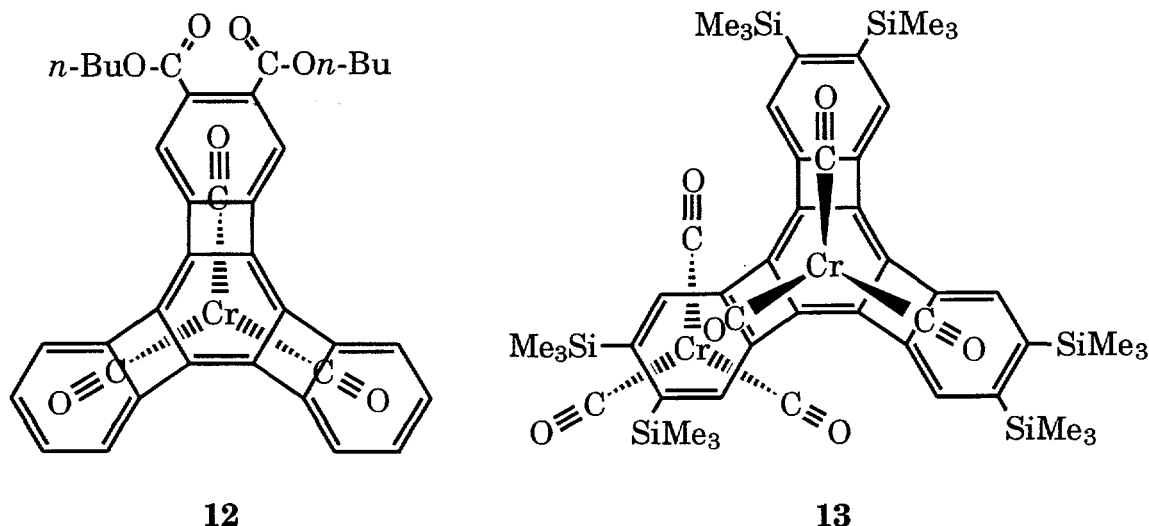


Figure 4. Structures of *angular*-terphenylene (**11a**) and starphenylene (**11b**)

Because the C_{3v} symmetry of *endo*-Cr(CO)₃(η^6 -starphenylene) prevents the direct measurement of the arene barrier to rotation by variable-temperature NMR spectroscopy, desymmetrized complexes must be prepared before an activation barrier can be measured. Siegel and co-workers³⁸ prepared two Cr(CO)₃ complexes with lowered symmetry: one in which the starphenylene ligand substitution breaks the C_{3v} symmetry, *endo*-Cr(CO)₃(η^6 -2,3-dicarbobutoxystarphenylene) (**12**), and the other in which an additional Cr(CO)₃ fragment bound to one of the *exo* rings lowers the symmetry of the complex, *endo*-,*exo*-[Cr(CO)₃]₂(η^6 -, η^6 -hexakis(trimethylsilyl)starphenylene) (**13**). The former complex has an activation barrier of 11.1(5) kcal/mol; the latter has an activation barrier of 9.7(5)



kcal/mol. Comparison of the ΔG^\ddagger values calculated for the monometallic complexes *endo*-Cr(CO)₃(η^6 -angular-terphenylene) (9.4(5) kcal/mol) and **12** (11.1(5) kcal/mol) demonstrates that the greater localization of the double bonds in the central ring of **12** leads to a larger activation barrier.

The *endo* isomers of **12** and $\text{Cr}(\text{CO})_3(\eta^6\text{-angular-terphenylene})$ isomerize at 90 and 140°C, respectively, to the thermodynamically favored *exo* isomers. The authors suggested that this isomerization stems from a kinetic preference for initial attack at the more nucleophilic central ring and the thermodynamic stability of the *exo* metal complex. Isomerization of the starphenylene complex was proposed to occur by rotation to the trigonal prismatic conformation of the “cyclohexatriene” fragment, ring slippage to the “dimethylenecyclobutene” fragment, and then ring slippage to the *exo* benzene ring (Figure 5).

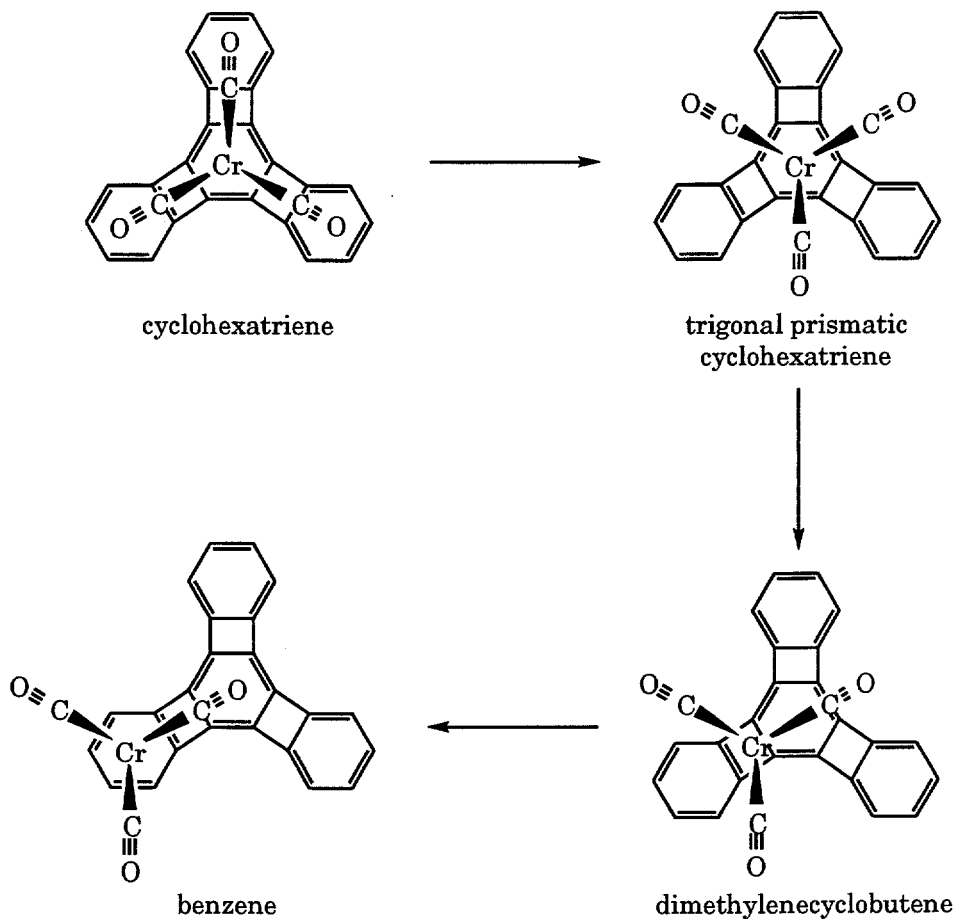


Figure 5. Proposed isomerization of *endo*- $\text{Cr}(\text{CO})_3(\eta^6\text{-starphenylene})$

DYNAMIC NMR STUDIES OF THE RESTRICTED ROTATION OF
THIOPHENES (Th) AND SELENOPHENES (Seln) IN THE
 $\text{Cr}(\text{CO})_3(\eta^5\text{-Th})$ AND $\text{Cr}(\text{CO})_3(\eta^5\text{-Seln})$ COMPLEXES

A paper submitted to *Organometallics* by
Michael J. Sanger and Robert J. Angelici*

Abstract

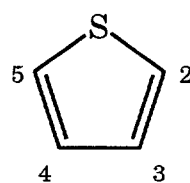
The reaction of $\text{Cr}(\text{CO})_6$ with thiophenes (Th) and selenophenes (Seln) produced $\text{Cr}(\text{CO})_3(\eta^5\text{-Th})$ (Th = T, 2-MeT, 2-EtT, 3-MeT, 2,5-Me₂T, and Me₄T) and $\text{Cr}(\text{CO})_3(\eta^5\text{-Seln})$ (Seln = Sel, 2-MeSel, and 2,5-Me₂Sel). Variable-temperature ¹³C NMR spectra of these complexes in dimethyl ether indicated that there is restricted rotation about the Cr-Th and -Seln bonds. Bandshape analyses of the ¹³C NMR spectra using DNMR5 gave activation parameters for ring rotation. Activation enthalpies (ΔH^\ddagger , kcal/mol) for these complexes increase in the following order: T (6.2), 3-MeT (6.5), 2-EtT (6.9), 2-MeT (7.1), Me₄T (7.4), 2,5-Me₂T (7.7), Sel (7.8), 2-MeSel (8.4), and 2,5-Me₂Sel (9.0). In general, alkyl substitution increases ΔH^\ddagger and α -substitution leads to a larger ΔH^\ddagger than β -substitution. Substitution of the S heteroatom by Se also increases ΔH^\ddagger . These results are discussed in terms of the relative electron densities on the heteroatom and the diene fragment, which were estimated using extended Hückel molecular orbital (EHMO) calculations. The structure of $\text{Cr}(\text{CO})_3(\eta^5\text{-2,5-Me}_2\text{T})$ was established by a single crystal X-ray diffraction study. The rotational

* All inquiries about this paper should be addressed to Dr. Robert J. Angelici.

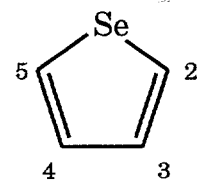
barriers for these complexes are larger than those of $\text{Cr}(\text{CO})_3(\eta^6\text{-arene})$ complexes presumably due to the strong interaction between the chromium and the heteroatom.

Introduction

Heterogeneous catalytic hydrodesulfurization (HDS) of petroleum-based feedstocks is crucial for both environmental and industrial reasons.² Of the organosulfur compounds present in petroleum, thiophene (T) and its alkyl-substituted derivatives (Th) are among the most difficult to desulfurize, presumably due to their aromaticity.³ For that reason, thiophene compounds and their organometallic transition metal complexes have been the focus of many HDS studies.⁴ Use of selenophene (Sel) as a model for HDS reactions is rather recent⁵



T



Sel

and is based primarily on the similarity of the chemistry of thiophenes (Th) and selenophenes (Sel).^{5,6} Selenophene compounds have the added benefit of an NMR active heteroatom (^{77}Se is a spin 1/2 nucleus that is 7.6% abundant)⁷ that could be useful in the elucidation of selenophene binding modes in transition metal complexes and on heterogeneous catalyst surfaces.⁵

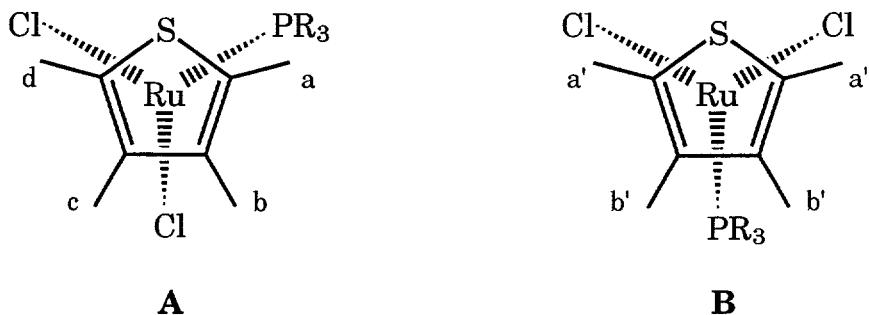
Although it is widely accepted that T and Sel possess some degree of aromaticity, attempts to quantify the relative aromaticities of this family of five-membered heterocycles with respect to each other and benzene have yielded

conflicting results.^{4b,6a,8} In general, however, studies indicate a decrease in aromaticity in the sequence benzene > T > Sel. Although this ordering indicates that T and Sel are less aromatic than benzene, it should be noted that the properties and reactivities of Th and Seln compounds are dominated by their aromaticity.^{6,9}

Without exception, transition metal complexes of thiophenes with the stoichiometry $ML_3(\eta^5\text{-Th})$ have pseudooctahedral structures in which the L ligands are approximately *trans* to the sulfur or a double bond of the Th ligand.^{4b,10} This orientation of the Th rings can be interpreted as indicating localized metal-thiophene bonding through the two double bonds and sulfur; however, it is possible that the metal-thiophene bonding is better described in terms of a delocalized electron system of roughly cylindrical symmetry. The former case implies a significant energy barrier to thiophene ring rotation; the latter would presumably allow relatively free rotation of the thiophene ring.

In the course of their investigations of the dimeric ruthenium-tetramethylthiophene (Me_4T) complex $[(\eta^5\text{-Me}_4\text{T})\text{RuCl}(\mu_2\text{-Cl})]_2$, Rauchfuss and co-workers^{10c} discovered striking differences in the ^1H NMR spectra of the $(\eta^5\text{-Me}_4\text{T})\text{RuCl}_2(\text{PR}_3)$ complexes for $\text{R} = \text{Me}$ or $n\text{-Bu}$ versus $\text{R} = \text{Ph}$ or $p\text{-tolyl}$. The ^1H NMR spectra of the PMe_3 and $\text{P}(n\text{-Bu})_3$ complexes showed two very sharp resonances at 24°C for the methyl peaks of Me_4T . The ^1H NMR of the PPh_3 and $\text{P}(p\text{-tolyl})_3$ complexes, however, showed two very broad resonances in the methyl region at room temperature. At -60°C , these broad resonances decoalesced into four methyl peaks of equal intensity. This observation is consistent with slowed metal-ring rotation to give structure **A** in which the sulfur is *trans* to a Cl, rather than the other rotamer **B** in which the PR_3 ligand is *trans* to the sulfur. It is not

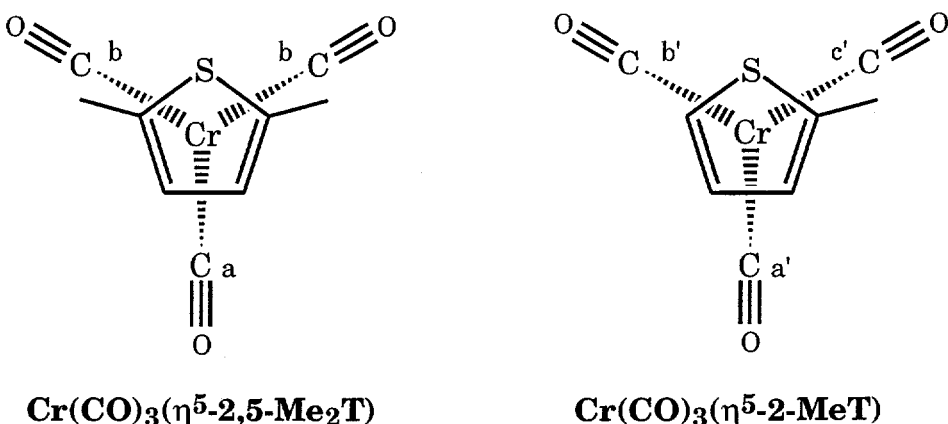
clear why **A** might be the most stable rotamer but the authors suggested that steric interactions between the Me_4T and PR_3 ligands are responsible for the relatively slow rate of rotation in the PPh_3 and $\text{P}(p\text{-tolyl})_3$ complexes.



Rotational barriers in $\text{Cr}(\text{CO})_3(\eta^6\text{-arene})$ complexes have been extensively studied and recently reviewed.¹¹ Generally, the barriers to arene rotation are low (less than 1 kcal/mol),¹² but in some cases the barrier can be substantially increased by steric¹³ or electronic¹⁴ modifications of the arene ligand. In particular, the chromium tricarbonyl complexes of aromatic rings that contain a distinct localization of the double bonds show relatively large rotational barriers of about 10 kcal/mol.^{14b,d} Given the fact that thiophene and selenophene are not as aromatic as benzene, it is not unreasonable to expect significant rotational barriers in the $\text{Cr}(\text{CO})_3(\eta^5\text{-Th})$ and $\text{Cr}(\text{CO})_3(\eta^5\text{-Seln})$ complexes. The ^{13}C NMR signals for the carbonyl ligands in these complexes provide an opportunity to monitor the ring rotation. The three carbonyls are equivalent when the ring rotates rapidly, but become inequivalent when the rotation is slowed on the NMR timescale, as seen for the 2,5-dimethylthiophene (2,5-Me₂T) and 2-methylthiophene (2-MeT) chromium tricarbonyl complexes (Chart I).

In this paper, we describe the synthesis and characterization of the series of $\eta^5\text{-Th}$ complexes $\text{Cr}(\text{CO})_3(\eta^5\text{-Th})$, where Th = T (**1**), 2-MeT (**2**), 2-ethylthio-

Chart I



phene (2-EtT) (**3**), 3-methylthiophene (3-MeT) (**4**), 2,5-Me₂T (**5**), and Me₄T (**6**), the η⁵-Seln complexes Cr(CO)₃(η⁵-Seln), where Seln = Sel (**7**), 2-methylselenophene (2-MeSel) (**8**), and 2,5-dimethylselenophene (2,5-Me₂Sel) (**9**), and the cationic, but isoelectronic, complex [Mn(CO)₃(η⁵-2,5-Me₂Sel)]OTf (**10**, OTf⁻ = CF₃SO₃⁻). The activation parameters (including ΔG_c[‡], T_c, ΔH[‡], and ΔS[‡]) for the restricted rotation of the thiophene and selenophene ligands in these complexes and the X-ray structure of Cr(CO)₃(η⁵-2,5-Me₂T) are also reported.

Experimental Section

General Procedures. All reactions were performed under a nitrogen atmosphere in purified solvents of reagent grade using standard Schlenk techniques¹⁵ unless otherwise stated. Hexanes, methylene chloride (CH₂Cl₂), chloroform (CHCl₃), and *n*-butyl ether (*n*-Bu₂O) were distilled from CaH₂, and THF was distilled under nitrogen from Na/benzophenone. The solvents were stored over 4-Å molecular sieves under nitrogen. The neutral alumina (Brockman, Activity I, 150 mesh) used for chromatography was deoxygenated at room temperature in

high vacuum for 16 h and then deactivated with 5 wt% nitrogen-saturated water, shaken, and stored under nitrogen.

The ^1H and $^{13}\text{C}\{^1\text{H}\}$ NMR spectra were recorded on a Nicolet NT-300 and a Varian VXR-300 spectrometer, respectively, using CDCl_3 (unless otherwise stated) as the solvent and internal lock. The ^1H NMR spectra (Table I) were referenced to internal SiMe_4 and the ^{13}C NMR spectra (Table II) were referenced to CDCl_3 (δ 77.0 ppm). The infrared spectra of the complexes (Table III) were measured in CH_2Cl_2 using a Nicolet 710 FT-IR spectrometer. Electron impact mass spectra (EIMS) were performed on a Finnigan 4000 or a Kratos MS-50 mass spectrometer. The photochemical reactions were performed under nitrogen in a quartz tube equipped with a nitrogen bubbler using a 450 W mercury UV lamp. The temperature of the photochemical reactions was maintained at -16°C by a Lauda RK 20 constant-temperature circulator.

The low-temperature ^{13}C NMR studies were performed on ^{13}CO -enriched samples (without spinning) using a Bruker WM-200 spectrometer. Temperatures were measured using a copper-constantan thermocouple, which was calibrated to within 1 K. The temperature-dependent ^{13}C NMR studies of the chromium-containing complexes were performed without ^1H decoupling using dimethyl ether (Me_2O) as the solvent, internal proton lock, and internal reference (δ 59.7 ppm) in a high-pressure 10-mm NMR tube. The low-temperature ^{13}C NMR studies of $[\text{Mn}(\text{CO})_3(\eta^5\text{-2,5-Me}_2\text{Sel})]\text{OTf}$ were performed using CD_3NO_2 as the internal lock and internal reference.

$\text{Cr}(\text{CO})_6$ was used as purchased from Strem Chemicals. Gaseous Me_2O and ^{13}CO (99.4 atom% ^{13}C) were used as purchased from Matheson. Thiophene was purified as described previously.¹⁶ Reagent grade CDCl_3 , CD_3NO_2 , 2-MeT,

Table I. ^1H NMR Chemical Shifts (δ) and Coupling Constants (Hz) for the Complexes in CDCl_3

Complex	$\text{H}(2)$	$\text{H}(3)$	$\text{H}(4)$	$\text{H}(5)$	Me	CH_2	$\text{J}_{2,5}$	$\text{J}_{3,4}$	$\text{J}_{3,5}$	$\text{J}_{4,5}$	J_{Et}
$\text{Cr}(\text{CO})_3(\eta^5\text{-T})$	5.37 <i>m</i>	5.59 <i>m</i>	5.59 <i>m</i>	5.37 <i>m</i>							
$\text{Cr}(\text{CO})_3(\eta^5\text{-2-MeT})$	5.33 <i>d</i>	5.52 <i>dd</i>	5.21 <i>d</i>	2.28							3.3
$\text{Cr}(\text{CO})_3(\eta^5\text{-2-EtT})$	5.35 <i>d</i>	5.53 <i>dd</i>	5.24 <i>d</i>	1.24 <i>t</i>	2.58 <i>q</i>						3.4
$\text{Cr}(\text{CO})_3(\eta^5\text{-3-MeT})$	5.13 <i>d</i>		5.49 <i>d</i>	5.37 <i>dd</i>	2.28						7.4
$\text{Cr}(\text{CO})_3(\eta^5\text{-2,5-Me}_2\text{T})$		5.27		2.22							3.3
$\text{Cr}(\text{CO})_3(\eta^5\text{-Me}_4\text{T})$				2.16 <i>a,b</i>							
$\text{Cr}(\text{CO})_3(\eta^5\text{-Sel})$	5.95 <i>m</i>	5.79 <i>m</i>	5.79 <i>m</i>	5.95 <i>m</i>							
$\text{Cr}(\text{CO})_3(\eta^5\text{-2-MeSel})$		5.47 <i>d</i>	5.74 <i>dd</i>	5.80 <i>d</i>	2.36						3.7
$\text{Cr}(\text{CO})_3(\eta^5\text{-2,5-Me}_2\text{Sel})$		5.43	5.43		2.31						
$[\text{Mn}(\text{CO})_3(\eta^5\text{-2,5-Me}_2\text{Sel})]\text{OTf}^c$	6.60	6.60		2.57							
T	7.31 <i>m</i>	7.10 <i>m</i>	7.31 <i>m</i>								
2-MeT	6.74 <i>dd</i>	6.87 <i>dd</i>	7.05 <i>dd</i>	2.48							3.4
2-EtT	6.79 <i>dd</i>	6.91 <i>dd</i>	7.10 <i>dd</i>	1.31 <i>t</i>							5.1
3-MeT	6.87 <i>d</i>	6.88 <i>d</i>	7.18 <i>dd</i>	2.26							7.5
2,5-Me ₂ T		6.51		2.40							
Me ₄ T				2.00 <i>a</i>							
				2.30 <i>b</i>							
Sel	8.01 <i>m</i>	7.34 <i>m</i>	7.34 <i>m</i>	8.01 <i>m</i>							
2-MeSel		6.91 <i>d</i>	7.09 <i>dd</i>	7.74 <i>d</i>	2.58						
2,5-Me ₂ Sel		6.65	6.65		2.50						

a $\text{Me}(3,4)$. *b* $\text{Me}(2,5)$. *c* in CD_3NO_2 .

Table II. $^{13}\text{C}\{^1\text{H}\}$ NMR Chemical Shifts (δ) for the Complexes in CDCl_3

Complex	C(2)	C(3)	C(4)	C(5)	Me	CH_2	CO
$\text{Cr}(\text{CO})_3(\eta^5\text{-T})$	85.87	91.24	91.24	85.87			232.79
$\text{Cr}(\text{CO})_3(\eta^5\text{-2-MeT})$	106.58	91.58	92.19	84.79	15.54		233.26
$\text{Cr}(\text{CO})_3(\eta^5\text{-2-EtT})$	114.69	89.89	92.24	84.68	15.30	23.30	233.32
$\text{Cr}(\text{CO})_3(\eta^5\text{-3-MeT})$	84.15	109.34	93.93	86.60	15.23		233.41
$\text{Cr}(\text{CO})_3(\eta^5\text{-2,5-Me}_2\text{T})$	105.44	92.16	92.16	105.44	15.80		233.68
$\text{Cr}(\text{CO})_3(\eta^5\text{-Me}_4\text{T})$	100.32	108.69	108.69	100.32	13.24 ^a		234.74
					14.23 ^b		
$\text{Cr}(\text{CO})_3(\eta^5\text{-Sel})$	91.63	91.91	91.91	91.63			233.04
$\text{Cr}(\text{CO})_3(\eta^5\text{-2-MeSel})$	113.82	92.64	92.68	91.01	18.08		233.44
$\text{Cr}(\text{CO})_3(\eta^5\text{-2,5-Me}_2\text{Sel})$	113.27	93.11	93.11	113.27	18.40		233.86
$[\text{Mn}(\text{CO})_3(\eta^5\text{-2,5-Me}_2\text{Sel})]\text{OTf}^c$	128.92	100.10	100.10	128.92	18.07		218.37
T	125.13	126.87	126.87	125.13			
2-MeT	139.60	125.13	126.89	123.05	15.05		
2-EtT	147.44	123.27	126.69	122.67	16.09	23.29	
3-MeT	120.48	137.55	129.23	125.16	15.45		
2,5-Me ₂ T	137.38	124.77	124.77	137.38	15.22		
Me ₄ T	127.80	133.04	133.04	127.80	12.74 ^a		
					13.05 ^b		
Sel	129.41	130.37	130.37	129.41			
2-MeSel	146.48	127.64	129.34	128.42	17.89		
2,5-Me ₂ Sel	144.33	127.12	127.12	144.33	18.14		

^a Me(3,4). ^b Me(2,5). ^c in CD_3NO_2 .

Table III. Infrared Absorptions (cm⁻¹) for the Complexes in CH₂Cl₂

Complex	ν_{CO}^a
Cr(CO) ₃ (η^5 -T)	1968, 1886, 1870
Cr(CO) ₃ (η^5 -2-MeT)	1963, 1880, 1870
Cr(CO) ₃ (η^5 -2-EtT)	1962, 1878, 1865
Cr(CO) ₃ (η^5 -3-MeT)	1964, 1883, 1868
Cr(CO) ₃ (η^5 -2,5-Me ₂ T)	1958, 1870, 1862
Cr(CO) ₃ (η^5 -Me ₄ T)	1951, 1868, 1849
Cr(CO) ₃ (η^5 -Sel)	1967, 1890, 1869
Cr(CO) ₃ (η^5 -2-MeSel)	1963, 1884, 1863
Cr(CO) ₃ (η^5 -2,5-Me ₂ Sel)	1958, 1878, 1859
[Mn(CO) ₃ (η^5 -2,5-Me ₂ Sel)]OTf	2069, 2011, 2000

^a Relative intensities are vs, s (*br*), and s (*br*).

2-EtT, 3-MeT, 2,5-Me₂T, and *cis*-cyclooctene were purchased from Aldrich and used without further purification. CD₂Cl₂ and CD₃OD were used as purchased from Cambridge Isotopes Laboratory. Me₄T,¹⁷ Sel,¹⁸ 2-MeSel,¹⁹ 2,5-Me₂Sel,¹⁹ and [Mn(CO)₃(η^5 -2,5-Me₂Sel)]OTf^{5b} were prepared by literature methods.

Preparation of the Cr(CO)₃(η^5 -Th) and Cr(CO)₃(η^5 -Seln) Complexes

(1-9). To a solution of 0.22 g (1.0 mmol) of Cr(CO)₆ in 10 mL of *n*-Bu₂O and 1 mL of THF was added 5 mmol of the thiophene or selenophene ligand. The mixture was refluxed with stirring under nitrogen for 3.5 h, during which time the solution slowly changed from colorless to dark red. The volatile components, including Cr(CO)₆, were removed *in vacuo* for 10 to 15 min at room temperature

and the resulting orange powder was extracted with hexanes-CH₂Cl₂ (10:1) and chromatographed on neutral alumina (2 cm x 20 cm). The orange band containing the product was eluted with 1:1 hexanes-CH₂Cl₂ and evaporated to dryness. The resulting solid was dissolved in a minimum amount of CH₂Cl₂ and layered with hexanes. This solution was allowed to slowly mix overnight at -20°C. The yields for Cr(CO)₃(η^5 -3-MeT) (**4**) and Cr(CO)₃(η^5 -2,5-Me₂Sel) (**9**) were 18% and 58%, respectively; when corrected for recovered Cr(CO)₆, the yields based on reacted Cr(CO)₆ were 85% and 93%, respectively. These values are representative of the yields for the other alkyl-substituted thiophene and selenophene complexes. The Cr(CO)₃(η^5 -Th) and Cr(CO)₃(η^5 -Sel) complexes were positively identified by their ¹H NMR spectra in CDCl₃,^{5b,20} which are given in Table I.

Preparation of ¹³CO-Enriched Cr(CO)₆. The ¹³CO-enriched Cr(CO)₆ was prepared by a modified literature method.²¹ A solution of Cr(CO)₅(COE) was prepared by UV irradiation of 0.223 g of Cr(CO)₆ in 20 mL of hexanes and 1 mL of *cis*-cyclooctene (COE) for 4 h at -16°C. The solution was filtered and slowly cooled to -78°C, which resulted in bright yellow crystals of Cr(CO)₅(COE) (0.20 g, 64%; ν_{CO} in hexanes: 2071 *w*, 1954 *s*, *br* cm⁻¹). A solution of 0.20 g of Cr(CO)₅(COE) dissolved in 20 mL of hexanes was frozen in a liquid nitrogen bath and the flask was evacuated. The solution was thawed and the ¹³C-enriched CO was bubbled in through a rubber septum using a metal needle connected via Tygon tubing to the lecture bottle. While stirring for 30 min at room temperature, the solution slowly turned from bright yellow to a colorless liquid. Filtering this solution and cooling it to -78°C precipitated Cr(CO)₅(¹³CO) in essentially quantitative yield based on Cr(CO)₅(COE). A ¹³CO enrichment value (the percent of

the total number of CO ligands that are ^{13}CO of 11.8% was calculated for the labelled $\text{Cr}(\text{CO})_6$ from the relative intensities of the molecular ion peaks in the mass spectrum of the labelled complex. The ^{13}CO -enriched $\text{Cr}(\text{CO})_3(\eta^5\text{-Th})$ and $\text{Cr}(\text{CO})_3(\eta^5\text{-Sel})$ complexes were produced as stated above, using equal weights of unlabelled $\text{Cr}(\text{CO})_6$ and the ^{13}CO -enriched $\text{Cr}(\text{CO})_6$ as the starting material.

Preparation of ^{13}CO -Enriched $\text{Mn}(\text{CO})_5\text{Br}$. The ^{13}CO -enriched $\text{Mn}(\text{CO})_5\text{Br}$ was prepared by a modification of a literature method.²² A solution of $(\text{CO})_4\text{Mn}-(\mu_2\text{-Br})_2\text{Mn}(\text{CO})_4$ was prepared by refluxing a solution of 0.151 g of $\text{Mn}(\text{CO})_5\text{Br}$ in 20 mL of CHCl_3 under nitrogen for 4 h. Cooling the solution to 0°C using an ice bath resulted in the formation of a red-brown powder of $\text{Mn}_2(\text{CO})_8\text{Br}_2$ (0.121 g, 89%; ν_{CO} in CHCl_3 : 2102 *m*, 2045 *vs*, 2013 *s*, 1977 *s* cm^{-1}). A solution of 0.121 g of $\text{Mn}_2(\text{CO})_8\text{Br}_2$ in 20 mL of CHCl_3 was frozen in a liquid nitrogen bath and the flask was evacuated. The ^{13}C -enriched CO was condensed into the flask at -196°C; the solution was thawed and allowed to stir at room temperature overnight. Cooling the solution to 0°C in an ice bath gave a precipitate of $\text{Mn}(\text{CO})_4-(^{13}\text{CO})\text{Br}$ in essentially quantitative yield. The ^{13}CO -labelled $[\text{Mn}(\text{CO})_3(\eta^5\text{-2,5-Me}_2\text{Sel})]\text{OTf}$ was prepared according to a literature procedure using the labelled $\text{Mn}(\text{CO})_5\text{Br}$.^{5b}

X-Ray Diffraction Study of $\text{Cr}(\text{CO})_3(\eta^5\text{-2,5-Me}_2\text{T})$ (5). A single crystal of **5** suitable for X-ray diffraction was obtained by layering a CH_2Cl_2 solution of the complex with hexanes and allowing the solution to mix at -20°C; the crystal was mounted on a glass fiber. The cell constants for data collection were determined from a list of reflections found by an automated search routine. Pertinent data

collection and reduction information is given in Table IV. Lorentz and polarization corrections were applied. A correction based on a decay in the standard reflections of 1.9% was applied to the data. An absorption correction based on a series of ψ -scans was applied. The agreement factor for the averaging of observed reflections was 1.1% based on F . The centric space group $P2_1/c$ was unambiguously determined by the systematic absences. The positions of all non-hydrogen atoms were determined by direct methods.²³ All non-hydrogen atoms were refined with anisotropic thermal parameters. After the least-squares converged, all hydrogen atoms were found in a difference Fourier map. These were placed into the model with isotropic temperature factors set equal to 1.0 times

**Table IV. Crystal and Data Collection Parameters for
 $\text{Cr}(\text{CO})_3(\eta^5\text{-2,5-Me}_2\text{T})$ (5)**

Formula	$\text{CrSC}_9\text{H}_8\text{O}_3$
Formula weight	248.22
Space Group	$P2_1/c$
a , Å	6.725(2)
b , Å	12.348(1)
c , Å	12.485(4)
α , deg	90
β , deg	104.14(2)
γ , deg	90
V , Å ³	1005.3(5)
Z	4

Table IV. (continued)

d_{calc} , g/cm ³	1.64
Crystal size, mm	0.35 x 0.30 x 0.25
$\mu(\text{MoK}\alpha)$, cm ⁻¹	12.8
Data collection instrument	Enraf-Nonius CAD4
Radiation (monochromated in incident beam)	MoK α ($\lambda = 0.71073 \text{ \AA}$)
Orientation reflections:	
number; range (2 θ), deg	25; 18.3 < 2 θ < 31.6
Temperature, °C	-50(1)
Scan Method	θ -2 θ
Data collection range (2 θ), deg	4.0-50.0
Number of data collected:	3686
Number of unique data, total:	1758
with $F_o^2 > 3\sigma(F_o^2)$:	1479
Number of parameters refined	127
Trans. factors: max.; min. (ψ -scans)	0.998; 0.959
R^a	0.022
R_w^b	0.034
Quality-of-fit indicator ^c	1.01
Largest shift/esd, final cycle	0.00
<u>Largest peak, e/Å³</u>	<u>0.23(3)</u>

^a $R = \sum ||F_o| - |F_c|| / \sum |F_o|$.

^b $R_w = [\sum w(|F_o| - |F_c|)^2 / \sum w |F_o|^2]^{1/2}$; $w = 1/\sigma^2(|F_o|)$.

^c Quality-of-fit = $[\sum w(|F_o| - |F_c|)^2 / (N_{obs} - N_{parameters})]^{1/2}$.

the isotropic equivalent of the attached atom. The hydrogen atom positions were not refined in the final least-squares cycle. An ORTEP drawing of **5** is given in Figure 1. Bond distances, selected angles, and atomic positional parameters for **5** are presented in Tables V and VI.

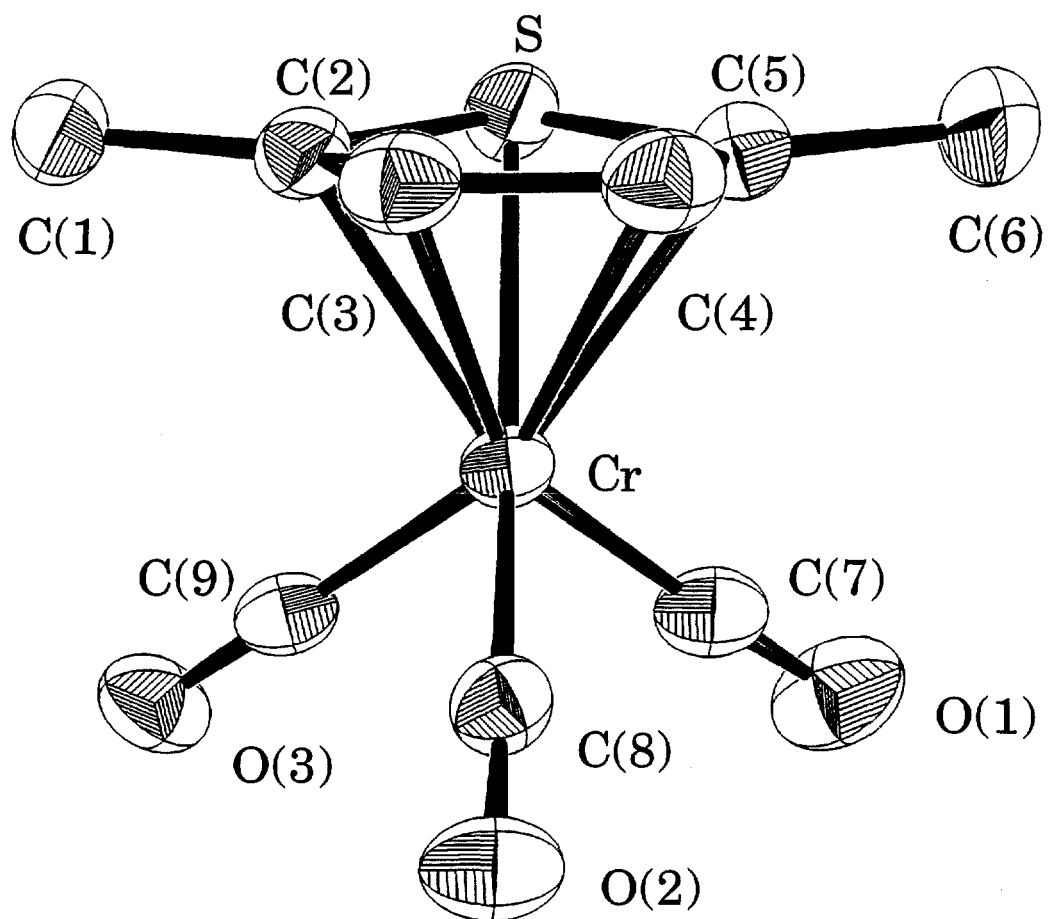


Figure 1. ORTEP drawing of $\text{Cr}(\text{CO})_3(\eta^5\text{-2,5-Me}_2\text{T})$ (**5**).

Table V. Bond Distances (Å)^a and Selected Angles (deg)^a for Cr(CO)₃(η⁵-2,5-Me₂T) (5)

Atoms	Distance	Atoms	Distance
Cr-S	2.3757(6)	S-C(5)	1.758(2)
Cr-C(2)	2.210(2)	C(1)-C(2)	1.496(3)
Cr-C(3)	2.206(2)	C(2)-C(3)	1.383(3)
Cr-C(4)	2.213(2)	C(3)-C(4)	1.422(3)
Cr-C(5)	2.213(2)	C(4)-C(5)	1.385(3)
Cr-C(7)	1.837(2)	C(5)-C(6)	1.499(3)
Cr-C(8)	1.837(2)	C(7)-O(1)	1.152(2)
Cr-C(9)	1.832(2)	C(8)-O(2)	1.144(3)
S-C(2)	1.754(2)	C(9)-O(3)	1.157(2)

Atoms	Angle	Atoms	Angle
C(7)-Cr-C(8)	90.15(8)	C(1)-C(2)-C(3)	128.7(2)
C(7)-Cr-C(9)	92.11(9)	C(2)-C(3)-C(4)	113.4(2)
C(8)-Cr-C(9)	86.35(8)	C(3)-C(4)-C(5)	113.5(2)
Cr-C(7)-O(1)	177.5(2)	C(4)-C(5)-C(6)	129.1(2)
Cr-C(8)-O(2)	178.2(2)	C(4)-C(5)-S	110.3(1)
Cr-C(9)-O(3)	177.0(1)	C(6)-C(5)-S	120.2(2)
S-C(2)-C(1)	120.3(1)	C(2)-S-C(5)	91.9(1)
S-C(2)-C(3)	110.6(1)		

^a Numbers in parentheses are estimated standard deviations in the least significant digits.

Table VI. Positional Parameters for $\text{Cr}(\text{CO})_3(\eta^5\text{-2,5-Me}_2\text{T})$ (5)

Atom	x	y	z	$B, a \text{ \AA}^2$
Cr	0.50427(4)	0.19908(2)	0.32686(2)	2.253(6)
S	0.85713(7)	0.18768(3)	0.41913(4)	2.833(9)
C(1)	0.7918(3)	-0.0221(2)	0.3275(2)	3.39(4)
C(2)	0.7652(3)	0.0974(1)	0.3098(1)	2.68(3)
C(3)	0.6927(3)	0.1532(2)	0.2120(1)	2.92(4)
C(4)	0.7010(3)	0.2676(2)	0.2252(2)	3.06(4)
C(5)	0.7783(3)	0.3005(1)	0.3334(2)	2.96(4)
C(6)	0.8206(3)	0.4129(2)	0.3787(2)	3.96(5)
C(7)	0.4014(3)	0.2996(2)	0.4075(2)	3.05(4)
C(8)	0.2684(3)	0.2078(1)	0.2159(2)	2.69(3)
C(9)	0.3797(3)	0.0873(2)	0.3816(2)	2.86(4)
O(1)	0.3411(2)	0.3655(1)	0.4569(1)	4.58(3)
O(2)	0.1196(2)	0.2108(1)	0.1480(1)	3.91(3)
O(3)	0.2957(2)	0.0159(1)	0.4116(1)	3.94(3)

^a Anisotropically refined atoms are given in the form of the isotropic equivalent displacement parameter defined as: $(4/3)[a^2B(1,1) + b^2B(2,2) + c^2B(3,3) + ab(\cos \gamma)B(1,2) + ac(\cos \beta)B(1,3) + bc(\cos \alpha)B(2,3)]$.

Extended Hückel Molecular Orbital (EHMO) Calculations. The molecular structures of the Th and Seln ligands and selected $\text{Cr}(\text{CO})_3(\eta^5\text{-Th})$ complexes were calculated using the extended Hückel method.²⁴ The orbital exponents were obtained from standard tables²⁵ and the orbital energies for the atoms were evaluated from atomic spectral tables.²⁶ It should be noted that valence 3d orbitals were not included for the sulfur atom. The bond distances and angles

for the free thiophene and selenophene ligands were taken from the structures of free T²⁷ and Sel.²⁸ The bond distances and angles for the Cr(CO)₃(η^5 -Th) complexes were taken from the molecular structure (Table V) of Cr(CO)₃(η^5 -2,5-Me₂T) (*vide infra*).

Bandshape Analysis. Rate constants for the Th and Sel ring rotations were calculated using the DNMR5²⁹ subroutine (QCPE³⁰ No. 365) of NMRI³¹ which uses an iterative nonlinear least-squares regression analysis to obtain the best fit of the experimental spectra. The reliability of the program was determined by calculating the activation parameters of neat N,N-dimethylformamide, which was distilled over CaH₂ before use. The resulting activation parameters ($\Delta H^\ddagger = 22.3(4)$ kcal/mol and $\Delta S^\ddagger = 6.6(11)$ cal/mol K) are in good agreement with the reported values of 23.8(2) kcal/mol for ΔH^\ddagger and 6.6(4) cal/mol K for ΔS^\ddagger .³² The ¹³C NMR spectra of the carbonyl ligands were analyzed as $A_3 \rightleftharpoons B_2C$ for the metal complexes with symmetric Th and Sel ligands (T, 2,5-Me₂T, Me₄T, Sel, and 2,5-Me₂Sel) and as $A_3 \rightleftharpoons BCD$ for the metal complexes with asymmetric Th and Sel ligands (2-MeT, 2-EtT, 3-MeT, and 2-MeSel). The linewidths were measured at several slow exchange temperatures and are independent of temperature. The bandshape calculations were performed on extracted spectra from δ 232 to 240 ppm. The chemical shifts, rate constant (k), baseline increment, and baseline tilt were optimized in the iterative calculations.

Activation parameters were obtained from the slope and intercept of Eyring plots (eq 1)³³ of $\ln(hk/kk_bT)$ versus $1/T$, where h is Planck's constant,

$$\ln \left(\frac{hk}{\kappa k_b T} \right) = - \frac{\Delta G^\ddagger}{RT} = - \frac{\Delta H^\ddagger}{RT} + \frac{\Delta S^\ddagger}{R} \quad (1)$$

(κ) of 1 was used in these calculations. The errors reported for ΔH^\ddagger and ΔS^\ddagger are the estimated standard deviations from the linear least-squares analysis of the Eyring plots. An Eyring plot of the rate constants for $\text{Cr}(\text{CO})_3(\eta^5\text{-2,5-Me}_2\text{T})$ is given in Figure 2.

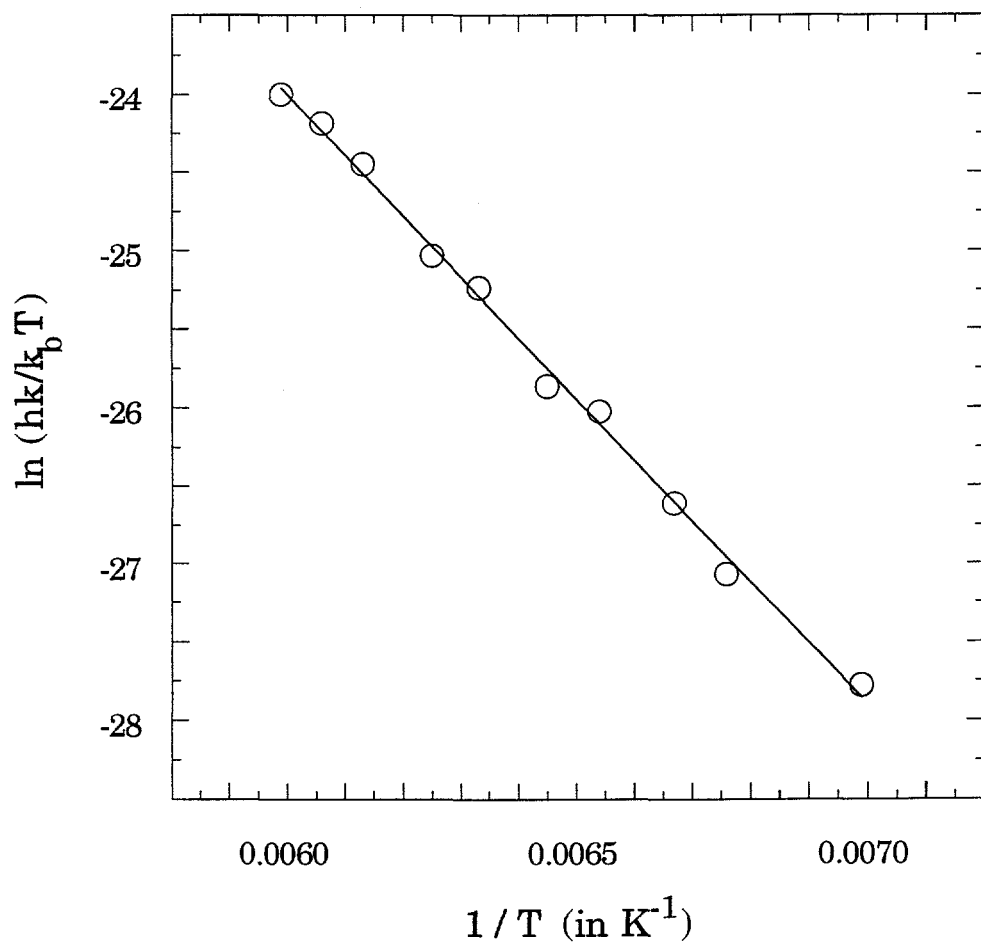
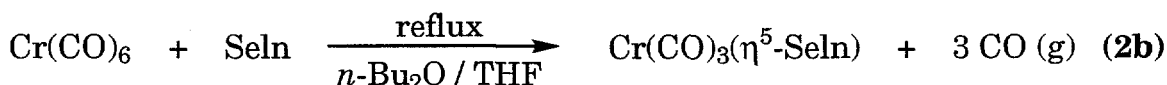
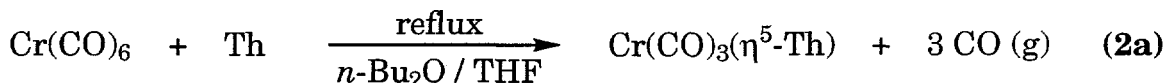


Figure 2. Eyring plot for $\text{Cr}(\text{CO})_3(\eta^5\text{-2,5-Me}_2\text{T})$ (5).

Results and Discussion

Synthesis and Characterization of the $\text{Cr}(\text{CO})_3(\eta^5\text{-Th})$ and $\text{Cr}(\text{CO})_3(\eta^5\text{-Seln})$ Complexes.

Chromium tricarbonyl thiophene and selenophene complexes, $\text{Cr}(\text{CO})_3(\eta^5\text{-Th})$ and $\text{Cr}(\text{CO})_3(\eta^5\text{-Seln})$, have been prepared by a variety of methods.^{20,34} The synthetic route used in this study (eq 2) is a modification of



one used for the preparation of chromium tricarbonyl arene complexes.³⁵ This method is useful for the synthesis of the chromium tricarbonyl complexes of thiophene, selenophene, and their alkyl-substituted derivatives. The advantage of this method is that the complexes can be made in one step without the need to isolate air-sensitive intermediates such as $\text{Cr}(\text{CO})_3(\text{NCMe})_3$ or $\text{Cr}(\text{CO})_3(\text{NC}_5\text{H}_5)_3$.^{34b,d} However, the yields for these complexes are only moderate to poor (58% for Seln = 2,5-Me₂Sel and 18% for Th = 3-MeT); attempts to increase the yield by additional heating resulted in substantial decomposition due to the thermal instability of these complexes. The $\text{Cr}(\text{CO})_3(\eta^5\text{-Th})$ and $\text{Cr}(\text{CO})_3(\eta^5\text{-Seln})$ complexes exhibit moderate thermal and air sensitivity, especially in solution and should be handled under nitrogen; however, they are stable for prolonged periods of time (greater than two years) in the solid state when stored under nitrogen at reduced temperatures (-20°C). All of the $\text{Cr}(\text{CO})_3(\eta^5\text{-Th})$ complexes were previously reported²⁰ and were positively identified in this study by their ¹H NMR spectra in CDCl₃. The ¹H NMR assignments for the $\text{Cr}(\text{CO})_3(\eta^5\text{-Seln})$ complexes^{5b} were made by comparison to the analogous $\text{Cr}(\text{CO})_3(\eta^5\text{-Th})$ complexes.

Th) complexes and were aided by the fact that the 2- and 5-hydrogen (α protons) peaks in the Seln complexes show ^{77}Se satellites but the 3- and 4-hydrogen (β protons) peaks do not.

The ^1H NMR spectra for the $\text{Cr}(\text{CO})_3(\eta^5\text{-Th})$ and $\text{Cr}(\text{CO})_3(\eta^5\text{-Seln})$ complexes are given in Table I and show a dramatic upfield shift of the aromatic protons upon metal complexation (1.2-2.1 ppm). It has been suggested previously³⁶ for $\text{Cr}(\text{CO})_3(\eta^6\text{-arene})$ complexes that this upfield shift is based on a reduction of π -electron density and ring current in the aromatic ring or on a magnetic anisotropy effect of the electric field arising from the metal-ring dipole. Dipole moments measured for $\text{Cr}(\text{CO})_3(\eta^5\text{-Th})$ complexes are larger than those of the $\text{Cr}(\text{CO})_3(\eta^6\text{-arene})$ complexes;³⁷ this has been attributed to the large dipole moment of the Cr-S bond. In the case of $[\text{Mn}(\text{CO})_3(\eta^5\text{-2,5-Me}_2\text{Sel})]\text{OTf}$ and other cationic metal-arene complexes, the positive charge on the metal increases the downfield shift and this results in a smaller total upfield shift of the aromatic protons upon metal complexation;^{16,38} in dicationic metal-arene complexes, the downfield shift caused by the positive charge is large enough to overcome the upfield shift and these complexes show proton shifts downfield from the free ligands.³⁹

The upfield shift of the aromatic protons in the $\text{Cr}(\text{CO})_3(\eta^5\text{-Th})$ and $\text{Cr}(\text{CO})_3(\eta^5\text{-Seln})$ complexes shows several trends with respect to alkyl and heteroatom substitution. It has been noted previously²⁰ for $\text{Cr}(\text{CO})_3(\eta^5\text{-Th})$ complexes that within the same complex, aromatic protons in the α positions are shifted upfield to a larger degree than protons in the β positions. The α protons in these complexes are shifted from 1.7 to 2.1 ppm upfield from the free ligands, whereas the upfield shift of the β protons ranges from 1.2 to 1.6 ppm. Jackson,

et al.,⁴⁰ have suggested that aromatic protons that are eclipsed with CO ligands are deshielded relative to those that are not. Octahedral coordination in $\text{Cr}(\text{CO})_3(\eta^5\text{-Th})$ or $\text{Cr}(\text{CO})_3(\eta^5\text{-Sel})$ results in a structure (Chart I) in which the α protons are eclipsed to the metal carbonyls; consequently, the α protons should be deshielded to a larger extent than the β protons. However, this is inconsistent with the experimental evidence.

The addition of alkyl groups to the thiophene ring reduces the upfield shift of the aromatic protons upon complexation. This is evidenced by the decreasing shift of the H(4) proton relative to the free ligands in $\text{Cr}(\text{CO})_3(\eta^5\text{-Th})$ for Th = T (1.51 ppm), 2-MeT (1.35 ppm), and 2,5-Me₂T (1.24 ppm). Similar trends for the proton shifts are seen in the methyl-substituted selenophene complexes. Substitution of the S heteroatom by Se does not greatly affect the β proton upfield shifts, as noted in the H(4) shifts upon complexation in the T and Sel (1.55 ppm) complexes. The upfield shifts in the α protons, however, are somewhat affected by heteroatom substitution. Substitution of S with Se leads to a 0.12 ppm increase in the upfield shift, as seen for the H(2) protons in the T (1.94 ppm) and Sel (2.06 ppm) complexes.

Upon metal complexation, the proton-proton coupling constants (${}^3J_{HH}$ and ${}^4J_{HH}$) show a marked decrease from values found for the free ligands (Table I). This decrease is dependent upon the position of the protons in question: the decrease in J values is larger for α than for β protons. This is demonstrated by the fact that $J_{2,5}$, the coupling constant between two α protons, for Th = 3-MeT decreases to 1.6 Hz, a value that is 53% of that seen for the free ligand (3.0 Hz); however, the values for $J_{3,4}$, the coupling constant between the two β protons, decreases to only 80-85% of the value seen for the free ligands (Th, Sel = 2-MeT,

2-EtT, and 2-MeSel). $J_{4,5}$, which represents the coupling of an α and β proton, shows a decrease from the value in the free ligand of 65-70% (Th, Seln = 2-MeT, 2-EtT, 3-MeT, and 2-MeSel) which is intermediate between the two values listed above. It has been previously suggested³⁶ for chromium tricarbonyl arene complexes that this decrease in proton-proton coupling constants can be related to a slight decrease in the electron density at the aromatic protons which results in smaller proton-proton coupling constants. The larger decrease in J values for the α protons suggests that the α carbons in the thiophene and selenophene rings interact more strongly with the metal atom than the β carbons. This is consistent with the fact that the α protons are shifted upfield to a larger extent than the β protons in these complexes.

Upon coordination to the metal, the methyl protons on the thiophene and selenophene rings show rather small shifts (0.02 to 0.22 ppm). It is interesting to note that methyl groups in the α positions are shifted upfield whereas methyl groups in the β positions are shifted downfield.

The $^{13}\text{C}\{^1\text{H}\}$ peaks for the $\text{Cr}(\text{CO})_3(\eta^5\text{-Th})$ and $\text{Cr}(\text{CO})_3(\eta^5\text{-Sel})$ complexes are given in Table II and have not been previously reported. The ^{13}C peak assignments for the $\text{Cr}(\text{CO})_3(\eta^5\text{-Th})$ (Th = T, 2-MeT, 2-EtT, and 3-MeT) and the $\text{Cr}(\text{CO})_3(\eta^5\text{-Sel})$ (Sel = Sel and 2-MeSel) complexes were made using HETCOR experiments. Since a HETCOR spectrum correlates peaks of the ^1H NMR spectrum to the peaks in the ^{13}C spectrum, these studies allow the assignment of all ^{13}C NMR peaks to specific carbon atoms in the complexes. As in the ^1H NMR studies, the ^{13}C NMR spectra of the $\text{Cr}(\text{CO})_3(\eta^5\text{-Th})$ and $\text{Cr}(\text{CO})_3(\eta^5\text{-Sel})$ complexes show a dramatic upfield shift of the aromatic carbons upon metal complexation (24-39 ppm). Similar upfield shifts in chromium tricarbonyl

arene complexes have been rationalized in terms of a change in the mobile bond order of the C-C bonds,⁴¹ a change in the hybridization of the carbon atoms from sp^2 to sp^3 upon metal coordination,⁴² or the presence of a net negative charge on the carbon atoms.⁴³ Calculations for $Cr(CO)_3(\eta^6-C_6H_6)$ using self-consistent charge and configuration molecular orbital theory (SCCCMO) and the Pople-Karplus equation correctly predicted an upfield shift of the aromatic carbons and a downfield shift of the carbonyl ligands with respect to free CO upon metal complexation.⁴⁴

For a given Th or Seln ligand, the α carbons are shifted upfield to a larger extent than the β carbons upon complexation. This can be seen in the upfield shifts of the α carbons (39.26 ppm) versus the β carbons (35.63 ppm) in $Cr(CO)_3(\eta^5-T)$. Addition of methyl groups to the thiophene ring results in a smaller upfield shift of the aromatic carbons, as evidenced by the smaller shifts of C(4) in $Cr(CO)_3(\eta^5-Th)$ for Th = T, 2-MeT (34.70 ppm), and 2,5-Me₂T (32.61 ppm). It is interesting to note that the upfield shift of an aromatic carbon is smaller when its hydrogen is replaced by a methyl group. Consequently, the upfield shift for 2-MeT in $Cr(CO)_3(\eta^5-2-MeT)$ is larger for the C(5) atom (38.26 ppm) than it is for C(2) (33.02 ppm). Similar trends are seen in the methyl-substituted selenophene complexes. Substitution of the heteroatom from S to Se leads to a larger upfield shift on the β carbons and a smaller upfield shift in the α carbons. This trend is demonstrated by comparison of the upfield shifts of C(4) (36.66 ppm) and C(5) (37.41 ppm) in $Cr(CO)_3(\eta^5-2-MeSel)$ with those values (34.70 and 38.26 ppm, respectively) in $Cr(CO)_3(\eta^5-2-MeT)$.

The ¹³C NMR chemical shift of the carbonyl peaks in $Cr(CO)_3(\eta^5-Th)$ and $Cr(CO)_3(\eta^5-Seln)$ demonstrate a definite trend with methyl and heteroatom sub-

stitution. The CO peak in these complexes shows a downfield shift upon addition of alkyl groups to the thiophene or selenophene rings. A similar trend was observed⁴⁵ in the substituted $\text{Cr}(\text{CO})_3(\eta^6\text{-C}_6\text{H}_{6-x}\text{R}_x)$ complexes in which the CO resonance is shifted upfield with respect to the benzene complex when electron-withdrawing and π -acceptor groups such as Cl, F, CO_2Me , or CF_3 are bound to the ring; similarly, the carbonyl resonances are shifted downfield with respect to $\text{Cr}(\text{CO})_3(\eta^6\text{-C}_6\text{H}_6)$ with the addition of electron-donating and π -donor groups such as Me, OMe, or NMe_2 . A comparison of Th and Seln complexes shows that substitution of the S heteroatom by Se results in a 0.2 ppm downfield shift of the CO resonance. This downfield shift suggests that the selenophenes donate more electron density to the metal than the analogous thiophenes. This is consistent with the larger upfield shift of the α protons in selenophene versus the thiophene complexes.

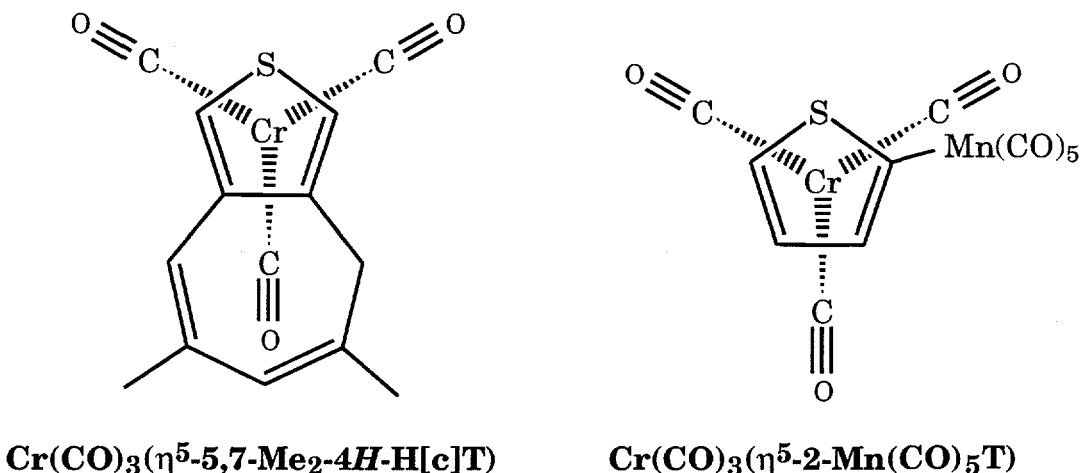
The aromatic carbons of the $[\text{Mn}(\text{CO})_3(\eta^5\text{-2,5-Me}_2\text{Sel})]\text{OTf}$ complex are shifted upfield from the free ligand, but these shifts are still downfield with respect to $\text{Cr}(\text{CO})_3(\eta^5\text{-2,5-Me}_2\text{Sel})$. The β carbons show an upfield shift of 27 ppm; the α carbons, which have a methyl group attached instead of a hydrogen, are only shifted upfield by about 15 ppm. Similar upfield shifts in the $^{13}\text{C}^{(1\text{H})}$ NMR spectrum were seen in the methyl-substituted derivatives of $[\text{Mn}(\text{CO})_3(\eta^6\text{-C}_6\text{H}_6)]\text{I}_3$.^{38a}

The infrared spectra of the η^5 -thiophene and -selenophene complexes were measured in CH_2Cl_2 and are given in Table III. Each spectrum contains three bands in the metal-carbonyl region, which is indicative of slow metal-ring rotation on the IR timescale. The peak at highest energy is very sharp and intense; the other two peaks are strong, but broadened with respect to the first peak, and

are close in energy. In concentrated or impure samples, it is not uncommon for the two lower energy peaks to appear as one, very broad peak. The IR bands in the $\text{Cr}(\text{CO})_3(\eta^5\text{-Th})$ and $\text{Cr}(\text{CO})_3(\eta^5\text{-Sel})$ complexes shift to lower energy with increasing alkyl substitution. This is consistent with a previous IR study^{34d} of $\text{Cr}(\text{CO})_3(\eta^5\text{-Th})$ complexes in which a correlation was observed between the decreasing carbonyl frequencies and the electron-donating power of the substituents, as measured by the Hammett parameter σ_p . Comparison of $\text{Cr}(\text{CO})_3(\eta^5\text{-Th})$ and $\text{Cr}(\text{CO})_3(\eta^5\text{-Sel})$ shows that their ν_{CO} values are very similar, which suggests that thiophene and selenophene donate comparable electron density to the metal. As noted above, trends in the ^{13}CO chemical shifts suggest that a Sel ligand donates slightly more electron density to the metal than the analogous Th ligand. A correlation was observed in this study between the ^{13}C NMR chemical shift of the CO ligands (δ_{CO}) and the ν_{CO} band at highest energy for the $\text{Cr}(\text{CO})_3(\eta^5\text{-Th})$ and $\text{Cr}(\text{CO})_3(\eta^5\text{-Sel})$ complexes ($\nu_{\text{CO}} = 4079 - 9.068 \delta_{\text{CO}}$, $R = 0.974$). A similar correlation was noted for the δ_{CO} and ν_{CO} values in the series of $\text{Cr}(\text{CO})_3(\eta^6\text{-C}_6\text{H}_5\text{X})$ complexes ($R = 0.964$ and 0.976 for the two ν_{CO} bands).^{45a} The ν_{CO} bands of $[\text{Mn}(\text{CO})_3(\eta^5\text{-2,5-Me}_2\text{Sel})]\text{OTf}$ are shifted to higher energy by $110\text{-}140 \text{ cm}^{-1}$ from the neutral $\text{Cr}(\text{CO})_3(\eta^5\text{-2,5-Me}_2\text{Sel})$. This is consistent with the cationic manganese complex having less electron density at the metal for back-donation to the CO ligands than the chromium complex.

Structure of $\text{Cr}(\text{CO})_3(\eta^5\text{-2,5-Me}_2\text{T})$ (5). The structure (Figure 1) of $\text{Cr}(\text{CO})_3(\eta^5\text{-2,5-Me}_2\text{T})$ (5) indicates that the thiophene ring binds to the chromium tricarbonyl fragment with the sulfur atom *trans* to one of the CO ligands. This conformation is the same as those found in $\text{Cr}(\text{CO})_3(\eta^5\text{-T})$ ^{10a} (a structure that is

complicated by a three-fold disorder of the thiophene ring), in the 5,7-dimethyl-4*H*-cyclohepta[c]thiophene (5,7-Me₂-4*H*-H[c]T) complex Cr(CO)₃(η^5 -5,7-Me₂-4*H*-H[c]T),^{10b} and in the 2-thienyl manganese pentacarbonyl (2-Mn(CO)₅T) complex Cr(CO)₃(η^5 -2-Mn(CO)₅T).^{10e} Thus, the three coordination sites of the ligand



(the two double bonds and the sulfur) and the three carbonyls occupy approximately octahedral coordination sites around the d⁶ Cr(0) metal atom in **5**. The crystal structure of the *endo* complex of chromium tricarbonyl *angular*-terphenylene,⁴⁶ an arene that exhibits a distinct localization of the double bonds in the central ring,⁴⁷ also contains an octahedrally-coordinated chromium(0) atom. The thiophene ligand in **5** is best described as a planar diene unit (± 0.002 Å) with the sulfur atom slightly (0.0959(5) Å) above that plane. The dihedral angle defined by the diene plane and the plane containing S, C(2), and C(5) is 4.5(4)°. The distortion of the planar ligand upon complexation to the chromium atom is probably due more to the fact that the Cr-S bond length is longer than that of a Cr-C bond than to any loss of thiophene aromaticity. The Cr-S bond length of 2.3757(6) Å in **5** is comparable to Cr-S distances of 2.355(2) Å in Cr(CO)₂(η^1 (S)-

1,3-dithiane)(η^6 -C₆H₆)⁴⁸ and 2.331(1) Å in Cr(CO)₅(η^1 (S)-2,5-dihydrothiophene-1-oxide).⁴⁹ Similarly, the average Cr-C(Th) bond length of 2.211(2) Å in **5** is comparable to the average Cr-C(C₆H₆) distance of 2.229(2) Å in Cr(CO)₃(η^6 -C₆H₆).⁵⁰ The C(2)-S and C(5)-S bond lengths of 1.754(2) and 1.758(2) Å in **5** are longer than that of 1.714(1) Å in free thiophene.²⁷ Similarly, the C(2)-C(3) (1.383(3) Å) and C(4)-C(5) (1.385(3) Å) distances are longer than the corresponding distance in free thiophene (1.370(2) Å); the C(3)-C(4) distances in **5** (1.422(3) Å) and free thiophene (1.424(2) Å) are the same within experimental error. Lengthening of the C-S and the C-C double bonds in thiophene upon metal coordination is consistent with either electron donation from the π -orbitals of the ring to the metal or an increased population of the π^* antibonding orbitals on the thiophene ligand due to back-bonding interactions with the metal atom.⁵¹ The idea that the chromium tricarbonyl fragment is capable of π^* back-donation to arene rings is supported by the molecular structures of Cr(CO)₃(η^6 -C₆Et₆), [Cr(CO)₂(NO)(η^6 -C₆Et₆)]BF₄, and [Cr(CO)(CS)(NO)(η^6 -C₆Et₆)]BF₄ in which the substitution of CO by NO⁺ and CS results in increased arene centroid-chromium distances (1.725, 1.795, and 1.803 Å, respectively).^{13f} This bond lengthening implies that the chromium-arene interaction has a substantial π^* metal-to-ligand back-bonding contribution that is weakened by strong π -accepting ligands. Similarly, SCF MS-X α calculations of the CpFe(η^6 -C₆H₆)⁺ cation (where Cp = η^5 -C₅H₅) suggested that the filled 3d orbitals on the iron atom interact to a much larger extent with the empty π^* orbitals on benzene than those on the cyclopentadienyl ligand.⁵²

Comparison of **5** with [(η^4 -COD)Rh(η^5 -2,5-Me₂T)]BF₄⁵³ (where COD is 1,5-cyclooctadiene) allows us to comment on relative distortions of the 2,5-Me₂T

ligand upon complexation to chromium and rhodium. In contrast to **5**, the C(2)-C(3) and C(4)-C(5) bonds that are formally double bonds in the free ligand are now longer than the formal C-C single bond (C(3)-C(4)) in the Rh complex (1.400(8) and 1.377(8) Å, respectively). The C-S bond lengths of 1.764(6) and 1.743(6) Å in the Rh complex are the same within experimental error to the C-S bond lengths in **5**. From this comparison, it is obvious that the 2,5-Me₂T ligand is distorted from the structure of free thiophene to a greater extent in the Rh complex than in **5**.

EHMO Calculations. The total energies of the Cr(CO)₃(η^5 -Th) complexes where Th = T, 2-MeT, 3-MeT, 2,5-Me₂T, and Me₄T were calculated using the extended Hückel method, assuming perfect three-fold symmetry of the Cr(CO)₃ fragment using the Cr-C and C-O distances (Table V) from **5**. In order to estimate the energy barrier for thiophene ring rotation, the total energy of Cr(CO)₃(η^5 -T) was optimized with respect to the orientation of the thiophene ring relative to the Cr(CO)₃ fragment. The conformation of lowest energy occurs when the S atom is *trans* to a carbonyl ligand and is consistent with the molecular structure of **5**; the highest energy conformer contains a chromium atom in an approximately trigonal prismatic coordination site (S eclipsed with a CO ligand). The energy difference between these two conformers is 0.174 eV (4.01 kcal/mol) which is similar to the experimental value of ΔH^\ddagger (6.2 kcal/mol). Similar calculations performed for Cr(CO)₃(η^5 -2-MeT) and Cr(CO)₃(η^5 -3-MeT) predict a low energy conformer with octahedral coordination that is 0.225 eV (5.18 kcal/mol) and 0.227 eV (5.24 kcal/mol), respectively, more stable than the trigonal prismatic conformer. The Cr(CO)₃(η^5 -2,5-Me₂T) and Cr(CO)₃(η^5 -Me₄T) complexes

are also calculated to have an octahedral low-energy conformer; however, the calculated rotational barrier for both of these complexes is 0.224 eV (5.16 kcal/mol), which is the same as that for the 2-MeT and 3-MeT complexes. The fact that the EHMO results show no difference in the rotational barriers for the 2-MeT, 3-MeT, 2,5-Me₂T, and Me₄T complexes indicates that these calculations are not useful in explaining trends in the activation parameters for thiophene ring rotation in these complexes.

EHMO calculations of the free Th and Seln ligands, however, appear to be more useful. The bond distances and angles for the heteroatom skeleton of the free Th and Seln ligands were taken from the microwave structures of T²⁷ and Sel.²⁸ The C-C and C-H bond lengths for the alkyl substituents were taken from a table of distances determined by X-ray and neutron diffraction studies of organic compounds.⁵⁴ Table VII contains the orbital populations for the p_z (π) orbitals of the heterocyclic rings as well as the total π -electron density in the ring (E + Σ C) and the difference in the electron populations of the heteroatom and the diene (E - Σ C). The total π -electron densities on T (6.000 e⁻) and Sel (6.001 e⁻) demonstrate that the protons do not donate any electron density to the metal. Addition of alkyl groups to the T and Sel ligands, however, increases the electron density in the ring. These calculations suggest that a methyl group donates comparable electron density to the ring in either the 2- or 3-position (0.017 and 0.014 e⁻, respectively). This is consistent with IR studies (Table III and reference 34d) of the Cr(CO)₃(η^5 -Th) complexes which demonstrate that the energy of the vCO bands is essentially unaffected by the position of the substituents (α versus β) on the Th ring. The calculations also suggest that an ethyl group donates more electron density to the ring than a methyl group, which is also supported by the

Table VII. Orbital Populations (e⁻) for the π Orbitals in the Th and Seln Ligands

Ligand	C(2)	C(3)	C(4)	C(5)	E	ΣC^a	$E + \Sigma C^b$	$E - \Sigma C^c$
T	1.059	1.127	1.127	1.059	1.628	4.372	6.000	-2.744
2-MeT	0.996	1.170	1.126	1.081	1.644	4.373	6.017	-2.729
2-EtT	0.987	1.180	1.126	1.086	1.648	4.379	6.027	-2.731
3-MeT	1.105	1.071	1.143	1.058	1.637	4.377	6.014	-2.740
2,5-Me ₂ T	1.017	1.171	1.171	1.017	1.659	4.376	6.035	-2.717
Me ₄ T	1.062	1.129	1.129	1.062	1.675	4.382	6.057	-2.707
Sel	1.022	1.101	1.101	1.022	1.755	4.246	6.001	-2.491
2-MeSel	0.957	1.150	1.099	1.050	1.765	4.256	6.021	-2.491
2,5-Me ₂ Sel	0.983	1.149	1.149	0.983	1.774	4.264	6.038	-2.490

^a Total orbital population for the four aromatic carbons.

^b Total orbital population for the aromatic ring.

^c Difference in orbital populations of the heteroatom (E) and the four carbons.

vCO data (Table III). The orbital populations of the carbon atoms show two distinct trends: β carbons tend to have more π -electron density than α carbons (1.127 and 1.059 e⁻, respectively, in T) and replacement of a hydrogen with a methyl group results in a lower electron density at that carbon, as evidenced by the populations at C(2) (0.996 e⁻) and C(5) (1.081 e⁻) in 2-MeT. The orbital population of the heteroatom also increases with increasing alkyl substitution. Comparison of the electron densities at S in 2-MeT (1.644 e⁻) and 3-MeT (1.637 e⁻) supports the conclusions made previously⁵⁵ that methyl substitution at the 2-position donates more electron density to the sulfur than a methyl in the

3-position and is consistent with the fact that dissociative substitution of Th by PPh_3 in $\text{CpRe}(\text{CO})_2(\eta^1(\text{S})\text{-Th})^{55}$ and $[\text{CpRu}(\text{CO})_2(\eta^1(\text{S})\text{-Th})]\text{BF}_4^{56}$ occurs at a slower rate for Th = 2-MeT than for Th = 3-MeT.

Activation Parameters for the Restricted Th and Seln Rotation. The ^{13}C NMR spectra of the ^{13}CO -labelled $\text{Cr}(\text{CO})_3(\eta^5\text{-Th})$ and $\text{Cr}(\text{CO})_3(\eta^5\text{-Seln})$ complexes were measured using dimethyl ether (mp = -141°C , bp = -25°C) as the solvent, internal proton lock, and internal reference. The spectra were measured in 2 to 5 K increments from just above the melting point of the solvent (132 K) to the point where the CO signal appeared as a sharp singlet (typically, 10 to 20 K above the coalescence temperature). At low temperatures, the carbonyl spectra of $\text{Cr}(\text{CO})_3(\eta^5\text{-Th})$ and $\text{Cr}(\text{CO})_3(\eta^5\text{-Seln})$ appear as two singlets of relative intensity 2:1 for the symmetric heterocycles (Th = T, 2,5-Me₂T, Me₄T; Seln = Sel, 2,5-Me₂Sel) and as three singlets of equal relative intensity for the asymmetric heterocycles (Th = 2-MeT, 2-EtT, 3-MeT; Seln = 2-MeSel). The experimental and theoretical bandshapes for the $\text{Cr}(\text{CO})_3(\eta^5\text{-2-MeT})$ and $\text{Cr}(\text{CO})_3(\eta^5\text{-2,5-Me}_2\text{T})$ complexes are given in Figures 3 and 4, respectively. The enthalpy of activation (ΔH^\ddagger), the entropy of activation (ΔS^\ddagger), the coalescence temperature (T_c), and the free energy of activation at coalescence (ΔG_c^\ddagger) determined from Eyring plots are given in Table VIII. Values of ΔG_c^\ddagger at T_c for the coalescence of an unequally populated doublet measured by NMR can be calculated⁵⁷ from the expression in eq 3, where $\delta\nu$ is the NMR chemical shift difference of the two peaks at slow exchange in Hz, and X is a parameter which depends on the value of the population

$$\Delta G_c^\ddagger \text{ (eq 3)} = R T_c \ln \left(\frac{k_b T_c X}{h \pi \delta\nu (1 - \Delta P)} \right) \quad (3)$$

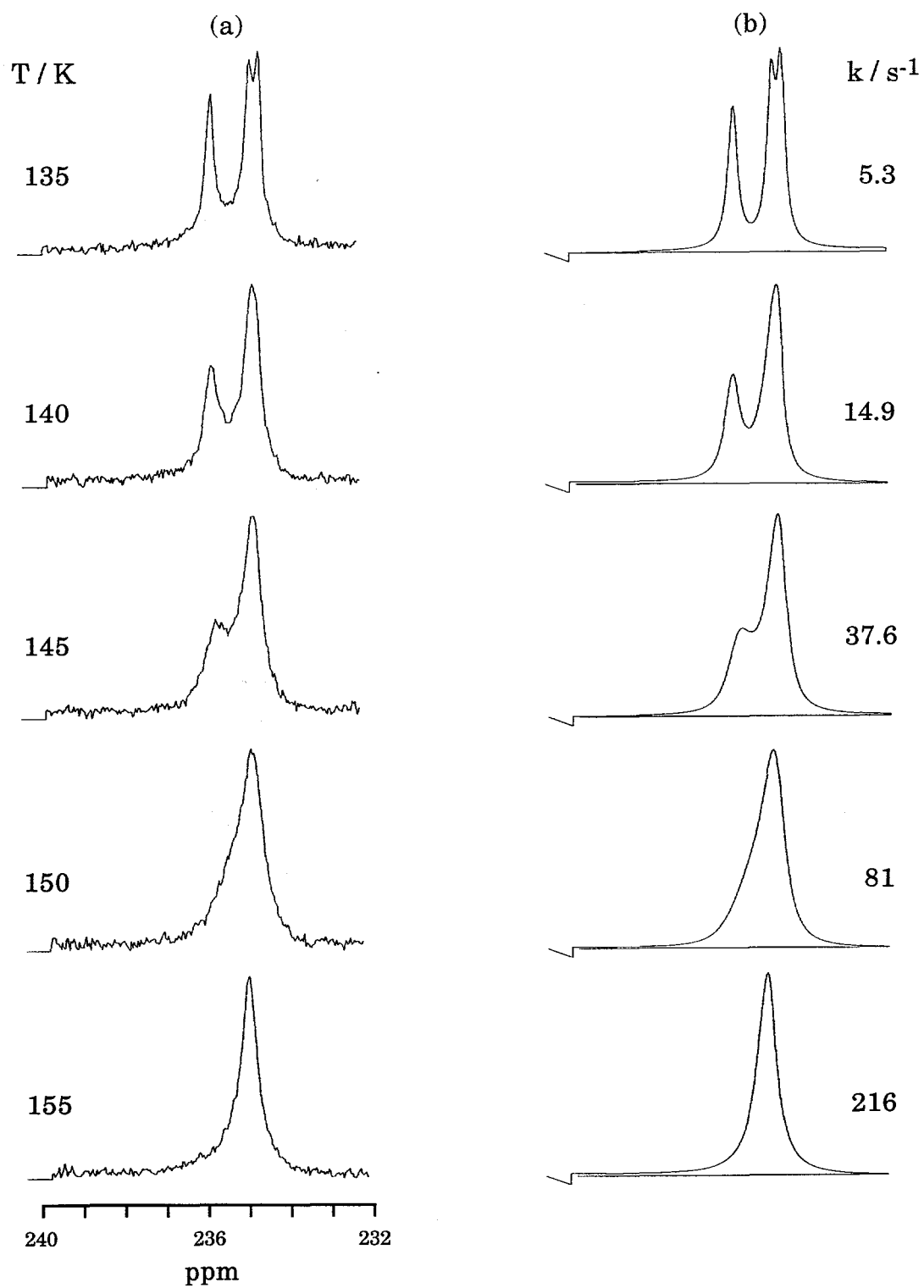


Figure 3. Variable-temperature ^{13}C NMR of $\text{Cr}(\text{CO})_3(\eta^5\text{-2-MeT})$ (**2**):
 (a) observed, (b) calculated

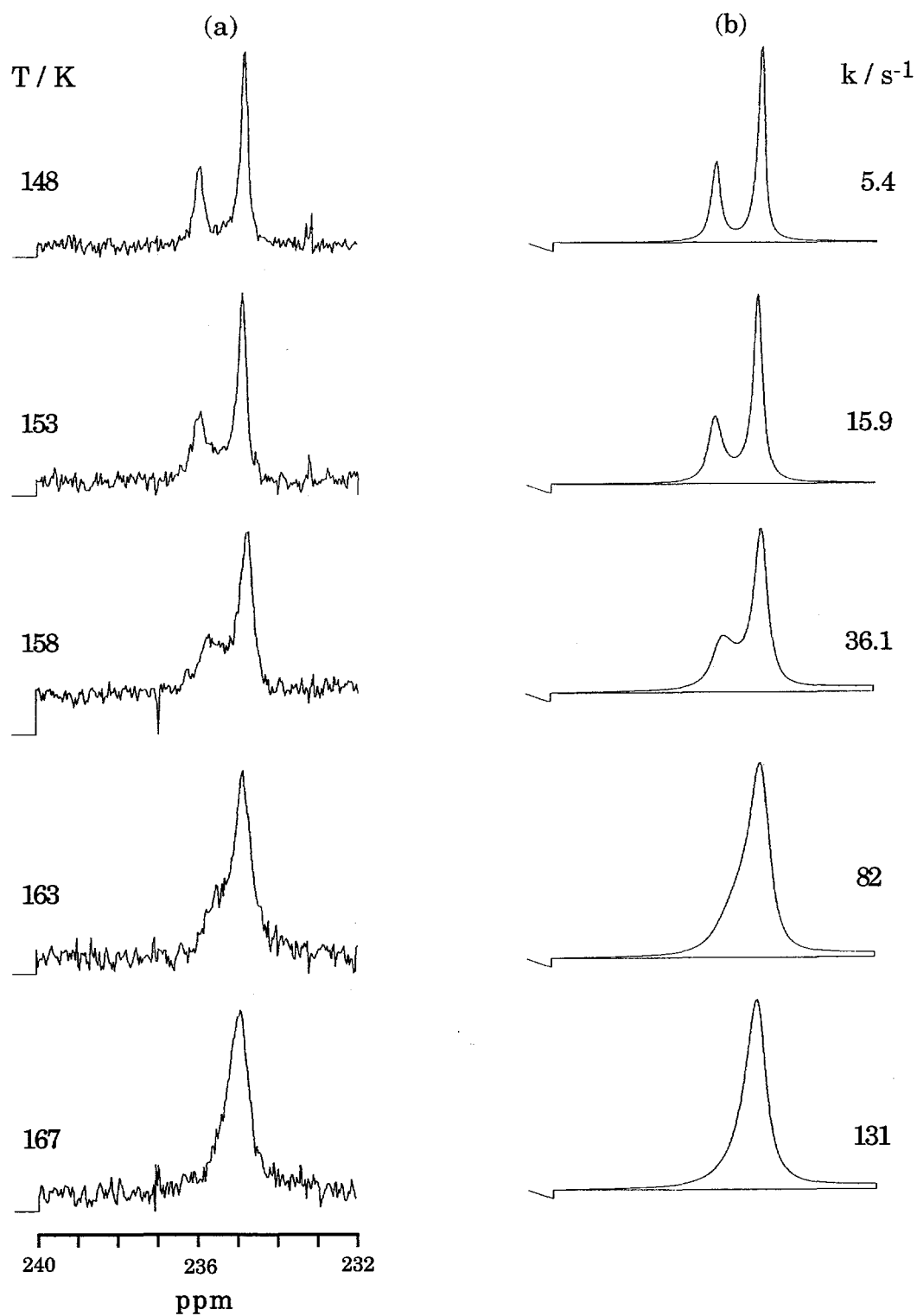


Figure 4. Variable-temperature ^{13}C NMR of $\text{Cr}(\text{CO})_3(\eta^5\text{-2,5-Me}_2\text{T})$ (**5**):
(a) observed, (b) calculated

Table VIII. Activation Parameters for Restricted Rotation in the $\text{Cr}(\text{CO})_3(\eta^5\text{-Th})$ and $\text{Cr}(\text{CO})_3(\eta^5\text{-Seln})$ Complexes

Ligand	ΔH^\ddagger , kcal/mol	ΔS^\ddagger , cal/mol K	T_c , K	ΔG_c^\ddagger , kcal/mol	ΔG_c^\ddagger (eq 3), ^a kcal/mol
T	6.2(2)	-1.6(12)	132	6.42(5)	6.40
2-MeT	7.1(3)	-1.1(19)	147	7.25(5)	—
2-EtT	6.9(3)	-1.4(19)	145	7.08(5)	—
3-MeT	6.5(3)	-1.2(23)	138	6.66(5)	—
2,5-Me ₂ T	7.7(2)	-1.3(10)	161	7.94(5)	7.90
Me ₄ T	7.4(4)	-1.7(30)	158	7.63(5)	7.67
Sel	7.8(2)	-1.5(14)	163	7.99(5)	7.92
2-MeSel	8.4(2)	-1.2(11)	178	8.64(5)	—
2,5-Me ₂ Sel	9.0(3)	-1.3(15)	185	9.20(5)	9.13

^a From eq 3 and reference 57.

difference ΔP . For the symmetric Th and Seln ligands, ΔP is 0.33 and the corresponding value of X is 2.0823. For the case of an equally populated doublet, ΔP is zero, X is equal to $\sqrt{2}$, and eq 3 reduces to the widely used equation to estimate ΔG_c^\ddagger .³³ Unfortunately, there is no simple equation to calculate ΔG_c^\ddagger for the asymmetric Th and Seln complexes that give a 1:1:1 set of singlets. Comparison of the measured ΔG_c^\ddagger values and the values calculated from eq 3, ΔG_c^\ddagger (eq 3), (Table VIII) reveals that the two ΔG_c^\ddagger values are the same within experimental error.

The ΔS^\ddagger values for these complexes are all very similar to each other (from -1.9 to -1.1 cal/mol K) and show no real trends with respect to heteroatom or alkyl substitution. Although the ΔS^\ddagger values are all slightly negative, which is

indicative of a more ordered transition state, almost all of them are equal to zero within experimental error. The errors reported for ΔH^\ddagger and ΔS^\ddagger are conservative estimates given by the linear least-squares fit to the Eyring equation (eq 1). Because the ΔS^\ddagger values in the $\text{Cr}(\text{CO})_3(\eta^5\text{-Th})$ and $\text{Cr}(\text{CO})_3(\eta^5\text{-Seln})$ complexes are similar to each other, both ΔH^\ddagger and ΔG_c^\ddagger follow the same trends.

The ΔH^\ddagger values for the $\text{Cr}(\text{CO})_3(\eta^5\text{-Th})$ complexes, where Th = T (6.2(2) kcal/mol), 2-MeT (7.1(3) kcal/mol), and 2,5-Me₂T (7.7(2) kcal/mol), demonstrate that the addition of a methyl group to the α -position of the thiophene ring increases ΔH^\ddagger by 0.6 to 0.9 kcal/mol. EHMO calculations presented in this work imply that the addition of methyl groups to the thiophene ring increases the π -electron density in the ring which, in turn, donates more electron density to the metal. This has been supported by the ¹³C NMR and IR results discussed above. The increased electron density shared by the metal and the ring results in the larger ΔH^\ddagger values upon methyl substitution. The calculations also suggest that the increased electron density appears mainly on the S atom, as evidenced by an increase of 0.031 e⁻ in the S π -electron density but only 0.004 e⁻ in the diene π -electron density in 2,5-Me₂T with respect to T. These results suggest that the ΔH^\ddagger values are primarily dependent on the π -electron density on the heteroatom. The $\text{Cr}(\text{CO})_3(\eta^5\text{-Seln})$ complexes show a similar trend in ΔH^\ddagger upon α -methyl substitution.

Although the EHMO calculations imply that 2-MeT and the isomeric 3-MeT ligands have comparable total π -electron densities, the ΔH^\ddagger values for the $\text{Cr}(\text{CO})_3(\eta^5\text{-2-MeT})$ complex is 0.6 kcal/mol higher than that of $\text{Cr}(\text{CO})_3(\eta^5\text{-3-MeT})$. These values imply that ΔH^\ddagger is dependent not only on the total π -electron density but also on the relative electron densities on the S and the diene frag-

ment in the ring. Comparison of the ΔH^\ddagger values for $\text{Cr}(\text{CO})_3(\eta^5\text{-T})$ and $\text{Cr}(\text{CO})_3(\eta^5\text{-2-MeT})$ demonstrates that increasing the π -electron density on the sulfur without changing the diene electron density leads to an increased activation barrier in these complexes. On the other hand, an increase in the electron density on the diene fragment, which presumably occurs to a greater extent in $\text{Cr}(\text{CO})_3(\eta^5\text{-3-MeT})$, would strengthen the metal-diene interaction and reduce the dominating influence of the Cr-S bond; this would be expected to give a smaller activation barrier, as is observed for $\text{Cr}(\text{CO})_3(\eta^5\text{-3-MeT})$ as compared with $\text{Cr}(\text{CO})_3(\eta^5\text{-2-MeT})$.

Substitution of the methyl group with an ethyl group results in comparable ΔH^\ddagger values for $\text{Cr}(\text{CO})_3(\eta^5\text{-2-MeT})$ (7.1(3) kcal/mol) and $\text{Cr}(\text{CO})_3(\eta^5\text{-2-EtT})$ (6.9(3) kcal/mol). EHMO calculations suggest that 2-EtT has a greater total π -electron density than 2-MeT; however, the difference in the orbital populations of the sulfur atom and the four carbons ($E - \Sigma C$) for 2-MeT and 2-EtT is very similar. In general, there is a very good linear correlation ($\Delta H^\ddagger = 156 + 54.6(E - \Sigma C)$, $R = 0.997$) between the ΔH^\ddagger values and the difference ($E - \Sigma C$) in the π -electron density on the sulfur and the diene fragment for the $\text{Cr}(\text{CO})_3(\eta^5\text{-Th})$ complexes, where Th = T, 2-MeT, 2-EtT, 3-MeT, and 2,5-Me₂T (all Th except Me₄T). The ΔH^\ddagger value of 7.4(4) kcal/mol for $\text{Cr}(\text{CO})_3(\eta^5\text{-Me}_4\text{T})$ is much lower than expected; in fact, the ΔH^\ddagger value for the Me₄T complex is lower than that for the 2,5-Me₂T complex. This suggests that the addition of two methyl groups to the ring lowers the activation barrier and is inconsistent with the trend seen in every other complex upon alkyl substitution in this study. In fact, extrapolation of the correlation between ΔH^\ddagger and ($E - \Sigma C$) mentioned previously for the Th complexes to

Me₄T results in a theoretical ΔH^\ddagger value of 8.3 kcal/mol for Cr(CO)₃(η^5 -Me₄T), a value that is 0.9 kcal/mol larger than experimentally measured.

A comparison of the activation barriers for Cr(CO)₃(η^5 -Th) and Cr(CO)₃(η^5 -Sel) complexes demonstrates that the substitution of S by Se increases the ΔH^\ddagger values by 1.3 to 1.6 kcal/mol. EHMO calculations for the free ligands suggest that the Sel ligands have slightly higher π -electron densities than the analogous Th ligands; this is supported by the ¹³C NMR data for the CO ligands. The difference between activation barriers for Cr(CO)₃(η^5 -T) and Cr(CO)₃(η^5 -Sel) is, as expected, reflected in a large difference in the relative electron densities of the heteroatom and the diene fragment (E - Σ C) in the T (-2.744 e⁻) and Sel (-2.491 e⁻) ligands. This is also true for the other Cr(CO)₃(η^5 -Th) and Cr(CO)₃(η^5 -Sel) complexes. Studies that have measured the aromaticities of the T and Sel ligands generally agree that T is more aromatic than Sel.⁸ In particular, it has been reported that the π bonding in Sel is more localized on the heteroatom and the two double bonds than in the case of the T ligand.^{6a} EHMO calculations of the Th and Sel ligands (Table VII) demonstrate that there is an increased electron density on the Se heteroatom and a decreased electron density on the diene fragment of the Sel ligands with respect to the analogous Th ligands. This is in agreement with our assumption that increasing the electron density on the heteroatom and decreasing the electron density on the diene fragment raises the activation barrier.

It should be noted that in the case of the Sel ligands, methyl substitution increases the electron density on the Se atom and the diene fragment equally, as evidenced by the constant E - Σ C values in the Sel ligands. Thus, the activation barriers in the Sel complexes should increase to a smaller extent upon methyl

substitution than in the analogous Th complexes, as observed. The addition of two methyl groups at the α -position in $\text{Cr}(\text{CO})_3(\eta^5\text{-T})$ increases the ΔH^\ddagger value by 1.5 kcal/mol; similar substitution of the $\text{Cr}(\text{CO})_3(\eta^5\text{-Sel})$ complex increases the ΔH^\ddagger value by only 1.2 kcal/mol.

Attempts to measure the activation barrier of the cationic $[\text{Mn}(\text{CO})_3(\eta^5\text{-2,5-Me}_2\text{Sel})]\text{OTf}$ complex were limited because the complex, while rather soluble in CD_2Cl_2 ($\text{mp} = -95^\circ\text{C}$) at room temperature, becomes only sparingly soluble at temperatures approaching -95°C and precipitates out of solution as yellow needles. Consequently, we were unable to measure the $^{13}\text{C}\{^1\text{H}\}$ NMR spectrum of **10** in CD_2Cl_2 at low temperatures. The solvents CD_3OD , CD_3COCD_3 , and CD_3CN could not be used because these coordinating solvents are known to rapidly displace $\eta^5\text{-Th}$ and $\eta^5\text{-Sel}$ ligands from metal complexes^{4b,16,38c-d} including **10**.^{5b} The $^{13}\text{C}\{^1\text{H}\}$ NMR spectrum of **10** was measured in CD_3NO_2 down to the solvent melting point ($\text{mp} = -29^\circ\text{C}$). At this temperature, the ^{13}C NMR resonance for the carbonyl ligands was still a very sharp singlet. Assuming that the δv value for **10** is similar to that (63 Hz) for the isoelectronic $\text{Cr}(\text{CO})_3(\eta^5\text{-2,5-Me}_2\text{Sel})$ complex, the maximum ΔG_c^\ddagger value can be estimated from eq 3 to be 11.77 kcal/mol. This estimate, however, does not establish whether the activation barrier for $[\text{Mn}(\text{CO})_3(\eta^5\text{-2,5-Me}_2\text{Sel})]\text{OTf}$ is higher or lower than that of $\text{Cr}(\text{CO})_3(\eta^5\text{-2,5-Me}_2\text{Sel})$. Based on our conclusion that a strong metal-selenium bond would lead to a higher barrier to rotation, we expected that the cationic (+1) d^6 $\text{Mn}(\text{I})$ complex would yield a stronger M-Se bond than that in the neutral d^6 $\text{Cr}(\text{0})$ complex. Although it has not been possible to determine this, the relatively high coalescence temperature ($T_c = 20^\circ\text{C}$) for $(\eta^5\text{-Me}_4\text{T})\text{RuCl}_2(\text{PPh}_3)$ may

be an indication that the more positive oxidation state of Ru(II) leads to stronger sulfur to Ru(II) bonding, which leads to the higher rotational barrier.

Acknowledgment. The authors thank Dr. Clifford LeMaster of Boise State University for his insightful discussions on the topic of DNMR5 and Drs. Karen Ann Smith and Dave Scott of the ISU Instrument Services for their help with the NMRI version of DNMR5. We would also like to thank Dr. Victor G. Young, Jr., of the ISU Molecular Structure Laboratory for determining the structure of **5**, Dr. Gordon J. Miller for his assistance in the EHMO calculations, and Carter J. White for the preparation of selenophene and its methyl-substituted derivatives.

Supplementary Materials

Data Collection. A reddish-colored crystal of the title compound (**5**) was attached to the tip of a glass fiber and mounted on the diffractometer for data collection at $-50 \pm 1^\circ\text{C}$. The cell constants for data collection were determined from a list of reflections found by an automated search routine. Pertinent data collection and reduction information is given in Table IV.

Lorentz and polarization corrections were applied. A correction based on a decay in the standard reflections of 1.9% was applied to the data. An absorption correction based on a series of ψ -scans was applied. The agreement factor for the averaging of observed reflections was 1.1% (based on F).

Structure Solution and Refinement. The centric space group $\text{P}2_1/c$ was unambiguously determined by the systematic absences. The positions of all non-

hydrogen atoms were determined by direct methods.^{23b} All non-hydrogen atoms were refined with anisotropic thermal parameters. After the least-squares converged, all hydrogen atoms were found in a difference Fourier map. These were placed into the model with isotropic temperature factors set equal to 1.0 times the isotropic equivalent of the attached atom. The hydrogen atom positions were not refined in a riding model.

X-ray data collection and structure solution were carried out at the Iowa State Molecular Structure Laboratory. Refinement calculations were performed on a Digital Equipment Corp. MicroVAX II computer using the CAD4-SDP programs.^{23a}

Table IX. Additional Positional Parameters for Cr(CO)₃(η⁵-2,5-Me₂T)

Atom	x	y	z	B, ^a Å ²
H(11)	0.769	-0.040	0.397	2.4*
H(12)	0.928	-0.042	0.326	2.4*
H(13)	0.697	-0.060	0.271	2.4*
H(31)	0.642	0.119	0.143	1.3*
H(41)	0.658	0.317	0.166	1.3*
H(61)	0.964	0.425	0.392	4.5*
H(62)	0.781	0.416	0.447	4.5*
H(63)	0.748	0.466	0.329	4.5*

^a Starred atoms were refined isotropically.

**Table X. General Displacement Parameter Expressions ^a (U's)
for Cr(CO)₃(η^5 -2,5-Me₂T)**

Atom	U(1,1)	U(2,2)	U(3,3)	U(1,2)	U(1,3)	U(2,3)
Cr	0.0243(1)	0.0332(2)	0.0264(1)	0.0020(1)	0.0029(1)	0.0015(1)
S	0.0294(2)	0.0357(2)	0.0366(2)	0.0021(2)	-0.0034(2)	-0.0050(2)
C(1)	0.0361(9)	0.0368(9)	0.052(1)	0.0030(8)	0.0039(8)	-0.0079(9)
C(2)	0.0260(8)	0.0361(8)	0.0376(8)	0.0000(7)	0.0035(7)	-0.0082(7)
C(3)	0.0320(8)	0.048(1)	0.0322(8)	-0.0010(8)	0.0097(7)	-0.0053(8)
C(4)	0.0333(9)	0.046(1)	0.0394(8)	0.0014(8)	0.0133(7)	0.0067(8)
C(5)	0.0306(8)	0.0334(9)	0.048(1)	0.0008(7)	0.0083(7)	0.0031(8)
C(6)	0.045(1)	0.0332(9)	0.070(1)	-0.0028(9)	0.011(1)	-0.0049(9)
C(7)	0.0313(9)	0.050(1)	0.0320(8)	0.0008(8)	0.0022(7)	0.0013(8)
C(8)	0.0340(8)	0.0350(9)	0.0327(8)	0.0033(7)	0.0071(7)	0.0036(7)
C(9)	0.0278(8)	0.0438(9)	0.0339(8)	0.0060(8)	0.0013(7)	0.0037(8)
O(1)	0.0572(8)	0.0668(9)	0.0515(7)	0.0127(7)	0.0161(6)	-0.0173(7)
O(2)	0.0336(7)	0.0650(9)	0.0420(7)	0.0040(7)	-0.0061(6)	0.0038(6)
O(3)	0.0423(7)	0.0511(7)	0.0547(7)	-0.0081(7)	0.0087(6)	0.0136(7)

^a The form of the anisotropic displacement parameter is:

$$\exp[-2\pi^2[h^2a^2U(1,1) + k^2b^2U(2,2) + l^2c^2U(3,3) + 2hkabU(1,2) + 2hlacU(1,3) + 2klbcU(2,3)]]$$
, where a, b, and c are reciprocal lattice constants.

Table XI. Bond Angles (deg)^a for Cr(CO)₃(η^5 -2,5-Me₂T)

Atoms	Angle	Atoms	Angle
S-Cr-C(2)	44.79(5)	C(7)-Cr-C(9)	92.11(9)
S-Cr-C(3)	68.65(5)	C(8)-Cr-C(9)	86.35(8)
S-Cr-C(4)	68.58(6)	Cr-S-C(2)	62.58(6)
S-Cr-C(5)	44.87(5)	Cr-S-C(5)	62.65(7)
S-Cr-C(7)	103.85(6)	C(2)-S-C(5)	91.9(1)
S-Cr-C(8)	161.04(7)	Cr-C(2)-S	72.63(6)
S-Cr-C(9)	105.53(6)	Cr-C(2)-C(1)	128.0(1)
C(2)-Cr-C(3)	36.51(7)	Cr-C(2)-C(3)	71.6(1)
C(2)-Cr-C(4)	64.04(7)	S-C(2)-C(1)	120.3(1)
C(2)-Cr-C(5)	69.60(7)	S-C(2)-C(3)	110.6(1)
C(2)-Cr-C(7)	148.31(8)	C(1)-C(2)-C(3)	128.7(2)
C(2)-Cr-C(8)	121.37(8)	Cr-C(3)-C(2)	71.9(1)
C(2)-Cr-C(9)	93.08(8)	Cr-C(3)-C(4)	71.5(1)
C(3)-Cr-C(4)	37.53(8)	C(2)-C(3)-C(4)	113.4(2)
C(3)-Cr-C(5)	64.17(8)	Cr-C(4)-C(3)	71.0(1)
C(3)-Cr-C(7)	151.96(9)	Cr-C(4)-C(5)	71.8(1)
C(3)-Cr-C(8)	92.99(8)	C(3)-C(4)-C(5)	113.5(2)
C(3)-Cr-C(9)	115.88(8)	Cr-C(5)-S	72.47(7)
C(4)-Cr-C(5)	36.47(8)	Cr-C(5)-C(4)	71.8(1)
C(4)-Cr-C(7)	114.46(8)	Cr-C(5)-C(6)	128.1(2)
C(4)-Cr-C(8)	94.13(8)	S-C(5)-C(4)	110.3(1)
C(4)-Cr-C(9)	153.41(8)	S-C(5)-C(6)	120.2(2)
C(5)-Cr-C(7)	91.09(8)	C(4)-C(5)-C(6)	129.1(2)
C(5)-Cr-C(8)	123.57(8)	Cr-C(7)-O(1)	177.5(2)
C(5)-Cr-C(9)	149.90(8)	Cr-C(8)-O(2)	178.2(2)
C(7)-Cr-C(8)	90.15(8)	Cr-C(9)-O(3)	177.0(2)

^a Numbers in parentheses are estimated standard deviations in the least significant digits.

Table XII. Torsion Angles (deg)^a for Cr(CO)₃(η^5 -2,5-Me₂T)

Atoms	Angle	Atoms	Angle
C(2)-Cr-S-C(5)	108.08(10)	C(7)-Cr-C(2)-C(1)	105.31(19)
C(3)-Cr-S-C(2)	-33.78(9)	C(7)-Cr-C(2)-C(3)	-129.48(15)
C(3)-Cr-S-C(5)	74.30(9)	C(8)-Cr-C(2)-S	163.35(7)
C(4)-Cr-S-C(2)	-74.20(9)	C(8)-Cr-C(2)-C(1)	-81.36(17)
C(4)-Cr-S-C(5)	33.88(9)	C(8)-Cr-C(2)-C(3)	43.85(14)
C(5)-Cr-S-C(2)	-108.08(10)	C(9)-Cr-C(2)-S	-109.05(7)
C(7)-Cr-S-C(2)	174.62(9)	C(9)-Cr-C(2)-C(1)	6.24(17)
C(7)-Cr-S-C(5)	-77.30(9)	C(9)-Cr-C(2)-C(3)	131.45(12)
C(8)-Cr-S-C(2)	-48.86(18)	S-Cr-C(3)-C(2)	41.18(9)
C(8)-Cr-S-C(5)	59.22(18)	S-Cr-C(3)-C(4)	-82.25(10)
C(9)-Cr-S-C(2)	78.42(9)	C(2)-Cr-C(3)-C(4)	-123.42(16)
C(9)-Cr-S-C(5)	-173.50(9)	C(4)-Cr-C(3)-C(2)	123.42(16)
S-Cr-C(2)-C(1)	115.29(18)	C(5)-Cr-C(3)-C(2)	90.17(12)
S-Cr-C(2)-C(3)	-119.50(13)	C(5)-Cr-C(3)-C(4)	-33.25(11)
C(3)-Cr-C(2)-S	119.50(13)	C(7)-Cr-C(3)-C(2)	120.39(17)
C(3)-Cr-C(2)-C(1)	-125.2(2)	C(7)-Cr-C(3)-C(4)	-3.0(2)
C(4)-Cr-C(2)-S	85.06(8)	C(8)-Cr-C(3)-C(2)	-143.68(11)
C(4)-Cr-C(2)-C(1)	-159.65(18)	C(8)-Cr-C(3)-C(4)	92.90(11)
C(4)-Cr-C(2)-C(3)	-34.44(11)	C(9)-Cr-C(3)-C(2)	-56.29(13)
C(5)-Cr-C(2)-S	45.69(7)	C(9)-Cr-C(3)-C(4)	-179.71(12)
C(5)-Cr-C(2)-C(1)	160.98(18)	S-Cr-C(4)-C(3)	82.46(10)
C(5)-Cr-C(2)-C(3)	-73.80(12)	S-Cr-C(4)-C(5)	-41.42(10)
C(7)-Cr-C(2)-S	-9.98(17)	C(2)-Cr-C(4)-C(3)	33.52(10)

Table XII. (continued)

Atoms	Angle	Atoms	Angle
C(2)-Cr-C(4)-C(5)	-90.36(12)	C(8)-Cr-C(5)-C(4)	-41.22(14)
C(3)-Cr-C(4)-C(5)	-123.88(16)	C(8)-Cr-C(5)-C(6)	84.60(19)
C(5)-Cr-C(4)-C(3)	123.88(16)	C(9)-Cr-C(5)-S	12.56(18)
C(7)-Cr-C(4)-C(3)	178.43(11)	C(9)-Cr-C(5)-C(4)	131.76(16)
C(7)-Cr-C(4)-C(5)	54.55(13)	C(9)-Cr-C(5)-C(6)	-102.4(2)
C(8)-Cr-C(4)-C(3)	-89.52(11)	S-Cr-C(7)-O(1)	67.11(3.91)
C(8)-Cr-C(4)-C(5)	146.60(12)	C(2)-Cr-C(7)-O(1)	74.34(3.93)
C(9)-Cr-C(4)-C(3)	0.6(2)	C(3)-Cr-C(7)-O(1)	-3.33(4.01)
C(9)-Cr-C(4)-C(5)	-123.30(17)	C(4)-Cr-C(7)-O(1)	-5.36(3.93)
S-Cr-C(5)-C(4)	119.20(13)	C(5)-Cr-C(7)-O(1)	23.61(3.91)
S-Cr-C(5)-C(6)	-115.0(2)	C(8)-Cr-C(7)-O(1)	-99.97(3.91)
C(2)-Cr-C(5)-S	-45.61(6)	C(9)-Cr-C(7)-O(1)	173.68(3.90)
C(2)-Cr-C(5)-C(4)	73.59(12)	S-Cr-C(8)-O(2)	125.64(5.14)
C(2)-Cr-C(5)-C(6)	-160.58(19)	C(2)-Cr-C(8)-O(2)	87.22(5.21)
C(3)-Cr-C(5)-S	-85.01(8)	C(3)-Cr-C(8)-O(2)	111.59(5.21)
C(3)-Cr-C(5)-C(4)	34.19(11)	C(4)-Cr-C(8)-O(2)	149.19(5.20)
C(3)-Cr-C(5)-C(6)	160.0(2)	C(5)-Cr-C(8)-O(2)	172.31(5.17)
C(4)-Cr-C(5)-S	-119.20(13)	C(7)-Cr-C(8)-O(2)	-96.28(5.21)
C(4)-Cr-C(5)-C(6)	125.8(2)	C(9)-Cr-C(8)-O(2)	-4.17(5.21)
C(7)-Cr-C(5)-S	108.67(8)	S-Cr-C(9)-O(3)	-140.95(3.09)
C(7)-Cr-C(5)-C(4)	-132.13(12)	C(2)-Cr-C(9)-O(3)	-97.22(3.10)
C(7)-Cr-C(5)-C(6)	-6.30(18)	C(3)-Cr-C(9)-O(3)	-67.51(3.11)
C(8)-Cr-C(5)-S	-160.43(7)	C(4)-Cr-C(9)-O(3)	-67.90(3.14)

Table XII. (continued)

Atoms	Angle	Atoms	Angle
C(5)-Cr-C(9)-O(3)	-150.11(3.02)	Cr-C(2)-C(3)-C(4)	59.60(15)
C(7)-Cr-C(9)-O(3)	114.05(3.10)	S-C(2)-C(3)-Cr	-62.55(10)
C(8)-Cr-C(9)-O(3)	24.04(3.10)	S-C(2)-C(3)-C(4)	-3.0(2)
Cr-S-C(2)-C(1)	-124.31(16)	C(1)-C(2)-C(3)-Cr	124.4(2)
Cr-S-C(2)-C(3)	61.93(12)	C(1)-C(2)-C(3)-C(4)	-176.04(18)
C(5)-S-C(2)-Cr	-57.66(7)	Cr-C(3)-C(4)-C(5)	59.29(15)
C(5)-S-C(2)-C(1)	178.03(16)	C(2)-C(3)-C(4)-Cr	-59.82(14)
C(5)-S-C(2)-C(3)	4.27(15)	C(2)-C(3)-C(4)-C(5)	-0.5(3)
Cr-S-C(5)-C(4)	-62.15(13)	Cr-C(4)-C(5)-S	62.59(10)
Cr-S-C(5)-C(6)	124.41(18)	Cr-C(4)-C(5)-C(6)	-124.7(2)
C(2)-S-C(5)-Cr	57.60(7)	C(3)-C(4)-C(5)-Cr	-58.85(15)
C(2)-S-C(5)-C(4)	-4.55(16)	C(3)-C(4)-C(5)-S	3.7(2)
C(2)-S-C(5)-C(6)	-177.99(17)	C(3)-C(4)-C(5)-C(6)	176.4(2)

^a Numbers in parentheses are estimated standard deviations in the least significant digits.

Table XIII. Least-Squares Planes for Cr(CO)₃(η⁵-2,5-Me₂T)**Orthonormal Equation of Plane 1:**

$$0.9887(2) X + 0.0095(9) Y - 0.1497(15) Z = 3.603(6)$$

Crystallographic Equation of Plane 1:

$$6.6486(15) X + 0.117(12) Y - 4.82(5) Z = 3.603(6)$$

Atom ^a	X	Y	Z	Distance ^b
C(1)*	4.3269	-0.2723	3.9657	0.079(2)
C(2)	4.2021	1.2029	3.7514	0.0014(18)
C(3)	4.0122	1.8919	2.5672	-0.0025(19)
C(4)	4.0278	3.3046	2.7265	0.003(2)
C(5)	4.2184	3.7105	4.0369	-0.001(2)
C(6)*	4.3647	5.0983	4.5851	0.074(2)
S*	4.4873	2.3176	5.0749	0.0959(5)

^a Starred atoms were not used in calculating the plane.

^b $\chi^2 = 4.5$

Orthonormal Equation of Plane 2:

$$0.9739(3) X + 0.0194(11) Y - 0.2263(11) Z = 3.267(7)$$

Crystallographic Equation of Plane 2:

$$6.5490(18) X + 0.240(13) Y - 5.71(5) Z = 3.267(7)$$

Atom	X	Y	Z	Distance
C(2)	4.2021	1.2029	3.7514	0.0000(18)
C(5)	4.2184	3.7105	4.0369	0.000(2)
S	4.4873	2.3176	5.0749	0.0000(5)

Dihedral Angle between Planes 1 and 2: 4.5(4)°

Table XIII. (continued)**Orthonormal Equation of Plane 3:**

$$0.9820(1) X + 0.0146(5) Y - 0.1882(7) Z = 3.476(4)$$

Crystallographic Equation of Plane 3:

$$6.6038(9) X + 0.180(6) Y - 5.27(4) Z = 3.476(4)$$

Atom	X	Y	Z	Distance ^a
C(1)	4.3269	-0.2723	3.9657	0.023(2)
C(2)	4.2021	1.2029	3.7514	-0.0379(18)
C(3)	4.0122	1.8919	2.5672	0.0086(19)
C(4)	4.0278	3.3046	2.7265	0.015(2)
C(5)	4.2184	3.7105	4.0369	-0.039(2)
C(6)	4.3647	5.0983	4.5851	0.022(2)
S	4.4873	2.3176	5.0749	0.0094(5)

^a $\chi^2 = 1481.5$

Dihedral Angle between Planes 1 and 3: 2.3(6) $^\circ$

Dihedral Angle between Planes 2 and 3: 2.3(6) $^\circ$

Table XIV. Rate constants (s⁻¹) for the Cr(CO)₃(η^5 -Th)

Temperature	T	2-MeT	2-EtT	3-MeT
131 K			4.0(9)	21.6(11)
133 K	80(8)		7.4(10)	34.0(18)
135 K	109(4)		10.2(13)	48(3)
138 K	188(9)	9.5(4)	20.8(19)	72(27)
140 K	232(6) ^a	14.9(6)	28(2)	109(21)
143 K		25.1(8)	39.4(9)	212(76)
145 K		37.6(2)	56(3)	
148 K		49(6)	88(4)	
150 K		81(3)	134(37)	
153 K		124(16)	295(94)	
155 K		216(21)		
158 K				
160 K				
163 K				
165 K				
168 K				
170 K				
173 K				
175 K				
178 K				
180 K				
183 K				
185 K				
188 K				
190 K				
193 K				
195 K				

^a T = 139 K. ^b T = 167 K. ^c T = 169 K. ^d T = 176 K.

and $\text{Cr}(\text{CO})_3(\eta^5\text{-Sel})$ Complexes

2,5-Me ₂ T	Me ₄ T	Sel	2-MeSel	2,5-Me ₂ Sel
	0.6(2)			
	3.8(2)			
2.6(6)	8.8(19)			
5.4(1)	12(2)	5.2(4)		
8.6(2)	35(7)	7.4(9)		
15.9(3)	49(5)	14.0(11)	1.5(5)	
18.9(3)	54(4)	17.4(10)		
36.1(12)	91(12)	29.2(14)	3.9(8)	
44.8(12)	125(7)	37(2)	6.2(18)	
82(4)	160(13)	60(4)	8.7(15)	1.5(2)
108(5)		101(16)	12.3(10)	
131(7)		142(10)	21.1(15)	4.3(5)
			34(3)	4.2(6) ^c
				9.0(3)
			67(4)	14.7(12)
			77(9)	16.9(7) ^d
			111(10)	31(2)
			181(57)	36(2)
				57(6)
				81(3)
				91(5)
				122(3)
				199(2)

Values of $10^4 F_{\text{obs}}$ and $10^4 F_{\text{calc}}$

H	K	L	F _{obs}	F _{calc}	SigF	H	K	L	F _{obs}	F _{calc}	SigF	H	K	L	F _{obs}	F _{calc}	SigF	
-	-	-	-	-	-	-	-	-	-	-	-	-	-	-	-	-	-	-
0	0	2	798	798	7	0	3	13	63	62	64	3	0	12	6	158	153	4
0	0	4	951	946	9	0	3	14	127	130	5	0	12	7	44	45	4	
0	0	6	240	237	2	0	4	0	374	352	2	0	12	7	119	116	6	
0	0	8	557	577	7	0	4	1	965	931	4	0	7	9	176	170	4	
0	0	10	96	92	3	0	4	2	360	338	2	0	7	10	297	296	4	
0	0	12	314	316	4	0	4	3	108	99	2	0	7	11	116	107	3	
0	0	14	86	85	3	0	4	4	210	200	2	0	8	1	274	273	3	
0	0	16	377	367	2	0	4	5	304	313	2	0	8	2	133	138	3	
0	0	18	1265	1319	9	0	4	6	87	98	2	0	8	3	67	64	2	
0	0	20	495	483	2	0	4	7	333	340	3	0	8	4	317	324	4	
0	0	22	280	263	2	0	4	8	65	65	5	0	8	5	281	279	3	
0	0	24	68	65	2	0	4	9	235	240	4	0	8	6	127	128	4	
0	0	26	35	44	3	0	4	11	229	227	5	0	8	7	271	272	3	
0	0	28	116	109	3	0	4	12	181	183	4	0	8	8	226	223	4	
0	0	30	193	185	3	0	4	13	131	129	3	0	8	11	48	42	4	
0	0	32	123	125	5	0	5	1	610	595	3	0	8	12	239	235	4	
0	0	34	114	114	3	0	5	2	127	130	2	0	9	1	38	36	3	
0	0	36	606	614	3	0	5	3	234	258	2	0	9	2	610	626	3	
0	0	38	257	254	3	0	5	4	75	72	2	0	9	3	115	110	3	
0	0	40	239	235	4	0	5	5	40	32	2	0	9	4	278	287	5	
0	0	42	127	122	3	0	5	5	154	149	3	0	9	5	138	146	5	
0	0	44	1285	1330	4	0	5	6	159	160	5	0	9	10	302	293	5	
0	0	46	841	837	7	0	5	7	159	160	5	0	9	10	302	293	5	
0	0	48	606	614	3	0	5	8	159	160	5	0	9	11	43	41	5	
0	0	50	599	572	4	0	5	8	56	60	2	0	10	5	684	701	3	
0	0	52	129	118	3	0	5	9	349	343	8	0	10	0	106	104	3	
0	0	54	91	88	4	0	5	10	55	56	3	0	10	1	106	104	2	
0	0	56	22	25	5	0	5	11	303	293	6	0	10	2	151	157	4	
0	0	58	282	293	2	0	5	12	42	42	6	0	10	3	73	72	2	
0	0	60	149	149	3	0	5	13	93	92	3	0	10	4	327	337	3	
0	0	62	136	149	3	0	5	14	93	92	3	0	10	5	442	442	2	
0	0	64	316	325	5	0	6	0	442	442	2	0	10	5	87	86	2	
0	0	66	115	107	2	0	6	1	464	490	4	0	10	6	148	151	3	
0	0	68	311	314	5	0	6	1	455	455	3	0	10	7	209	207	4	
0	0	70	45	45	3	0	6	2	111	107	3	0	10	8	109	107	3	
0	0	72	295	294	2	0	6	3	327	316	2	0	10	9	82	82	3	
0	0	74	88	92	2	0	6	4	79	81	2	0	10	10	50	56	6	
0	0	76	243	243	4	0	6	4	79	81	2	0	10	10	50	56	6	
0	0	78	84	80	3	0	6	5	104	110	3	0	11	1	231	238	4	
0	0	80	325	325	5	0	6	6	0	442	442	2	0	11	2	287	291	4
0	0	82	115	107	2	0	6	7	283	281	3	0	11	3	98	95	2	
0	0	84	311	314	5	0	6	8	288	285	3	0	11	3	109	107	3	
0	0	86	45	45	3	0	6	9	135	133	3	0	11	4	109	107	3	
0	0	88	210	111	2	0	6	10	327	316	2	0	10	9	82	82	3	
0	0	90	174	174	2	0	6	11	178	178	6	0	11	6	82	82	2	
0	0	92	169	169	3	0	6	12	192	188	5	0	11	7	108	109	2	
0	0	94	59	64	3	0	6	13	192	188	5	0	11	7	231	238	4	
0	0	96	34	40	3	0	6	13	123	120	3	0	11	9	88	84	3	
0	0	98	115	107	2	0	6	14	140	149	3	0	12	0	207	206	4	
0	0	100	71	60	4	0	6	15	351	357	3	0	12	1	198	196	4	
0	0	102	311	30	3	0	7	2	351	357	3	0	12	2	112	108	3	
0	0	104	124	130	3	0	7	3	134	142	3	0	12	2	106	108	3	
0	0	106	169	174	2	0	7	4	91	85	2	0	12	3	124	128	3	
0	0	108	304	304	4	0	7	5	258	259	4	0	12	4	39	36	4	
0	0	110	290	285	4	0	7	6	63	62	2	0	12	5	140	138	3	
0	0	112	94	93	2	0	7	7	63	62	0	1	11	10	0	303	301	3

Values of $10^4 F_{\text{obs}}$ and $10^4 F_{\text{calc}}$

H	K	L	F _{obs}	F _{calc}	SigF	H	K	L	F _{obs}	F _{calc}	SigF	H	K	L	F _{obs}	F _{calc}	SigF		
1	2-14	230	221	4	1	3	6	147	137	3	1	5	4	141	147	8	1	7	2
2	2-13	148	145	3	1	3	7	206	211	5	1	5	5	610	606	3	1	7	3
1	2-12	162	161	9	1	3	8	255	252	3	1	5	6	111	114	3	1	7	4
1	2-11	53	51	3	1	3	9	512	521	8	1	5	7	79	75	2	1	7	5
1	2-10	121	121	3	1	3	10	131	128	3	1	5	6	107	106	3	1	7	6
1	2-9	117	120	3	1	3	11	77	78	3	1	5	9	446	451	3	1	7	7
1	2-8	158	160	3	1	4	13	259	257	4	1	5	11	62	60	3	1	7	8
1	2-6	642	640	2	1	4	12	119	119	4	1	6	13	239	235	4	1	7	9
1	2-5	480	482	3	1	4	11	62	54	7	1	6	12	81	77	3	1	7	10
1	2-4	314	305	2	1	4	9	33	37	4	1	6	11	103	107	2	1	7	11
1	2-3	75	76	3	1	4	8	251	260	4	1	6	10	64	62	3	1	7	12
1	2-2	883	884	5	1	4	7	368	368	7	1	6	9	126	132	3	1	7	13
1	2-1	683	666	6	1	4	6	62	60	2	1	6	8	51	44	6	1	6	6
1	2-0	494	475	3	1	4	5	803	798	2	1	6	7	340	342	3	1	6	4
1	2-1	142	134	2	1	4	4	108	100	2	1	6	6	239	244	3	1	6	3
1	2-2	151	141	2	1	4	3	746	724	2	1	6	5	403	409	3	1	6	2
1	2-3	532	508	2	1	4	2	221	212	2	1	6	4	62	62	2	1	6	1
1	2-4	340	310	4	1	4	1	922	916	2	1	6	3	299	299	2	1	6	0
1	2-5	442	446	3	1	4	0	41	45	2	1	6	2	123	126	3	1	6	1
1	2-6	333	356	3	1	4	1	497	441	2	1	6	1	341	351	5	1	6	3
1	2-7	446	446	4	1	4	2	39	46	5	1	6	0	114	114	3	1	6	4
1	2-8	301	308	3	1	4	3	475	445	2	1	6	1	261	257	2	1	6	5
1	2-9	99	97	2	1	4	4	164	167	2	1	6	2	152	145	3	1	6	6
1	2-10	113	116	4	1	4	6	110	109	3	1	6	3	161	145	3	1	6	7
1	2-11	65	63	3	1	4	7	679	693	6	1	6	4	66	61	2	1	6	8
1	2-12	70	69	3	1	4	6	76	81	2	1	6	5	164	172	3	1	6	9
1	2-13	41	35	4	1	4	9	89	86	2	1	6	6	190	193	3	1	6	10
1	2-13	71	68	3	1	4	10	62	61	3	1	6	7	565	569	3	1	6	11
1	2-12	122	131	3	1	4	11	115	116	4	1	6	8	76	81	7	1	6	12
1	2-11	113	110	3	1	4	12	59	55	5	1	6	9	161	161	4	1	6	13
1	2-10	217	218	5	1	4	13	42	39	4	1	6	10	80	81	2	1	6	14
1	2-9	79	72	2	1	5	13	81	78	3	1	6	11	79	71	3	1	6	15
1	2-8	182	179	3	1	5	12	72	72	6	1	7	12	132	130	4	1	7	16
1	2-7	551	541	9	1	5	11	134	132	3	1	7	11	91	92	2	1	7	17
1	2-6	213	193	2	1	5	10	109	114	3	1	7	10	115	119	3	1	7	18
1	2-5	72	86	2	1	5	9	284	293	3	1	7	9	71	73	2	1	7	19
1	2-4	443	441	2	1	5	7	437	440	12	1	7	8	119	124	3	1	7	20
1	2-3	1382	1407	18	1	5	5	527	533	2	1	7	7	281	290	3	1	7	21
1	3-2	560	535	6	1	5	4	152	152	3	1	7	6	80	80	3	1	7	22
1	3-1	138	133	2	1	5	3	991	976	2	1	7	5	252	251	3	1	7	23
1	3-0	121	114	3	1	5	2	223	212	6	1	7	4	436	443	3	1	7	24
1	3-1	43	39	3	1	5	1	299	285	2	1	7	3	629	632	3	1	7	25
1	3-2	130	127	2	1	5	0	241	231	3	1	7	2	338	339	3	1	7	26
1	3-3	124	139	4	1	5	1	128	97	2	1	7	1	506	497	6	1	7	27
1	3-4	499	463	3	1	5	2	28	30	3	1	7	0	25	19	3	1	7	28
1	3-5	954	960	2	1	5	3	213	224	2	1	7	1	57	45	3	1	7	29

Values of $10^4 F_{\text{obs}}$ and $10^4 F_{\text{calc}}$

H	K	L	F _{obs}	F _{calc}	SigF	H	K	L	F _{obs}	F _{calc}	SigF	H	K	L	F _{obs}	F _{calc}	SigF
1	10	-8	80	82	3	1	13	-6	65	59	3	2	1	4	820	824	2
1	10	-7	45	43	3	1	13	-5	136	139	3	2	1	5	169	174	3
1	10	-6	122	126	3	1	13	-4	75	77	3	2	1	6	213	216	3
1	10	-5	144	146	3	1	13	-3	265	268	4	2	1	7	197	195	3
1	10	-3	32	33	4	1	13	-2	107	115	6	2	1	8	45	42	3
1	10	-2	371	388	3	1	13	-1	76	75	3	2	1	9	67	61	6
1	10	-1	80	84	2	1	13	0	62	71	3	2	1	12	169	160	4
1	10	0	214	208	3	1	13	1	47	42	3	2	1	14	107	103	3
1	10	1	48	50	3	1	13	2	120	115	3	2	1	13	76	77	3
1	10	3	72	75	3	1	13	5	220	220	6	2	1	12	160	158	4
1	10	4	176	179	4	1	14	-4	37	40	5	2	2	-11	208	210	4
1	10	6	364	366	4	1	14	-3	128	126	3	2	2	-10	79	79	2
1	10	7	88	88	2	1	14	-2	65	59	3	2	2	-8	363	365	3
1	10	8	147	154	4	1	14	-1	187	191	4	2	2	-7	411	425	3
1	10	9	138	140	3	1	14	0	92	92	3	2	2	-7	458	464	8
1	11	-9	74	76	3	1	14	2	48	43	4	2	2	-6	153	150	4
1	11	-8	122	125	5	1	14	3	93	92	3	2	2	-5	175	178	2
1	11	-7	86	88	2	2	0	-14	126	124	3	2	2	-4	340	324	5
1	11	-6	64	69	3	2	0	-12	204	201	6	2	2	-2	312	288	3
1	11	-4	249	256	4	2	0	-10	201	209	5	2	2	-1	232	205	2
1	11	-3	104	102	3	2	0	-8	334	343	4	2	2	-1	159	159	5
1	11	-2	279	282	4	2	0	-6	544	557	2	2	0	-7	587	585	9
1	11	-1	43	48	6	2	0	-4	148	146	2	2	2	-4	355	355	2
1	11	0	63	66	2	2	0	-2	1461	1471	6	2	2	-3	388	377	3
1	11	1	55	60	3	2	0	0	607	572	2	2	2	-2	99	96	3
1	11	2	181	169	4	2	0	2	1342	1339	6	2	2	5	517	516	2
1	11	3	100	99	3	2	0	4	562	565	2	2	6	0	482	479	3
1	11	4	212	207	4	2	0	6	555	554	3	2	2	6	354	351	3
1	11	5	173	172	4	2	0	8	54	57	3	2	2	7	157	153	4
1	11	7	92	88	3	2	0	12	220	216	6	2	2	9	133	134	3
1	11	8	129	123	5	2	0	-14	106	103	3	2	2	10	107	107	3
1	12	-6	93	66	5	2	1	-12	44	42	3	2	2	11	72	75	2
1	12	-7	47	46	4	2	1	-11	78	81	2	2	2	12	60	64	3
1	12	-5	107	115	3	2	1	-10	278	282	7	2	2	-12	51	51	3
1	12	-4	195	199	4	2	1	-9	221	227	3	2	2	-11	107	104	3
1	12	-3	50	48	3	2	1	-8	215	229	3	2	2	-10	201	203	7
1	12	-2	112	71	3	2	1	-6	728	718	3	2	2	-9	422	429	3
1	12	-1	144	140	3	2	1	-5	203	204	2	2	2	-8	160	167	3
1	12	0	165	122	4	2	1	-4	572	576	2	2	2	-7	143	136	4
1	12	1	61	63	3	2	1	-3	61	55	2	2	2	-6	346	337	2
1	12	3	117	117	3	2	1	-2	195	179	2	2	2	-5	626	619	2
1	12	4	113	113	3	2	1	-1	36	38	2	2	2	-4	482	474	2
1	12	5	86	84	3	2	1	0	521	495	15	2	2	-3	706	688	2
1	12	6	114	117	3	2	1	1	137	124	2	2	2	-2	435	419	3
1	12	7	233	233	4	2	1	2	948	948	3	2	2	-1	279	272	2

Values of $10^4 F_{\text{obs}}$ and $10^4 F_{\text{calc}}$

	H	K	L	F _{obs}	F _{calc}	SigF		H	K	L	F _{obs}	F _{calc}	SigF		H	K	L	F _{obs}	F _{calc}	SigF			
2	5	5	250	244	4	2	7	5	35	30	5	2	10	-4	92	95	2	13	3	230	231	7	
2	5	6	61	2	2	7	6	146	149	3	2	10	-2	102	107	3	2	14	-1	98	95	4	
2	5	7	169	175	4	2	7	7	118	117	3	2	10	-1	139	143	3	2	14	0	38	32	5
2	5	8	97	96	3	2	7	9	136	142	4	2	10	0	182	171	4	2	14	1	149	150	4
2	5	9	101	102	3	2	7	10	63	61	3	2	10	1	103	103	3	0	-14	191	192	4	
2	5	10	56	58	3	2	7	11	88	86	4	2	10	2	334	333	3	3	-12	496	495	4	
2	5	11	217	214	7	2	8	12	94	96	5	2	10	4	179	171	4	3	0	8	327	336	3
2	5	12	83	78	5	2	8	11	70	70	4	2	10	5	56	52	7	3	0	-6	595	601	9
2	6	-13	144	141	3	2	8	10	110	115	3	2	10	6	292	289	4	3	0	-4	828	810	15
2	6	-11	143	147	3	2	8	-8	273	276	9	2	10	7	138	140	4	3	0	-2	215	227	3
2	6	-9	160	167	4	2	8	-7	59	58	3	2	11	-9	116	111	3	3	0	0	667	687	2
2	6	-8	128	127	3	2	8	-6	134	130	6	2	11	-8	178	174	4	3	0	2	279	284	6
2	6	-7	496	490	12	2	8	-5	113	113	3	2	11	-7	50	53	3	3	0	4	308	308	3
2	6	-6	304	312	3	2	8	-4	83	82	2	2	11	-6	164	167	4	3	0	6	375	373	3
2	6	-5	276	280	3	2	8	-3	55	54	2	2	11	-5	131	125	4	3	0	8	353	360	3
2	6	-4	193	193	5	2	8	-2	33	32	3	2	11	-4	218	215	4	3	0	10	88	93	3
2	6	-3	367	349	8	2	8	-1	180	178	4	2	11	-3	80	83	2	3	0	14	169	173	4
2	6	-2	57	56	3	2	8	0	335	334	4	2	11	-2	113	113	3	3	-12	101	96	2	
2	6	-1	265	259	3	2	8	1	198	204	5	2	11	-1	83	84	2	3	-11	131	136	3	
2	6	0	67	69	2	2	8	2	372	376	3	2	11	0	76	80	6	3	-10	347	351	3	
2	6	1	729	727	6	2	8	4	246	238	6	2	11	1	86	86	3	3	-9	155	156	4	
2	6	2	299	305	8	2	8	5	118	116	3	2	11	2	190	190	6	3	-8	118	116	3	
2	6	3	107	107	3	2	8	6	292	292	4	2	11	3	247	253	4	3	-7	169	173	4	
2	6	4	179	180	3	2	8	7	168	172	5	2	11	4	198	196	4	3	-6	98	100	3	
2	6	5	590	597	3	2	8	10	101	104	5	2	11	6	85	88	3	3	-5	144	149	3	
2	6	7	329	329	5	2	9	-11	89	88	3	2	11	7	81	83	3	3	-4	417	420	2	
2	6	8	62	60	3	2	9	-10	248	249	4	2	12	-8	49	48	4	3	-3	303	295	2	
2	6	9	108	108	3	2	9	-9	270	267	3	2	12	-7	243	237	6	3	-2	847	837	13	
2	6	10	128	133	2	9	-8	146	139	5	2	12	-6	131	125	7	3	-1	1	264	240	6	
2	6	11	118	112	3	2	9	-6	244	247	4	2	12	-5	60	58	3	3	1	1	75	84	2
2	6	12	204	206	4	2	9	-4	30	30	4	2	12	-4	62	58	3	3	1	2	528	535	11
2	7	-9	160	179	4	2	9	-3	175	177	3	2	12	-3	106	105	3	3	1	3	48	47	2
2	7	-8	223	231	4	2	9	-2	154	150	3	2	12	-2	84	84	3	3	1	4	501	502	3
2	7	-7	243	243	4	2	9	0	283	283	3	2	12	0	162	166	5	3	1	5	335	336	3
2	7	-6	333	336	3	2	9	1	47	46	3	2	12	-6	219	218	6	3	1	6	323	323	5
2	7	-5	387	378	10	2	9	3	189	180	3	2	12	2	51	54	5	3	1	7	158	158	4
2	7	-4	345	339	3	2	9	4	288	293	3	2	12	4	100	102	3	3	1	9	191	192	4
2	7	-3	457	449	5	2	9	6	119	117	3	2	12	6	106	109	3	3	1	10	349	353	10
2	7	-2	81	86	4	2	9	7	52	53	3	2	13	-5	169	174	6	3	-14	43	45	4	
2	7	-1	178	180	3	2	9	6	68	69	3	2	13	-4	126	128	3	3	-13	86	87	6	
2	7	0	147	151	3	2	9	9	77	75	4	2	13	-3	91	87	3	3	-12	312	239	9	
2	7	1	216	215	3	2	10	-10	123	126	4	2	13	-2	130	131	3	3	-11	143	149	3	
2	7	2	342	347	3	2	10	-8	194	194	4	2	13	-1	74	76	3	3	-9	225	224	3	
2	7	3	383	384	3	2	10	-7	83	86	2	2	13	0	70	66	3	3	-8	372	381	3	
2	7	4	377	384	3	2	10	-6	96	91	2	2	13	2	92	69	6	3	-7	304	305	5	

Values of $10^4 F_{\text{obs}}$ and $10^4 F_{\text{calc}}$

H	K	L	F _{obs}	F _{calc}	SigF	H	K	L	F _{obs}	F _{calc}	SigF	H	K	L	F _{obs}	F _{calc}	SigF
3	2	-6	210	215	3	3	4	-7	239	245	3	3	6	-1	707	706	6
3	2	-5	112	107	4	3	4	-6	307	308	3	3	6	0	205	210	3
3	2	-4	339	324	2	3	4	-5	361	383	3	3	6	1	198	199	3
3	2	-3	214	205	7	3	4	-4	70	74	4	3	6	2	92	95	2
3	2	-2	122	139	3	3	4	-3	221	220	3	3	6	3	221	220	3
3	2	-1	502	518	12	3	4	-2	191	192	3	3	6	5	96	93	2
3	2	0	605	609	7	3	4	-1	948	958	2	3	6	7	104	103	3
3	2	1	115	120	5	3	4	0	232	232	3	3	6	8	191	187	7
3	2	2	123	117	5	3	4	1	392	409	8	3	6	9	54	52	4
3	2	3	214	208	3	3	4	2	63	79	2	3	7	12	46	44	4
3	2	4	481	471	7	3	4	3	571	549	3	3	7	11	245	247	4
3	2	5	105	106	3	3	4	5	97	97	2	3	7	10	180	176	4
3	2	6	140	138	5	3	4	6	172	172	3	3	7	9	91	92	2
3	2	7	261	263	3	3	4	7	165	166	4	3	7	7	49	48	3
3	2	8	170	173	4	3	4	8	86	82	6	3	7	4	76	77	2
3	2	9	80	80	2	3	4	9	127	126	3	3	7	3	116	126	3
3	2	10	50	44	3	3	4	10	48	49	4	3	7	2	293	299	3
3	2	11	207	209	4	3	4	11	274	271	4	3	7	1	36	30	3
3	3	-14	66	68	3	3	5	-11	252	255	4	3	7	0	228	233	3
3	3	-11	268	292	4	3	5	-10	119	124	4	3	7	1	198	203	3
3	3	-10	126	125	3	3	5	-8	50	53	3	3	7	2	282	290	4
3	3	-9	117	124	5	3	5	-7	43	42	5	3	7	3	235	233	7
3	3	-7	311	302	3	3	5	-6	69	59	7	3	7	5	103	100	3
3	3	-6	189	186	4	3	5	-4	62	64	3	3	7	6	138	136	3
3	3	-4	90	95	5	3	5	-3	572	585	3	3	7	7	33	34	4
3	3	-3	322	339	2	3	5	-2	162	157	3	3	7	7	74	77	3
3	3	-2	359	358	2	3	5	-1	62	63	2	3	7	9	214	214	4
3	3	-1	464	464	2	3	5	1	658	652	6	3	7	10	240	234	5
3	3	0	63	66	2	3	5	2	128	125	6	3	8	12	187	177	4
3	3	1	718	722	5	3	5	3	293	301	3	3	8	11	68	65	3
3	3	2	368	364	8	3	5	5	147	144	3	3	8	10	51	47	3
3	3	3	196	188	3	3	5	7	127	127	5	3	8	9	170	177	4
3	3	4	144	149	5	3	5	6	75	81	3	3	8	8	263	269	4
3	3	5	75	61	2	3	5	9	350	344	10	3	8	7	251	259	4
3	3	6	161	160	10	3	5	10	74	67	3	3	8	6	197	187	3
3	3	7	217	228	4	3	5	11	248	250	4	3	8	5	202	199	5
3	3	8	71	73	3	3	6	-13	169	191	5	3	8	-4	220	227	3
3	3	9	253	258	4	3	6	-12	105	103	3	3	8	-3	39	41	4
3	3	10	229	230	4	3	6	-9	272	271	3	3	8	-2	50	45	3
3	3	11	171	167	4	3	6	-8	51	49	3	3	8	-1	216	220	3
3	3	12	52	48	6	3	6	-7	190	187	4	3	8	0	581	591	3
3	4	-14	239	240	4	3	6	-6	41	38	3	3	8	1	257	257	3
3	4	-13	100	100	3	3	6	-5	399	405	3	3	8	3	123	120	3
3	4	-10	96	95	2	3	6	-4	160	162	3	3	8	4	105	110	3
3	4	-9	259	264	3	3	6	-3	154	154	4	3	8	5	40	44	4
3	4	-6	113	113	3	3	6	-2	223	223	3	3	8	6	55	50	3

Values of $10^4 F_{\text{obs}}$ and $10^4 F_{\text{calc}}$

H	K	L	F _{obs}	F _{calc}	Sig _F	H	K	L	F _{obs}	F _{calc}	Sig _F	H	K	L	F _{obs}	F _{calc}	Sig _F	
3	12	-2	115	117	3	4	-14	147	147	4	-11	62	4	6	6	225	221	4
3	12	-1	197	202	4	4	-13	127	130	3	4	-10	31	29	4	6	7	205
3	12	0	150	154	5	4	-12	78	75	3	4	-7	231	237	3	4	7-12	88
3	12	1	45	46	4	4	-11	93	93	2	4	-6	101	104	2	4	7-11	91
3	12	2	93	92	4	4	-10	65	63	3	4	-5	409	415	3	4	7-9	153
3	12	3	68	69	3	4	-9	131	130	3	4	-3	279	286	3	4	7-8	158
3	12	4	72	71	3	4	-8	194	196	3	4	-2	55	56	4	4	7-7	168
3	13	-4	100	91	4	4	-7	322	325	3	4	-1	338	352	5	4	7-6	103
3	13	-3	207	204	4	4	-6	112	120	3	4	0	224	223	3	4	7-5	74
3	13	-1	115	110	5	4	-5	173	165	3	4	1	112	108	3	4	7-4	263
3	13	1	222	215	11	4	-3	280	282	6	4	3	198	198	5	4	7-3	196
3	13	2	63	63	3	4	-2	347	346	6	4	4	46	46	3	4	7-2	96
4	0	-14	211	210	6	4	-1	189	185	4	4	5	151	145	4	4	7-1	40
4	0	-12	138	141	5	4	0	98	101	2	4	7	287	289	4	4	7-0	76
4	0	-10	67	71	3	4	1	166	166	6	4	8	40	39	4	4	7-1	106
4	0	-8	254	252	9	4	2	371	382	4	4	10	51	53	4	4	7-3	286
4	0	-6	471	461	3	4	3	189	198	3	4	5-13	74	69	3	4	7-4	230
4	0	-4	146	139	5	4	2	33	35	4	4	5-11	135	136	3	4	7-5	238
4	0	-2	1126	1126	9	4	2	96	99	2	4	5-9	104	105	2	4	7-6	60
4	0	0	208	221	5	4	6	417	423	3	4	5-7	365	371	4	4	7-7	126
4	0	2	185	193	3	4	7	368	374	12	4	5-6	43	43	4	4	7-8	195
4	0	4	116	117	3	4	8	77	75	3	4	5-5	126	122	3	4	6-9	188
4	0	6	633	644	10	4	9	40	38	4	4	5-4	101	101	3	4	6-8	135
4	0	8	262	266	4	4	10	52	51	4	4	5-3	619	620	7	4	6-7	234
4	0	10	97	94	3	4	13	103	102	6	4	5-1	152	146	3	4	6-6	397
4	1	-13	99	99	3	4	12	87	83	2	4	0	34	33	4	4	6-5	54
4	1	-12	171	166	4	4	11	109	109	3	4	5-2	291	290	5	4	6-3	49
4	1	-11	129	131	3	4	10	86	86	2	4	5-2	121	120	3	4	6-2	237
4	1	-10	299	299	3	4	9	186	186	3	4	5-3	189	185	3	4	6-1	106
4	1	-8	400	402	3	4	8	265	264	3	4	4	120	126	3	4	6-0	67
4	1	-7	66	68	2	4	7	331	331	3	4	5	227	226	4	4	6-1	163
4	1	-6	47	40	5	4	5	312	322	3	4	5-7	184	180	6	4	6-2	193
4	1	-5	201	204	3	4	4	291	300	3	4	5-2	219	219	4	4	6-3	110
4	1	-4	895	903	5	4	3	325	334	3	4	6-11	41	39	4	4	6-2	241
4	1	-3	271	272	3	4	2	197	204	3	4	6-9	107	108	3	4	6-1	107
4	1	-2	363	362	3	4	1	83	77	2	4	6-8	59	63	3	4	6-6	292
4	1	0	195	188	3	4	0	61	60	3	4	6-7	141	145	7	4	6-7	92
4	1	1	157	153	4	4	2	235	239	6	4	6-6	137	139	4	4	6-10	113
4	1	2	91	87	6	4	3	263	267	4	4	6-5	380	380	4	4	6-9	57
4	1	3	85	87	2	4	3	221	223	4	4	6-4	145	146	3	4	6-8	266
4	1	4	537	553	3	4	5	310	315	4	4	6-3	81	75	4	4	6-7	25
4	1	5	170	169	3	4	6	134	137	3	4	6-2	231	232	3	4	6-6	142
4	1	7	51	49	3	4	7	164	167	5	4	6-1	286	279	7	4	6-4	446
4	1	8	474	469	4	4	6	278	279	7	4	6-0	33	33	4	4	6-3	32
4	1	9	193	193	5	4	9	209	205	4	4	6-1	39	36	3	4	6-0	164
4	1	10	122	122	3	4	113	141	141	3	4	6-3	241	251	3	4	6-1	203

Values of $10^6 F_{\text{obs}}$ and $10^6 F_{\text{calc}}$

H	K	L	F _{obs}	F _{calc}	SigF	H	K	L	F _{obs}	F _{calc}	SigF	H	K	L	F _{obs}	F _{calc}	SigF		
4	9	2	175	177	4	5	1	-8	273	278	3	5	3	0	99	95	2	115	113
4	9	3	159	156	5	5	1	-6	328	333	3	5	3	2	175	178	7	5	6
4	9	4	343	339	4	5	1	-5	72	75	2	5	3	3	417	422	9	5	6
4	9	5	49	47	4	5	1	-4	126	136	5	5	3	4	88	94	3	5	6
4	10	-6	162	161	4	5	1	-3	46	40	3	5	3	5	39	36	4	5	6
4	10	-6	365	368	4	5	1	-1	73	74	2	5	3	6	107	109	5	5	7
4	10	-5	54	56	3	5	1	0	65	63	4	5	3	7	94	92	3	5	7
4	10	-3	135	136	3	5	1	2	112	112	3	5	4	-12	50	48	7	5	7
4	10	-2	302	301	4	5	1	2	201	203	5	5	4	-11	154	152	5	5	7
4	10	0	138	142	4	5	1	3	111	111	3	5	4	-9	109	109	3	5	7
4	10	1	61	55	5	5	1	4	146	146	3	5	4	-7	311	310	3	5	7
4	10	2	149	147	4	5	1	5	166	167	4	5	4	-6	39	41	4	5	7
4	10	3	106	105	3	5	1	6	189	192	4	5	4	-5	90	82	2	5	7
4	10	5	116	117	3	5	1	8	110	112	6	5	4	-4	46	42	3	5	7
4	11	-8	126	117	3	5	2	-12	65	59	3	5	4	-1	212	206	3	5	7
4	11	-7	40	32	4	5	2	-11	102	101	4	5	4	0	196	197	7	5	7
4	11	-5	97	96	3	5	2	-10	118	116	3	5	4	1	621	625	9	5	7
4	11	-4	214	211	6	5	2	-8	216	214	4	5	4	2	93	93	3	5	7
4	11	-3	153	147	4	5	2	-7	239	240	3	5	4	4	98	99	6	5	7
4	11	-2	94	93	2	5	2	-6	269	271	3	5	4	5	385	389	4	5	7
4	11	-1	93	92	2	5	2	-5	333	336	4	5	4	5	108	108	3	5	7
4	11	0	82	81	3	5	2	-4	110	109	3	5	4	7	55	54	4	5	7
4	11	1	67	71	3	5	2	-3	112	116	3	5	5	-12	55	54	4	5	7
4	11	2	163	163	4	5	2	-2	206	204	4	5	5	-9	307	315	6	5	7
4	11	4	211	210	4	5	2	-1	173	169	3	5	5	-7	135	132	3	5	6
4	12	-5	162	154	6	5	2	0	434	438	3	5	5	-5	175	172	4	5	6
4	12	-3	71	71	3	5	2	1	439	493	5	5	5	-4	69	68	4	5	6
4	12	-2	74	71	3	5	2	2	392	398	3	5	5	-3	180	183	3	5	6
4	12	-1	123	120	3	5	2	3	122	123	4	5	5	-1	384	390	4	5	6
4	12	0	140	136	3	5	2	4	204	215	4	5	5	0	53	52	3	5	6
4	12	2	114	117	3	5	2	5	258	261	4	5	5	1	104	102	3	5	6
5	0	-12	82	82	3	5	2	6	282	287	5	5	5	3	400	397	4	5	6
5	0	-10	112	112	4	5	2	7	51	50	4	5	5	4	36	41	5	5	6
5	0	-8	382	387	3	5	2	8	52	49	4	5	5	6	56	55	4	5	6
5	0	-6	40	37	3	5	3	-12	129	127	4	5	5	7	49	51	4	5	6
5	0	-4	319	316	3	5	3	-11	168	167	4	5	6	-11	200	204	4	5	6
5	0	-2	230	233	3	5	3	-10	166	165	4	5	6	-9	117	115	3	5	6
5	0	0	465	479	6	5	3	-9	342	344	4	5	6	-8	142	139	6	5	6
5	0	2	297	291	3	5	3	-8	159	162	4	5	6	-7	270	270	4	5	6
5	0	4	274	283	10	5	3	-7	65	64	3	5	6	-6	34	35	4	5	6
5	0	6	254	260	10	5	3	-6	94	96	2	5	6	-5	117	124	3	5	6
5	0	8	61	61	6	5	3	-5	326	334	6	5	6	-3	151	159	3	5	6
5	1	-2	70	71	3	5	3	-4	182	183	3	5	6	-2	95	95	2	5	6
5	1	-1	49	52	3	5	3	-3	129	125	3	5	6	-1	270	271	7	5	6
5	1	-10	395	404	4	5	3	-2	92	91	3	5	6	0	206	209	4	5	6
5	1	-9	89	88	2	5	3	-1	242	241	5	5	6	1	462	467	7	5	6

Values of $10^4 \cdot F_{\text{obs}}$ and $10^4 \cdot F_{\text{calc}}$

H	K	L	F _{obs}	F _{calc}	Sigr	H	K	L	F _{obs}	F _{calc}	Sigr	H	K	L	F _{obs}	F _{calc}	Sigr	H	K	L	F _{obs}	F _{calc}	Sigr
5	10	-7	59	61	4	6	2	-4	140	137	3	6	5	4	63	62	3	7	0	0	77	79	3
5	10	-6	110	107	3	6	2	-3	55	54	3	6	5	5	118	117	3	7	0	2	163	164	5
5	10	-5	63	61	3	6	2	-2	309	311	9	6	6	-10	56	53	5	7	1	-3	57	61	4
5	10	-4	71	76	8	6	2	-1	271	272	4	6	6	-9	157	149	4	7	1	-6	197	192	4
5	10	-3	40	44	5	6	2	0	248	251	4	6	6	-8	87	87	3	7	1	-6	99	96	3
5	10	-2	46	44	4	6	2	2	114	117	3	6	6	-7	153	149	4	7	1	-5	137	138	3
5	10	-1	34	36	5	6	2	3	113	116	3	6	6	-5	54	52	3	7	1	-4	432	433	4
5	10	0	123	116	3	6	2	6	99	102	3	6	6	-4	70	69	3	7	1	-3	119	121	6
5	10	1	35	23	5	6	3	-11	231	229	6	6	6	-3	40	41	4	7	1	-2	79	79	3
5	10	2	95	90	3	6	3	-10	88	87	3	6	6	-1	354	358	7	7	1	0	147	146	10
5	11	-5	47	39	5	6	3	-5	48	41	3	6	6	0	165	165	10	7	1	2	181	181	4
5	11	-4	138	132	3	6	3	-4	166	160	4	6	6	1	103	105	3	7	1	3	126	130	3
5	11	-2	108	104	3	6	3	-3	392	392	5	6	6	3	218	220	4	7	2	-8	87	89	3
5	11	-1	69	72	4	6	3	-2	158	155	3	6	7	-9	82	76	3	7	2	-7	142	142	4
6	0	-12	140	142	3	6	3	-1	60	58	5	6	7	-8	47	47	4	7	2	-6	233	236	4
6	0	-8	186	192	6	6	3	0	36	36	4	6	7	-6	36	43	5	7	2	-5	179	177	4
6	0	-6	230	229	9	6	3	1	309	308	4	6	7	-5	172	169	6	7	2	-4	94	90	3
6	0	-4	267	269	4	6	3	2	118	120	3	6	7	-4	139	137	3	7	2	-3	62	62	3
6	0	-2	172	168	4	6	3	3	103	104	3	6	7	-3	282	286	4	7	2	-2	70	70	6
6	0	0	371	373	5	6	3	4	170	174	6	6	7	-2	184	187	4	7	2	1	54	52	4
6	0	2	89	86	2	6	3	5	64	60	7	6	7	-1	106	108	3	7	2	2	94	94	3
6	0	4	37	42	4	6	3	6	131	131	6	6	7	0	84	84	3	7	2	3	136	134	3
6	1	-12	79	79	3	6	4	-11	59	59	4	6	7	1	150	152	4	7	3	-9	64	56	3
6	1	-11	64	61	3	6	4	-9	247	243	4	6	7	2	130	132	3	7	3	-6	72	69	3
6	1	-10	130	130	4	6	4	-8	57	57	5	6	7	3	56	53	5	7	3	-5	183	178	4
6	1	-9	79	84	3	6	4	-7	88	83	3	6	8	-7	75	74	3	7	3	-4	161	161	4
6	1	-8	79	76	2	6	4	-6	67	69	4	6	8	-6	83	81	3	7	3	-3	167	167	5
6	1	-7	38	40	4	6	4	-5	172	172	5	6	8	-5	68	67	3	7	3	-1	83	86	3
6	1	-6	87	89	2	6	4	-3	39	41	4	6	8	-4	138	137	3	7	3	0	63	67	3
6	1	-4	146	135	5	6	4	-2	48	46	4	6	8	-3	57	56	4	7	3	1	49	47	4
6	1	-3	95	91	3	6	4	-1	457	453	4	6	8	-2	188	191	4	7	3	2	111	111	3
6	1	-2	347	347	3	6	4	1	172	173	4	6	8	-1	94	93	3	7	3	-1	170	170	8
6	1	-1	45	46	5	6	4	2	75	80	3	6	8	0	171	174	4	7	4	-8	68	70	3
6	1	0	151	155	6	6	4	3	168	167	4	6	8	-5	68	67	3	7	4	-7	212	199	4
6	1	1	42	39	4	6	4	4	68	69	4	6	9	-6	85	85	4	7	4	-6	47	43	6
6	1	2	209	209	4	6	4	5	101	99	4	6	9	-5	103	102	4	7	4	-5	295	288	4
6	1	4	90	94	3	6	5	-9	83	83	3	6	9	-4	201	197	4	7	4	-3	134	133	6
6	1	6	206	209	4	6	5	-7	139	141	5	6	9	-3	42	44	5	7	4	-1	56	56	4
6	2	-12	99	97	3	6	5	-5	70	70	3	6	9	-2	286	278	4	7	4	1	59	66	7
6	2	-11	82	83	5	6	5	-4	52	52	4	6	9	-1	78	77	4	7	4	2	47	50	5
6	2	-10	116	113	3	6	5	-3	377	373	4	6	9	0	42	42	5	7	5	-3	117	115	3
6	2	-9	141	141	3	6	5	-2	78	76	3	6	9	-10	48	45	4	7	5	-1	121	117	7
6	2	-8	147	148	5	6	5	-1	297	300	7	7	9	-8	149	150	4	7	5	-1	99	93	3
6	2	-7	113	115	2	6	5	0	54	54	3	7	7	-6	545	549	4	7	5	1	56	54	4
6	2	-6	188	192	4	6	5	1	275	275	5	7	7	-4	123	126	5	7	6	-6	110	110	3
6	2	-5	196	192	4	6	5	3	250	254	4	7	7	-2	196	192	4	7	6	-5	46	46	4

Values of $10^4 F_{\text{obs}}$ and $10^4 F_{\text{calc}}$

H	K	L	F _{obs}	F _{calc}	SigF	H	K	L	F _{obs}	F _{calc}	SigF	H	K	L	F _{obs}	F _{calc}	SigF	H	K	L	F _{obs}	F _{calc}	SigF						
-	-	-	-	-	-	-	-	-	-	-	-	-	-	-	-	-	-	-	-	-	-	-	-						
7	6	-4	66	65	3	7	6	-3	124	127	5	7	6	-2	62	62	5	7	6	-1	35	33	5	7	7	-4	170	165	7
7	7	-3	107	111	4	7	7	-2	59	53	4	7	7	-1	107	111	4	7	7	-2	59	53	4	-	-	-	-	-	-

References Cited

(1) Ames Laboratory is operated for the U. S. Department of Energy by Iowa State University under Contract No. W-7405-Eng-82. This research was supported by the Office of Basic Energy Sciences, Chemical Sciences Division.

(2) (a) Schuman, S. C.; Shalit, H. *Catal. Rev.*, **1970**, *4*, 245.
(b) Prins, R.; De Beer, V. H. J.; Somorjai, G. A. *Catal. Rev. -Sci. Eng.*, **1989**, *31*, 1.
(c) Manowitz, B.; Lipfert, F. W. In *Geochemistry of Sulfur in Fossil Fuels*; Orr, W. L. and White, C. M., Eds.; *ACS Symposium Series 429*; American Chemical Society: Washington, DC, 1990; pp 53-67.

(3) (a) Gates, B. C.; Katzer, J. R.; Schuit, G. C. A. *Chemistry of Catalytic Processes*; McGraw-Hill: New York, 1979; pp 390-447.
(b) Galpern, G. D. In *The Chemistry of Heterocyclic Compounds*; Gronowitz, S., Ed.; John Wiley and Sons, Inc.: New York, 1985; Vol. 44, part 1; pp. 325-351.
(c) *Geochemistry of Sulfur in Fossil Fuels*; Orr, W. L. and White, C. M., Eds. *ACS Symposium Series 429*; American Chemical Society: Washington, DC, 1990.

(4) (a) Angelici, R. J. *Acc. Chem. Res.*, **1988**, *21*, 387.
(b) Angelici, R. J. *Coord. Chem. Rev.*, **1990**, *105*, 61.
(c) Rauchfuss, T. B. *Prog. Inorg. Chem.*, **1991**, *39*, 259.
(d) Rosini, G. P.; Jones, W. D. *J. Am. Chem. Soc.*, **1992**, *114*, 10767.
(e) Selnaau, H. E.; Merola, J. S. *Organometallics*, **1993**, *12*, 1583.

(f) Bianchini, C.; Meli, A.; Peruzzini, M.; Vizza, F.; Frediani, P.; Herrera, V.; Sanchez-Delgado, R. A. *J. Am. Chem. Soc.*, **1993**, *115*, 7505.

(5) (a) Choi, M. -G.; Angelici, R. J. *J. Am. Chem. Soc.*, **1991**, *113*, 5651.
(b) White, C. J.; Choi, M. -G.; Angelici, R. J. To be submitted.

(6) (a) Magdesieva, N. N. *Adv. Heterocycl. Chem.*, **1970**, *12*, 1.
(b) Hörnfeldt, A. -B. *Adv. Heterocycl. Chem.*, **1982**, *30*, 127.
(c) Bird, C. W.; Cheeseman, G. W. H.; Hörnfeldt, A. -B. In *Comprehensive Heterocyclic Chemistry*; Katritzky, A. R. and Rees, C. W., Eds.; Pergamon Press: New York, 1984; Vol. 4; pp 935-971.

(7) (a) McFarlane, H. C. E.; McFarlane, W. In *NMR and the Periodic Table*; Harris, R. K. and Mann, B. E., Eds.; Academic Press: New York, 1978; pp 402-412.
(b) McFarlane, H. C. E.; McFarlane, W. In *NMR of Newly Accessible Nuclei*; Laszlo, P., Ed.; Academic Press: New York, 1983; Vol. 2; pp 275-290.

(8) (a) Pauling, L.; Sherman, J. *J. Chem. Phys.*, **1933**, *1*, 606.
(b) Klages, F. *Chem. Ber.*, **1949**, *82*, 358.
(c) Grasshof, H. *Chem. Ber.*, **1951**, *84*, 916.
(d) Cox, J. D. *Tetrahedron*, **1963**, *19*, 1175.
(e) Elvidge, J. A. *J. Chem. Soc., Chem. Commun.*, **1965**, 160.
(f) Davies, D. W. *J. Chem. Soc., Chem. Commun.*, **1965**, 258.
(g) De Jongh, H. A. P.; Wynberg, H. *Tetrahedron*, **1965**, *21*, 515.

- (h) Dewar, M. J. S. *Tetrahedron*, **1966**, *22*, *Suppl. 8*, 75.
- (i) Julg, A.; François, P. *Theor. Chim. Acta*, **1967**, *8*, 249.
- (j) Dewar, M. J. S.; Trinajstic, N. *J. Am. Chem. Soc.*, **1970**, *92*, 1453.
- (k) Fringuelli, R.; Marino, G.; Taticchi, A. *J. Chem. Soc., Perkin Trans. II*, **1974**, 332.
- (l) Cook, M. J.; Katritzky, A. R.; Linda, P. *Adv. Heterocycl. Chem.*, **1974**, *17*, 255.
- (m) Bird, C. W.; Cheeseman, G. W. H. In *Comprehensive Heterocyclic Chemistry*; Katritzky, A. R. and Rees, C. W., Eds.; Pergamon Press: New York, 1984; Vol. 4; pp 1-38.

(9) (a) Gronowitz, S. *Adv. Heterocycl. Chem.*, **1963**, *1*, 1.

(b) Marino, G. *Adv. Heterocycl. Chem.*, **1971**, *13*, 235.

(c) Meth-Cohn, O. In *Comprehensive Organic Chemistry*; Sammes, P. G., Ed.; Pergamon Press: New York, 1979; Vol. 4; pp 789-838.

(10) (a) Bailey, M. F.; Dahl, L. F. *Inorg. Chem.*, **1965**, *4*, 1306.

(b) Dusausoy, P. Y.; Protas, J.; Guillard, R. *Acta Crystallogr., Sect. B*, **1973**, *29*, 726.

(c) Lockemeyer, J. R.; Rauchfuss, T. B.; Rheingold, A. L.; Wilson, S. R. *J. Am. Chem. Soc.*, **1989**, *111*, 8828.

(d) Ganja, E. A.; Rauchfuss, T. B.; Stern, C. L. *Organometallics*, **1991**, *10*, 270.

(e) Waldbach, T. A.; van Rooyen, P. H.; Lotz, S. *Angew. Chem., Int. Ed. Engl.*, **1993**, *32*, 710.

(11) McGlinchey, M. J. *Adv. Organomet. Chem.*, **1992**, *34*, 285.

(12) (a) Albright, T. A.; Hofmann, P.; Hoffmann, R. *J. Am. Chem. Soc.*, **1977**, *99*, 7546.
(b) Albright, T. A. *Acc. Chem. Res.*, **1982**, *15*, 149.

(13) (a) McGlinchey, M. J.; Fletcher, J. L.; Sayer, B. G.; Bougeard, P.; Fagiani, R.; Lock, C. J. L.; Bain, A. D.; Rodger, C.; Kündig, E. P.; Astruc, D.; Hamon, J. -R.; Le Maux, P.; Top, S.; Jaouen, G. *J. Chem. Soc., Chem. Commun.*, **1983**, 634.
(b) Hunter, G.; Mislow, K. *J. Chem. Soc., Chem. Commun.*, **1984**, 172.
(c) McGlinchey, M. J.; Bougeard, P.; Sayer, B. G.; Hofer, R.; Lock, C. J. L. *J. Chem. Soc., Chem. Commun.*, **1984**, 789.
(d) Chudek, J. A.; Hunter, G.; MacKay, R. L.; Färber, G.; Weissensteiner, W. *J. Organomet. Chem.*, **1989**, *377*, C69.
(e) Downton, P. A.; Mailvaganam, B.; Frampton, C. S.; Sayer, B. G.; McGlinchey, M. J. *J. Am. Chem. Soc.*, **1990**, *112*, 27.
(f) Mailvaganam, B.; Frampton, C. S.; Top, S.; Sayer, B. G.; McGlinchey, M. J. *J. Am. Chem. Soc.*, **1991**, *113*, 1177.
(g) Kilway, K. V.; Siegel, J. S. *J. Am. Chem. Soc.*, **1991**, *113*, 2332.
(h) Chudek, J. A.; Hunter, G.; MacKay, R. L.; Kremminger, P.; Weissensteiner, W. *J. Chem. Soc., Dalton Trans.*, **1991**, 3337.
(i) Hunter, G.; MacKay, R. L.; Kremminger, P.; Weissensteiner, W. *J. Chem. Soc., Dalton Trans.*, **1991**, 3349.
(j) Kilway, K. V.; Siegel, J. S. *Organometallics*, **1992**, *11*, 1426.

(14) (a) Acampora, M.; Ceccon, A.; Dal Farra, M.; Giacometti, G.; Rigatti, G. *J. Chem. Soc., Perkin Trans. II*, **1977**, 483.

- (b) Nambu, M.; Siegel, J. S. *J. Am. Chem. Soc.*, **1988**, *110*, 3675.
- (c) Downton, P. A.; Sayer, B. G.; McGlinchey, M. J. *Organometallics*, **1992**, *11*, 3281.
- (d) Nambu, M.; Mohler, D. L.; Hardcastle, K.; Baldridge, K. K.; Siegel, J. S. *J. Am. Chem. Soc.*, **1993**, *115*, 6138.

(15) (a) Shriver, D. F.; Drezdzon, M. A. *The Manipulation of Air Sensitive Compounds*, 2nd ed.; John Wiley and Sons, Inc.: New York, 1986.

(b) *Experimental Organometallic Chemistry*; Wayda, A. L.; Darenbourg, M. Y., Eds.; ACS Symposium Series 357; American Chemical Society: Washington, D.C., 1987.

(16) Spies, G. H.; Angelici, R. J. *Organometallics*, **1987**, *6*, 1897.

(17) Dong, L.; Duckett, S. B.; Ohman, K. F.; Jones, W. D. *J. Am. Chem. Soc.*, **1992**, *114*, 151.

(18) (a) Gronowitz, S.; Frejd, T.; Moberg-Ogard, A.; Trege, L. *J. Heterocycl. Chem. (Engl. Transl.)*, **1976**, *13*, 1319.

(b) Mohmand, S.; Bargon, J.; Waltman, R. J. *J. Org. Chem.*, **1983**, *48*, 3544.

(19) Yuryev, Y. K.; Mezentsova, N. N.; Vaskovsky, V. E. *J. Gen. Chem. USSR (Engl. Transl.)*, **1957**, *27*, 3193.

(20) (a) Mangini, A.; Taddei, F. *Inorg. Chim. Acta*, **1968**, *2*, 12.

(b) Guillard, R.; Tirouflet, J.; Fournari, P. *J. Organomet. Chem.*, **1971**, *33*, 195.

(c) Segard, C.; Roques, B. -P.; Pommier, C.; Guiochon, G. *J. Organomet. Chem.*, **1974**, 77, 59.

(21) Grevels, F. -W.; Skibbe, V. *J. Chem. Soc., Chem. Commun.*, **1984**, 681.

(22) Bamford, C. H.; Burley, J. W.; Coldbeck, M. *J. Chem. Soc., Dalton Trans.*, **1972**, 1846.

(23) (a) *Enraf-Nonius Structure Determination Package*; Enraf Nonius: Delft, Holland. Neutral-atom scattering factors and anomalous scattering corrections were taken from *International Tables for X-ray Crystallography*; The Kynoch Press: Birmingham, England, 1974; Vol. IV.
(b) Sheldrick, G. M. *SHELXS-86*; Institut für Anorganische Chemie der Universität, Göttingen, F. R. G., 1986.

(24) Hoffmann, R. *J. Chem. Phys.*, **1963**, 39, 1397.

(25) Clementi, E.; Roetti, C. *At. Data Nucl. Data Tables*, **1974**, 14, 177.

(26) Moore, C. E. *At. Energy Levels Natl. Stand. Ref. Data Ser.*, **1971**, 35.

(27) Bak, B.; Christensen, D.; Hansen-Nygaard, L.; Rastrup-Andersen, J. *J. Mol. Spectrosc.*, **1961**, 7, 58.

(28) Brown, R. D.; Burden, F. R.; Godfrey, P. D. *J. Mol. Spectrosc.*, **1968**, 25, 415.

(29) Stephenson, D. S.; Binsch, G. *J. Magn. Reson.*, **1978**, 32, 145.

(30) Quantum Chemistry Program Exchange, Indiana University, Bloomington, IN.

(31) New Methods Research, Inc., Syracuse, NY.

(32) Neuman, R. C., Jr.; Jonas, V. *J. Org. Chem.*, **1974**, *39*, 925.

(33) Sandström, J. *Dynamic NMR Spectroscopy*; Academic Press: New York, 1982; pp 93-97.

(34) (a) Fischer, E. O.; Öfele, K. *Chem. Ber.*, **1958**, *91*, 2395.
(b) Segard, C.; Roques, B.; Pommier, C. *C. R. Acad. Sci., Ser. C*, **1971**, *272*, 2179.
(c) Moser, G. A.; Rausch, M. D. *Syn. React. Inorg. Met.-Org. Chem.*, **1974**, *4*, 37.
(d) Novi, M.; Guanti, G.; Dell'Erba, C. *J. Heterocycl. Chem. (Engl. Transl.)*, **1975**, *12*, 1055.

(35) Mahaffy, C. A. L.; Pauson, P. L. *Inorg. Synth.*, **1990**, *28*, 136.

(36) Emanuel, R. V.; Randall, E. W. *J. Chem. Soc. A*, **1969**, 3002.

(37) Lumbroso, H.; Segard, C.; Roques, B. *J. Organomet. Chem.*, **1973**, *61*, 249.

(38) (a) Brill, T. B.; Kotlar, A. J. *Inorg. Chem.*, **1974**, *13*, 470.
(b) Gill, T. P.; Mann, K. R. *Organometallics*, **1982**, *1*, 485.
(c) Lesch, D. A.; Richardson, J. W., Jr.; Jacobson, R. A.; Angelici, R. J. *J. Am. Chem. Soc.*, **1984**, *106*, 2901.

- (d) Huckett, S. C.; Sauer, N. N.; Angelici, R. J. *Organometallics*, **1987**, *6*, 591.
- (e) Hachgenei, J. W.; Angelici, R. J. *Angew. Chem., Int. Ed. Engl.*, **1987**, *26*, 909.
- (f) Hachgenei, J. W.; Angelici, R. J. *J. Organomet. Chem.*, **1988**, *355*, 359.
- (g) Hachgenei, J. W.; Angelici, R. J. *Organometallics*, **1989**, *8*, 14.

(39) (a) White, C.; Thompson, S. J.; Maitlis, P. M. *J. Chem. Soc., Dalton Trans.*, **1977**, 1654.

(b) Huckett, S. C.; Miller, L. L.; Jacobson, R. A.; Angelici, R. J. *Organometallics*, **1988**, *7*, 686.

(40) (a) Gracey, D. E. F.; Jackson, W. R.; Jennings, W. B.; Rennison, S. C.; Spratt, R. *J. Chem. Soc. B*, **1969**, 1210.

(b) Top, S.; Jaouen, G.; Vessières, A.; Abjean, J. -P.; Davoust, D.; Rodger, C. A.; Sayer, B. G.; McGlinchey, M. J. *Organometallics*, **1985**, *4*, 2143.

(c) Mailvaganam, B.; Perrier, R. E.; Sayer, B. G.; McCarry, B. E.; Bell, R. A.; McGlinchey, M. J. *J. Organomet. Chem.*, **1988**, *354*, 325.

(41) Mann, B. E. *J. Chem. Soc., Chem. Commun.*, **1971**, 976.

(42) Farnell, L. F.; Randall, E. W.; Rosenberg, E. *J. Chem. Soc., Chem. Commun.*, **1971**, 1078.

(43) Mann, B. E. *J. Chem. Soc., Dalton Trans.*, **1973**, 2012.

(44) Brown, D. A.; Chester, J. P.; Fitzpatrick, N. J.; King, I. J. *Inorg. Chem.*, **1977**, *16*, 2497.

(45) (a) Bodner, G. M.; Todd, L. J. *Inorg. Chem.*, **1974**, *13*, 1335.
(b) Hunter, A. D.; Mozol, V.; Tsai, S. D. *Organometallics*, **1992**, *11*, 2251.

(46) Nambu, M.; Hardcastle, K.; Baldridge, K. K.; Siegel, J. S. *J. Am. Chem. Soc.*, **1992**, *114*, 369.

(47) Diercks, R.; Vollhardt, K. P. C. *Angew. Chem., Int. Ed. Engl.*, **1986**, *25*, 266.

(48) Van Rooyen, P. H.; Dillen, J. L. M.; Lotz, S.; Schindehutte, M. *J. Organomet. Chem.*, **1984**, *273*, 61.

(49) (a) Spek, A. L. *Cryst. Struct. Commun.*, **1977**, *6*, 835.
(b) Eekhof, J. H.; Hogeveen, H.; Kellogg, R. M. *J. Organomet. Chem.*, **1978**, *161*, 361.

(50) Rees, B.; Coppens, P. *Acta Crystallogr., Sect. B*, **1973**, *29*, 2516.

(51) Zonnevylle, M. C.; Hoffmann, R.; Harris, S. *Surf. Sci.*, **1988**, *199*, 320.

(52) Le Beuze, A.; Lissillour, R.; Weber, J. *Organometallics*, **1993**, *12*, 47.

(53) Polam, J. R.; Porter, L. C. *Organometallics*, **1993**, *12*, 3504.

(54) Allen, F. H.; Kennard, O.; Watson, D. G.; Brammer, L.; Orpen, A. G.; Taylor, R. *J. Chem. Soc., Perkin Trans. II*, **1987**, S1.

(55) Choi, M. -G.; Angelici, R. J. *Inorg. Chem.*, **1991**, *30*, 1417.

(56) Benson, J. W.; Angelici, R. J. *Organometallics*, **1993**, *12*, 680.

(57) Shanan-Atidi, H.; Bar-Eli, K. H. *J. Phys. Chem.*, **1970**, *74*, 961.

GENERAL CONCLUSIONS

This research demonstrates that the rotational barriers of the alkyl-substituted thiophene (Th) and selenophene (Sel) ligands in $\text{Cr}(\text{CO})_3(\eta^5\text{-Th})$ and $\text{Cr}(\text{CO})_3(\eta^5\text{-Sel})$ can be measured at low temperatures using variable-temperature ^{13}C NMR spectroscopy. Activation enthalpies (ΔH^\ddagger , in kcal/mol) for these complexes increase in the following order: T (6.2), 3-MeT (6.5), 2-EtT (6.9), 2-MeT (7.1), Me₄T (7.4), 2,5-Me₂T (7.7), Sel (7.8), 2-MeSel (8.4), and 2,5-Me₂Sel (9.0). The fact that the activation barriers for these complexes are higher than those in the analogous alkyl-substituted benzene complexes is due to the relatively localized π bonding in the Th and Sel ligands which is directed at the heteroatom and the two double bonds.

In general, we suggest that the bonding between the chromium and the Th or Sel ligand is dominated by a strong metal-heteroatom (S or Se) bond and a weaker Cr-diene interaction. Any change in the Th or Sel ligand that results in increased π -electron density on the heteroatom should strengthen the Cr-heteroatom bond. The stronger Cr-S or -Se bond should enhance this localized picture of the metal-Th or -Sel bond and should lead to a higher activation barrier. On the other hand, any change in the Th or Sel ligand that leads to increased π -electron density on the diene fragment should strengthen the bond between the metal and the diene fragment. The stronger Cr-diene bond should reduce the dominating influence of the Cr-heteroatom bond and should lead to a smaller activation barrier.

REFERENCES CITED

- (1) Rees, B.; Coppens, P. *Acta Crystallogr., Sect. B*, **1973**, *29*, 2516.
- (2) Delise, P.; Allegra, G.; Mognaschi, E. R.; Chierico, A. *J. Chem. Soc., Faraday Trans. II*, **1975**, *71*, 207.
- (3) Van Steenwinkel, R. *Z. Naturforsch., Teil A*, **1969**, *24*, 1526.
- (4) Gryff-Keller, A.; Szczecinski, P.; Koziel, H. *Magn. Reson. Chem.*, **1990**, *28*, 25.
- (5) Chiu, N. -S.; Schäfer, L.; Seip, R. *J. Organomet. Chem.*, **1975**, *101*, 331.
- (6) Albright, T. A.; Hofmann, P.; Hoffmann, R. *J. Am. Chem. Soc.*, **1977**, *99*, 7546.
- (7) Jackson, W. R.; Pincombe, C. F.; Rae, I. D.; Thapebinkarn, S. *Aust. J. Chem.*, **1975**, *28*, 1535.
- (8) Jackson, W. R.; Pincombe, C. F.; Rae, I. D.; Rash, D.; Wilkinson, B. *Aust. J. Chem.*, **1976**, *29*, 2431.
- (9) Maricq, M. M.; Waugh, J. S.; Fletcher, J. L.; McGlinchey, M. J. *J. Am. Chem. Soc.*, **1978**, *100*, 6902.
- (10) (a) Hunter, G.; Iverson, D. J.; Mislow, K.; Blount, J. F. *J. Am. Chem. Soc.*, **1980**, *102*, 5942.
(b) Iverson, D. J.; Hunter, G.; Blount, J. F.; Damewood, J. R., Jr.; Mislow, K. *J. Am. Chem. Soc.*, **1981**, *103*, 6073.

(11) Pausak, S.; Tegenfeldt, J.; Waugh, J. S. *J. Chem. Phys.*, **1974**, *61*, 1338.

(12) Hunter, G.; Blount, J. F.; Damewood, J. R., Jr.; Iverson, D. J.; Mislow, K. *Organometallics*, **1982**, *1*, 448.

(13) (a) Bailey, M. F.; Dahl, L. F. *Inorg. Chem.*, **1965**, *4*, 1298.
(b) Bailey, M. F.; Dahl, L. F. *Inorg. Chem.*, **1965**, *4*, 1314.

(14) McGlinchey, M. J.; Fletcher, J. L.; Sayer, B. G.; Bougeard, P.; Faggiani, R.; Lock, C. J. L.; Bain, A. D.; Rodger, C.; Kündig, E. P.; Astruc, D.; Hamon, J. -R.; Le Maux, P.; Top, S.; Jaouen, G. *J. Chem. Soc., Chem. Commun.*, **1983**, 634.

(15) Mailvaganam, B.; Frampton, C. S.; Top, S.; Sayer, B. G.; McGlinchey, M. J. *J. Am. Chem. Soc.*, **1991**, *113*, 1177.

(16) Blount, J. F.; Hunter, G.; Mislow, K. *J. Chem. Soc., Chem. Commun.*, **1984**, 170.

(17) Hunter, G.; Weakley, T. J. R.; Weissensteiner, W. *J. Chem. Soc., Perkin Trans. II*, **1987**, 1633.

(18) (a) Kilway, K. V.; Siegel, J. S. *J. Am. Chem. Soc.*, **1991**, *113*, 2332.
(b) Kilway, K. V.; Siegel, J. S. *J. Am. Chem. Soc.*, **1992**, *114*, 255.

(19) Iverson, D. J.; Mislow, K. *Organometallics*, **1982**, *1*, 3.

(20) Hunter, G.; Weakley, T. J. R.; Mislow, K.; Wong, M. G. *J. Chem. Soc., Dalton Trans.*, **1986**, 577.

(21) Hunter, G.; Weakley, T. J. R.; Weissensteiner, W. *J. Chem. Soc., Dalton Trans.*, **1987**, 1545.

(22) Chudek, J. A.; Hunter, G.; MacKay, R. L.; Kremminger, P.; Schlägl, K.; Weissensteiner, W. *J. Chem. Soc., Dalton Trans.*, **1990**, 2001.

(23) Hunter, G.; MacKay, R. L.; Kremminger, P.; Weissensteiner, W. *J. Chem. Soc., Dalton Trans.*, **1991**, 3349.

(24) Hunter, G.; Mislow, K. *J. Chem. Soc., Chem. Commun.*, **1984**, 172.

(25) McGlinchey, M. J.; Bougeard, P.; Sayer, B. G.; Hofer, R.; Lock, C. J. L. *J. Chem. Soc., Chem. Commun.*, **1984**, 789.

(26) Chudek, J. A.; Hunter, G.; MacKay, R. L.; Kremminger, P.; Weissensteiner, W. *J. Chem. Soc., Dalton Trans.*, **1991**, 3337.

(27) Downton, P. A.; Mailvaganam, B.; Frampton, C. S.; Sayer, B. G.; McGlinchey, M. J. *J. Am. Chem. Soc.*, **1990**, *112*, 27.

(28) Kilway, K. V.; Siegel, J. S. *Organometallics*, **1992**, *11*, 1426.

(29) Kremminger, P.; Weissensteiner, W.; Kratky, C.; Hunter, G.; MacKay, R. L. *Monatsh. Chem.*, **1989**, *120*, 1175.

(30) Acampora, M.; Ceccon, A.; Dal Farra, M.; Giacometti, G.; Rigatti, G. *J. Chem. Soc., Perkin Trans. II*, **1977**, 483.

(31) Downton, P. A.; Sayer, B. G.; McGlinchey, M. J. *Organometallics*, **1992**, *11*, 3281.

(32) Albright, T. A.; Hoffmann, R.; Hofmann, P. *Chem. Ber.*, **1978**, *111*, 1591.

(33) Andrianov, V. G.; Struchkov, Y. T. *J. Struct. Chem. (Engl. Transl.)*, **1977**, *18*, 251.

(34) Koch, O.; Edelmann, F.; Behrens, U. *Chem. Ber.*, **1982**, *115*, 1313.

(35) Diercks, R.; Vollhardt, K. P. C. *Angew. Chem., Int. Ed. Engl.*, **1986**, *25*, 266.

(36) Diercks, R.; Vollhardt, K. P. C. *J. Am. Chem. Soc.*, **1986**, *108*, 3150.

(37) Nambu, M.; Hardcastle, K.; Baldridge, K. K.; Siegel, J. S. *J. Am. Chem. Soc.*, **1992**, *114*, 369.

(38) Nambu, M.; Mohler, D. L.; Hardcastle, K.; Baldridge, K. K.; Siegel, J. S. *J. Am. Chem. Soc.*, **1993**, *115*, 6138.